Neurogenic Tumors

9

Jin Han and Song Zhang

Neurogenic tumors represent approximately 20% of all adult tumors and 35% of all pediatric mediastinal tumors and are the most common cause of a posterior mediastinal mass, accounting for 20–47% of mediastinal tumors, and comprising approximately 80% of all posterior mediastinal tumors. Primary mediastinal neurogenic tumors are mostly benign, and malignant tumors are common in children, accounting for about 10% of mediastinal neurogenic tumors.

9.1 Origin and Classification

Mediastinal neurogenic tumors mostly originate from the spinal nerve and paraspinal sympathetic chain, and only a few originate from the vagus nerve, phrenic nerve, and pulmonary nerve. Mediastinal neurogenic tumors are generally grouped into three categories according to tumor origin within the mediastinal nervous tissues—namely, the peripheral nerves, sympathetic ganglia, or paraganglia.

Mediastinal neurogenic tumors can originate from cells of the nerve sheath, such as schwannomas, neurofibromas, and malignant schwannomas. The vast majority of adult mediastinal neurogenic tumors fall into this category. Schwannomas and neurofibromas are benign, slow-growing peripheral nerve sheath tumors that frequently originate from a spinal nerve root or intercostal nerve but may involve any thoracic nerve (including the vagus or phrenic nerve). Tumors growing on intradural nerve roots can expand outward through the intervertebral foramen and enlarge the intervertebral foramen; tumors of intercostal nerve origin can sometimes extend into the spinal canal, both of which make the tumor dumbbell shaped. Focal malignant schwannoma, primary malignant schwannoma, and neurofibrosarcoma are rare. They often invade adjacent tissues and cause distant metastases.

Mediastinal neurogenic tumors can originate from ganglion cells, such as ganglioneuroma, ganglioneuroblastoma, and neuroblastoma, and are more common in children and young people. Generally, ganglioneuromas are found in children older than 10 years, with a male predominance. Ganglioneuroma is a benign tumor, usually attached either to a sympathetic nerve or to an intercostal nerve trunk, protrudes outward in the paravertebral sulcus, and grows slowly. The tumor diameter is usually more than 5 cm. As a transitional tumor on the intermediate spectrum of disease between ganglioneuromas and neuroblastomas, Ganglioneuroblastoma includes elements of both malignant neuroblastoma and benign ganglioneuroma. Neuroblastoma is a highly malignant tumor, which is very rare and occurs in infants and young children. It tends to invade adjacent thoracic vertebrae and ribs. Hematogenous metastases are more common in liver and bone.

Mediastinal neurogenic tumors can originate from paraganglial cells, such as pheochromocytoma (chromaffin paraganglioma) and nonchromaffin paraganglioma (receptoma), and are rare clinically.

9.2 Schwannoma

Schwannomas are benign nerve sheath neoplasms of Schwann cells origin, and are the most common of the neurogenic mediastinal tumors. The peak incidence is 30–50 years, and there is no gender difference. According to the 2007 WHO central nervous system (CNS) tumor classification criteria, benign schwannomas are classified into three types: cellular schwannoma, plexiform schwannoma, and melanotic schwannoma. Malignant peripheral nerve sheath tumors (MPNSTs) are divided into epithelioid MPNST, MPNST with mesenchymal differentiation, melanotic MPNST, and MPNST with glandular differentiation. Capsule

J. Han
Department of Pulmonary and Critical Care Medicine, Yantaishan Hospital, Yantai, China

S. Zhang (✉)
Department of Respiratory and Critical Care Medicine, Shandong Provincial Hospital Affiliated to Shandong First Medical University, Shandong, china

S. Zhang (ed.), *Diagnostic Imaging of Mediastinal Diseases*, https://doi.org/10.1007/978-981-15-9930-9_9

of cellular schwannoma is relatively intact, with a disproportionate increase in nuclear division and atypical cells, and S100 is strongly positive. Plexiform schwannoma mainly consists of Antoni type A tissue, composed of cells with small spindle or wavy nuclei arrayed in cellular fascicles often with nuclear palisading. Immunohistochemistry demonstrates positive S100 and negative EMA. Melanotic schwannoma is rare and occurs more frequently in middle-aged people. Microscopically, the tumors are characterized by spindle and epithelioid cells arranged in interlacing fascicles, with marked accumulation of melanin in neoplastic cells and related melanophages.

In the 2016 edition of the new classification of CNS tumors, melanotic schwannoma is now classified as a distinct entity rather than as a variant. The reason is that it is both clinically (e.g., malignant behavior in a significant subset) and genetically (e.g., associations with Carney Complex and the *PRKAR1A* gene) distinct from conventional schwannoma. Because hybrid nerve sheath tumors are increasingly being recognized in a variety of combinations, they have been included in the 2016 CNS WHO; as such, this broad category was separated out as an entity, although it may well represent a group of tumors rather than one distinct subtype. Lastly, the 2016 CNS WHO now designates two subtypes of malignant MPNST: epithelioid MPNST and MPNST with perineurial differentiation. These were considered sufficiently distinct clinically to warrant designation as variants, whereas other subtypes such as MPNST with divergent differentiation (malignant Triton tumor, glandular MPNST, etc.) simply represent histologic patterns.

Depending on the growth location and tumor size of the schwannoma, patients may have different clinical manifestations. Under normal circumstances, because schwannomas tend to occur in the posterior mediastinum, most of them grow outward and easily cause pressure on the lung and heart. Therefore, patients often refer to chest tightness and suffocation as the first symptoms. Some patients may have chest pain or paresthesia due to tumor irritation to the pleura, and some have symptoms of nerve compression such as limb numbness. In addition, there are a considerable number of patients who have no obvious symptoms and are found during physical examination.

Benign schwannomas generally present as lobular spheroidal masses, solitary, well encapsulated, and sharply demarcated from the adjacent soft tissue. Large tumors may be cystic. It is also famous as "dumbbell tumor" as in posterior mediastinum, which originates from or extends into the vertebral canal. Malignant schwannomas may have local invasion, and the boundary between the tumor and surrounding tissues is unclear. Complete surgical resection is difficult and prone to recurrence.

Schwannoma has usually yellow cut surface and is rarely dark red/black due to hemorrhage. Microscopically, it is composed of Schwann cells within a background of loose reticular tissue. The tumor's features are that the hypercellular Antoni A and hypocellular Antoni B areas appear alternately, and most of the capsules are complete (Fig. 9.1). The relative content of the two components varies greatly. When the mass is large, it can contain two structures. When the mass is small, it often only appears in the Antoni A area. The Antoni A is mostly composed of compact spindle cells with palisading cell nuclei (Fig. 9.2), and there are Verocay bodies surrounded by oval nuclei. Sometimes mitotic figures are also seen. If the tumor has the typical characteristics of schwannomas, mitotic images can be ignored. The cell arrangement of the Antoni B area is more irregular and has fewer cell components. In the loose matrix, spindle or oval cells are scattered randomly. At the same time, microcapsule structures, fine collagen fibers, and varying amounts of inflammatory cell infiltration are often found in the matrix.

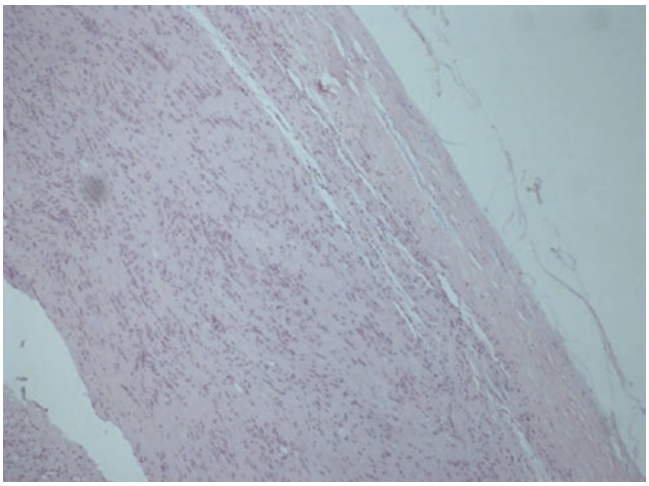

Fig. 9.1 Schwannoma with complete encapsulation (HE, ×100)

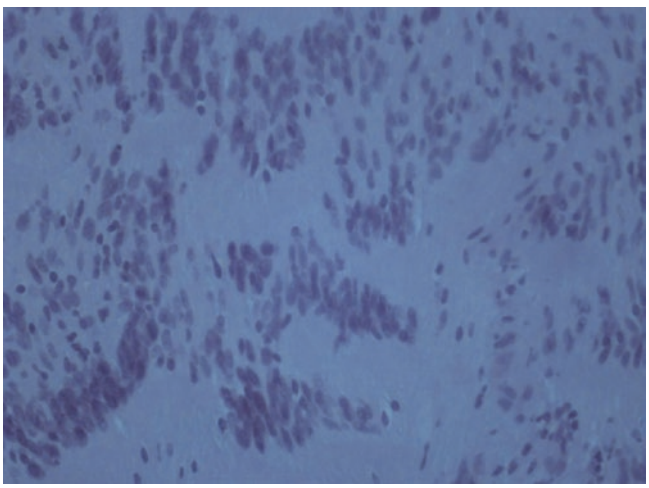

Fig. 9.2 Hypercellular Antoni A area with palisaded spindle cells (HE, ×400)

Large irregular blood vessels can be seen in the Antoni B area, which is also one of the characteristics of schwannoma. Malignant schwannomas show nucleus mitotic figures, cellular atypia, and invasion of surrounding tissues. The immunocytochemistry is positive for S100 (Fig. 9.3), Vimentin (Fig. 9.4), type IV collagen, calcineurin (CaN), basement membrane components (such as laminin) and nerve growth factor receptor (NGF), etc. Glial fibrillary acidic protein (GFAP) and CD68 may occasionally be focally positive. Tumor cells generally do not express CK, CD117, SMA, Desmin, NF, and desmosome.

Thoracal schwannoma is normally located in the posterior regions of the mediastinum. Chest CT shows a well-marginated paraspinal soft-tissue mass (Fig. 9.5), often containing areas of low attenuation corresponding to bleeding (Fig. 9.6) or cystic degeneration (Fig. 9.7).Calcification is seen in about 10% of schwannomas (Fig. 9.8), which may primarily be in a peripheral pattern, particularly in long-standing lesions with advanced degeneration (so-called ancient schwannomas). Fat can be seen in some lesions. Generally, the tumor is relatively small, no more than 5 cm. The tumor's density is lower than that of muscle tissue on unenhanced scan, which is mainly due to the loose arrangement of tumor cells, the large interstitial composition, and a large amount of intercellular edema fluid and mucus. In addition, Schwannomas have reduced attenuation compared to muscle tissues, which is related to the high moisture content in the mucus matrix of schwannoma cells. The homogeneous enhancement is shown in contrast-enhanced CT when the mass is small and more heterogeneous enhancement with larger schwannomas owing to cystic and hemorrhagic changes. Osseous pressure erosion may be present (Fig. 9.9). The tumors may be dumbbell shaped and grow into the spinal canal and paravertebral region, extending and squeezing through the spinal foramen, giving the narrow waist.

MRI is another auxiliary examination that can be used for the diagnosis of schwannoma. Heterogeneous mixed signals are often seen in the tumor. Compared with CT, MRI has good soft-tissue resolution and can perform multidirectional imaging. It can not only accurately display the location of the

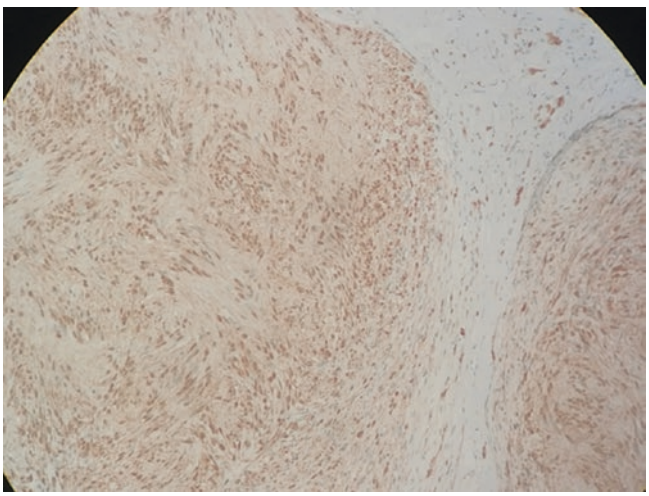

Fig. 9.3 The tumor exhibits diffuse positivity for S-100 (HE, ×200)

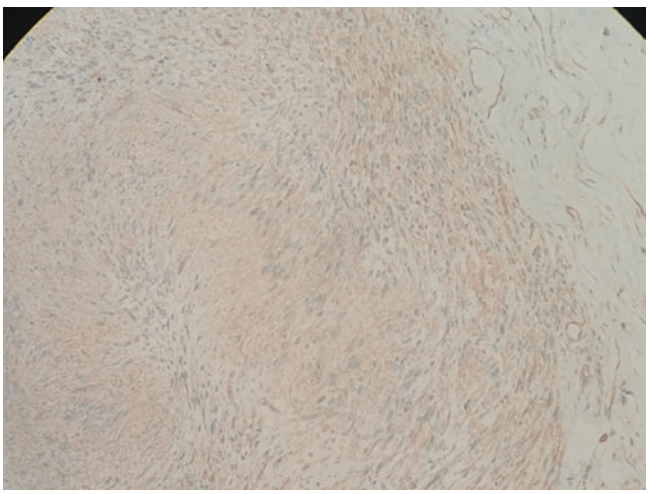

Fig. 9.4 The tumor exhibits diffuse positivity for Vimentin (HE, ×200)

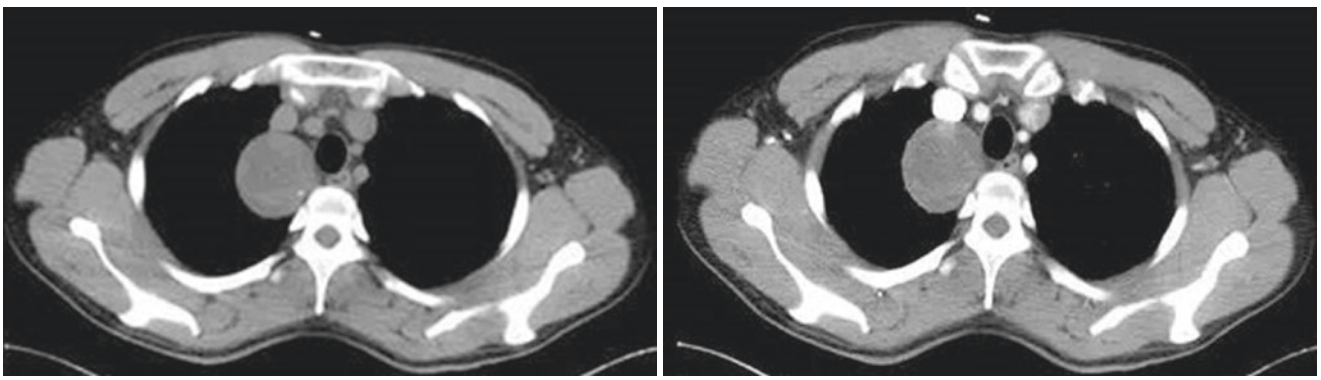

Fig. 9.5 A 31-year-old man complained of no sweat on the right forehead and drooping right eyelid. CT scan showed a clear boundary mass in the right superior mediastinum. The arterial phase showed slightly heterogeneous enhancement

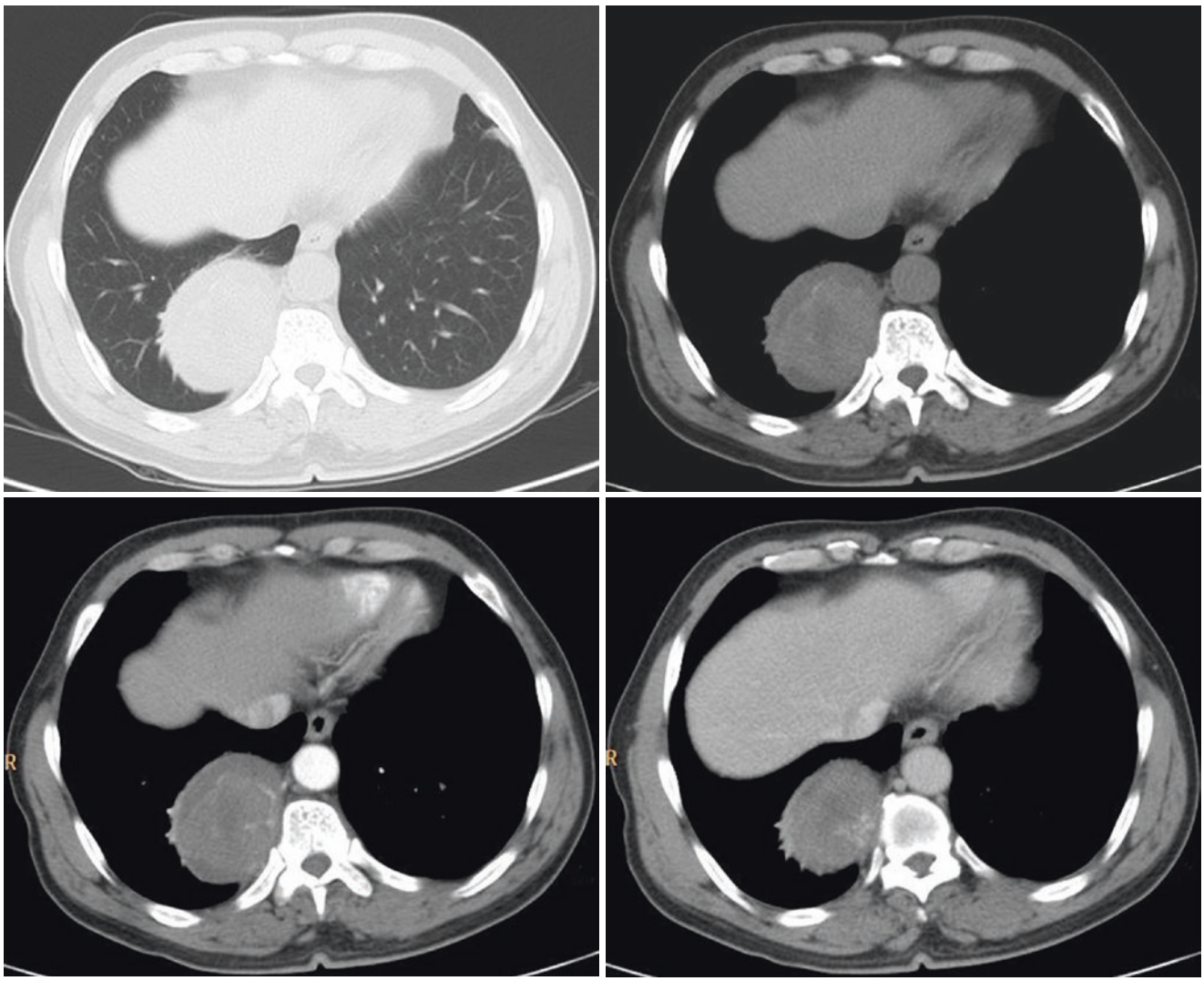

Fig. 9.6 A 58-year-old man with spherical soft tissue mass in the right posterior mediastinum. Unenhanced CT scan showed uneven density, the arterial phase of the contrast-enhanced CT scan showed slightly heterogeneous enhancement, and the venous phase showed delayed enhancement. Postoperative pathology revealed schwannoma with bleeding, necrosis, and degeneration

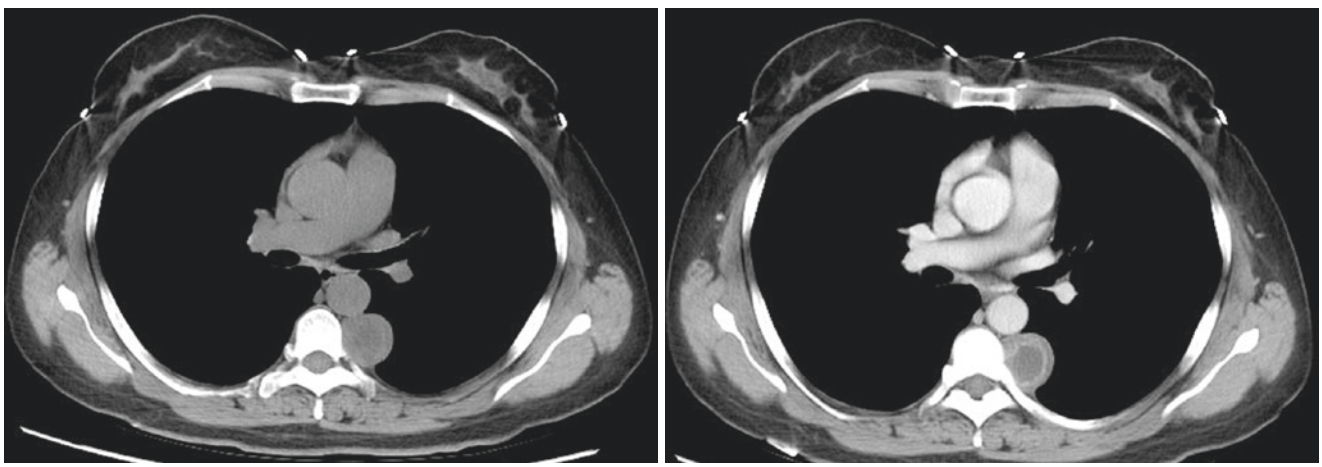

Fig. 9.7 A 47-year-old woman with paraspinal mass in the left posterior mediastinum. The contrast-enhanced scan showed a ring-shaped enhancement and a low-density change in the center. Pathology revealed schwannoma with cystic changes

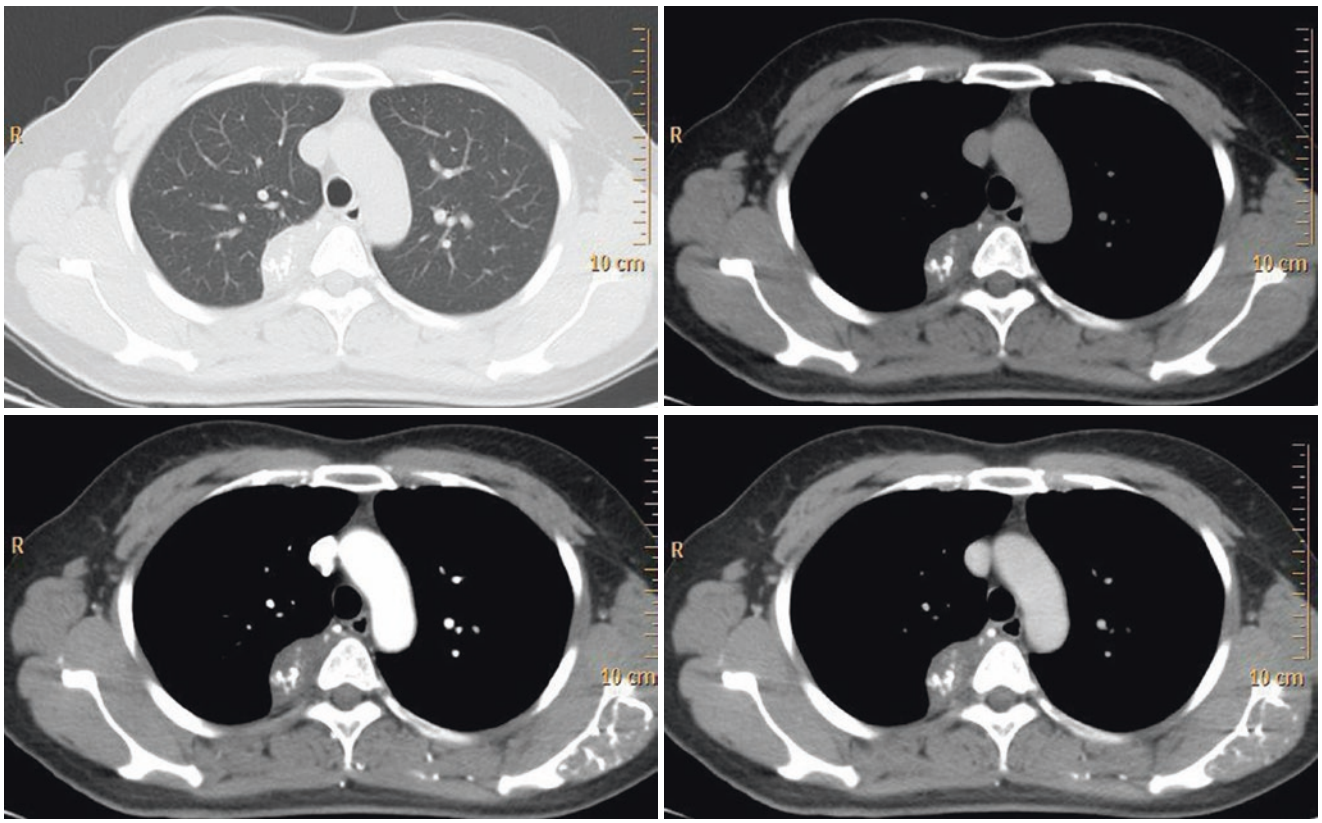

Fig. 9.8 A 36-year-old woman with right posterior mediastinal mass. Pathology revealed schwannoma with hemorrhage, necrosis, and calcifications

tumor, shape, and its relationship with peripheral blood vessels and nerves, but also show the characteristics of pathological signals of tumor tissue, suggesting pathological changes in tumors, such as mucus changes, collagen fibers, bleeding, and cystic changes. The limitations of MRI compared to CT are the limited radiographic evaluation of calcifications and poorer spatial resolution. Low to intermediate signal intensity on T1-weighted images, high signal intensity on T2-weighted images, and intense enhancement of solid components are shown in MRI on gadolinium-enhanced imaging, which can vary based on the ratio of collagenous fibrous tissues, myxomatous matrices, and tumor cells in the tumors. In schwannoma, Antoni A area cells have rich blood supply, and have a higher density on CT scan. The Antoni A component shows relatively low signal intensity on T2-weighted images and relatively strong contrast enhancement. Antoni B area cells have higher water content in the substrate. CT scan shows low density, whereas MRI shows very high signal intensity on T2-weighted images and gradual and weak contrast enhancement (Figs. 9.10, 9.11, 9.12, 9.13, 9.14, and 9.15).

9.3 Neurofibroma

Neurofibromas are usually homogeneous, well-marginated tumors caused by disorganized proliferation of all nerve elements, including Schwann cells, myelinated, and unmyelinated nerve fibers, and fibroblasts. Neurofibromas account for about 20% of mediastinal neurogenic tumors. The peak age of occurrence is 20–30 years. Localized neurofibromas have a true capsule or pseudocapsule. At microscopy, the tumors are hypocellular and consist of widely spaced spindle cells embedded in myxomatous and collagenous matrices.

Neurofibromas may be subdivided into three categories: solitary, diffuse, and plexiform. Solitary neurofibromas usually present as small polypoid masses. Solitary cutaneous neurofibroma is most common, and occurs sporadically in the majority of cases. Solitary neurofibromas may also involve a major nerve, and typically fusiform expansion of the nerve trunk (intraneural subtype) is resulted. Diffuse neurofibromas are usually characterized by a plaque-like enlargement in the head and neck region. Plexiform neurofibromas are large, complex tumors with a “bag of worms”

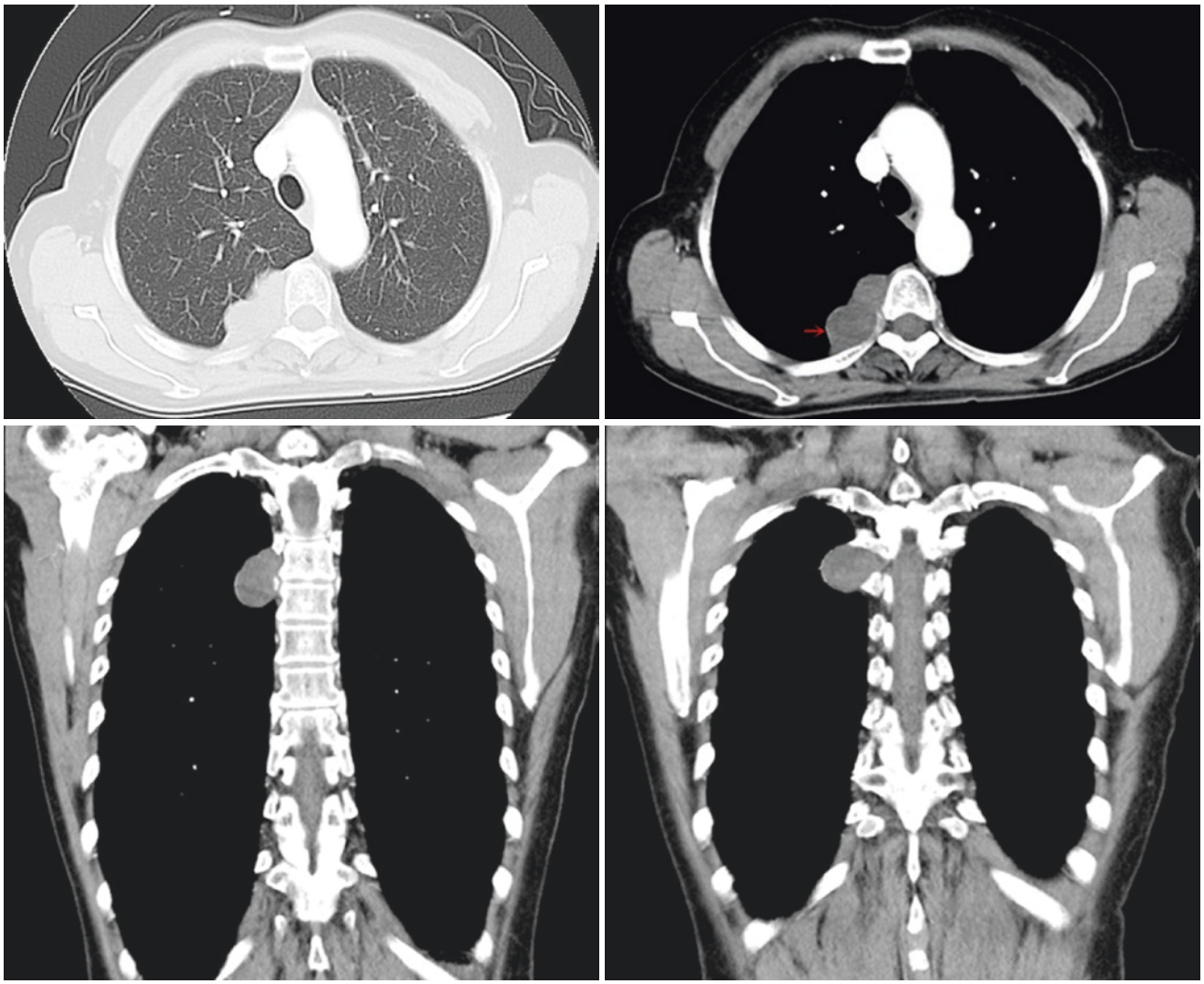

Fig. 9.9 A 62-year-old woman complained of chest pain for 20 days. CT showed right posterior mediastinal schwannoma with intact capsule (red arrow), and adjacent ribs were compressed

appearance, usually near large spinal roots. Most neurofibromas occur sporadically, although approximately 10% ultimately proved to be associated with neurofibromatosis type 1 (NF1). Diffuse and plexiform neurofibromas may be pigmented histologically and clinically. Sporadic and diffuse neurofibromas only rarely progress to MPNST. In diffuse neurofibromas, progression has been associated with multiple local recurrences. Plexiform neurofibromas are pathognomic of neurofibromatosis and have a significant risk of malignant transformation.

Neurofibromas grow slowly, rarely undergo degeneration, cyst formation, or bleeding, and are prone to relapse after resection. Intrathoracic neurofibromatosis often occurs in the posterior mediastinum, most of them originate from the sympathetic or spinal nerves. Neurogenic tumors located in the anterior mediastinum mostly originate from the intercostal or vagus nerve. The patients are mostly asymptomatic or with mild symptoms. Chest CT scan shows a low-density mass with clear boundaries. Contrast-enhanced CT image shows slight enhancement or no enhancement (Fig. 9.16). The density and enhancement degree of the tumor depends on the proportion of nerve sheath cells, collagen bundles.

9.4 Ganglioneuroma

Tumors caused by autonomic ganglion cells include the spectrum of benign ganglioneuromas, varying degrees of malignant ganglioneuroblastomas, and aggressively malignant neuroblastomas. In the United States, two histological classification systems are commonly used to stratify neuroblastic tumors into risk groups: the Shimada classification and the Pediatric Oncology Group (POG) classification. Both systems evaluate histological features, such as cellular

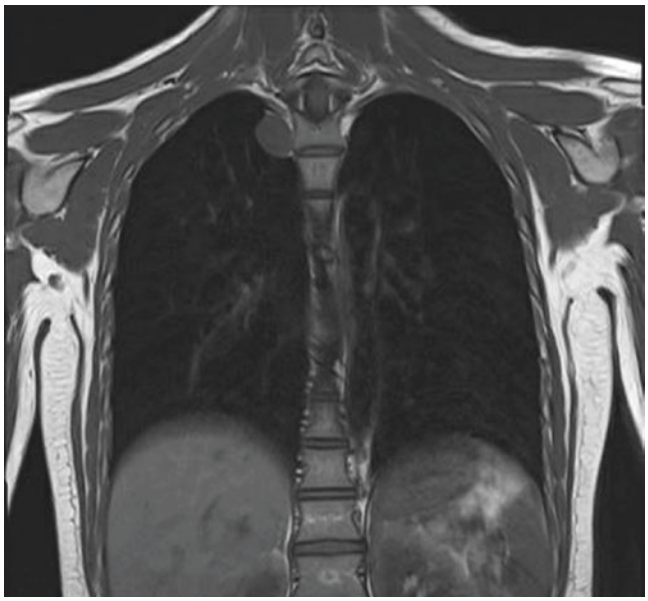

Fig. 9.10 A 15-year-old woman with right posterior mediastinal schwannoma. Coronal T1-weighted fat-saturated MRI scan shows low signal

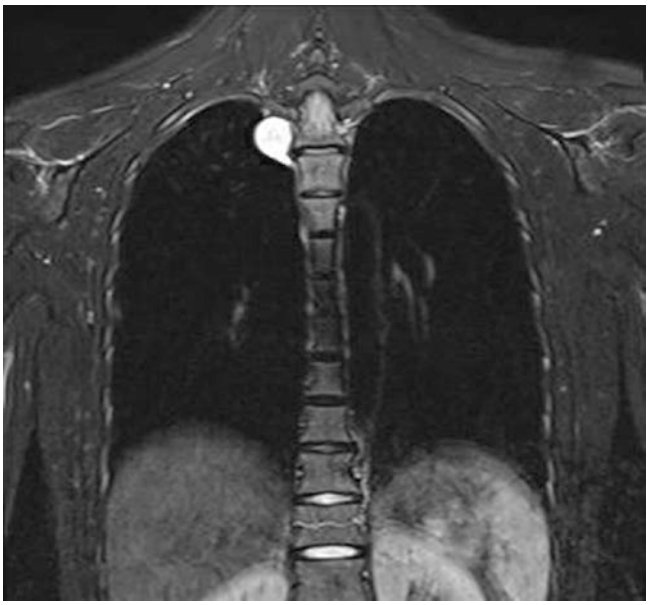

Fig. 9.12 Coronal T2-weighted fat-suppressed MRI scan shows high signal

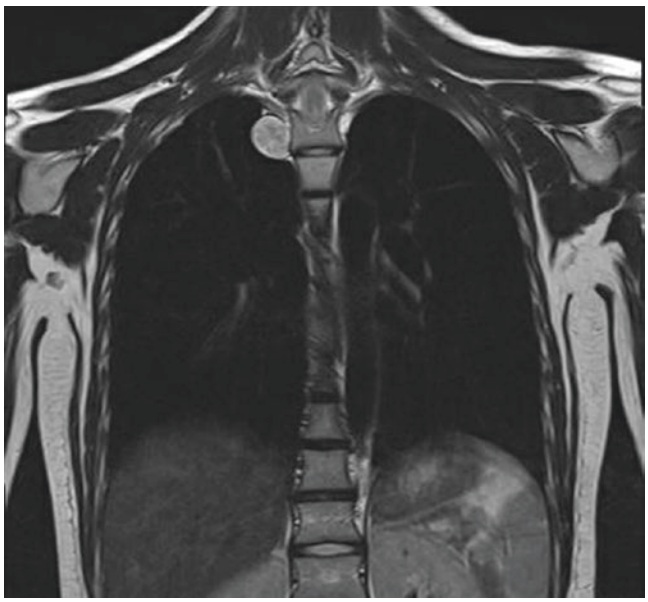

Fig. 9.11 Coronal T2-weighted fat-saturated MRI scan shows high signal

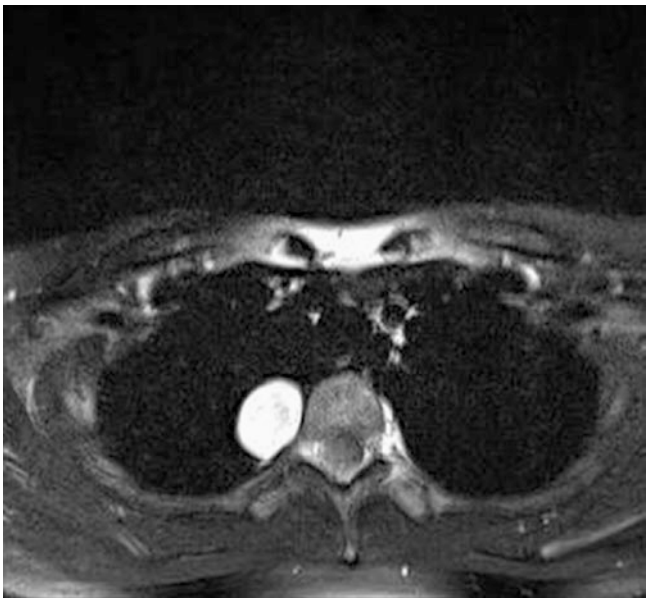

Fig. 9.13 Axial T2-weighted fat-suppressed MRI scan shows high signal

differentiation, to arrive at a prognostic classification (however, these are not staging systems). The POG system is only based on the degree of differentiation of the different histological components. Ganglioneuroma shows completely (100%) differentiated stromal and cellular components, neuroblastoma contains less than 50% differentiated elements, and ganglioneuroblastoma is intermediate (greater than 50% differentiated cells).

Grossly, ganglioneuroma may have a pseudocapsule and appear trabeculated or whorled. Microscopic features include a tumor consisting of Schwann cells, collagenous fibers, and rare vessels with isolated mature ganglion cells. There are no immature cells and no mitoses (Fig. 9.17). The ganglion cells vary in size and are mostly polygonal with abundant cytoplasm. Nissl particles can be seen, with two or more nucleoli.

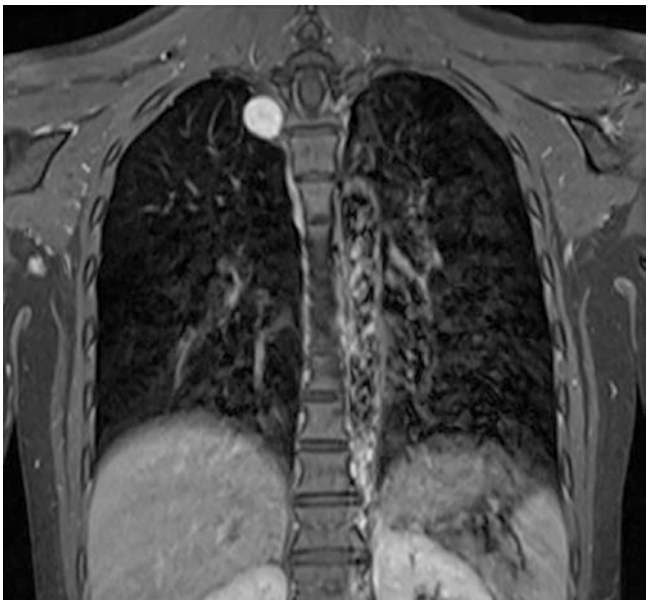

Fig. 9.14 Coronal contrast-enhanced T1-weighted fat-suppressed MRI scan shows heterogeneous enhancement

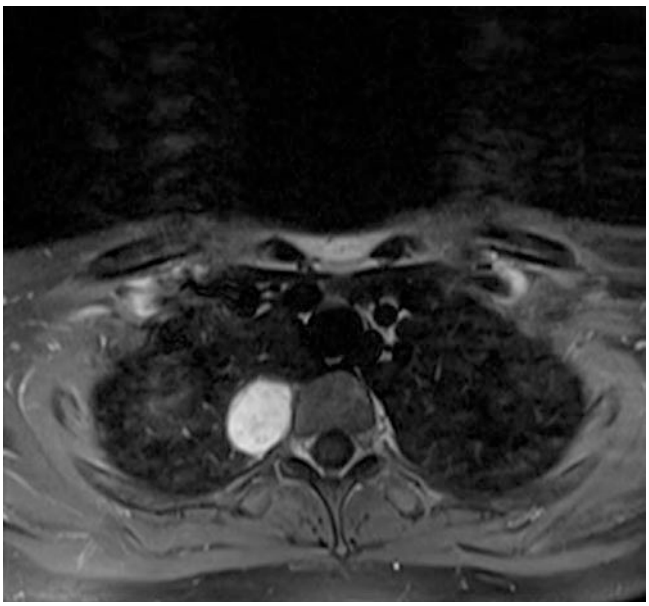

Fig. 9.15 Axial contrast-enhanced T1-weighted fat-suppressed MRI scan shows heterogeneous enhancement

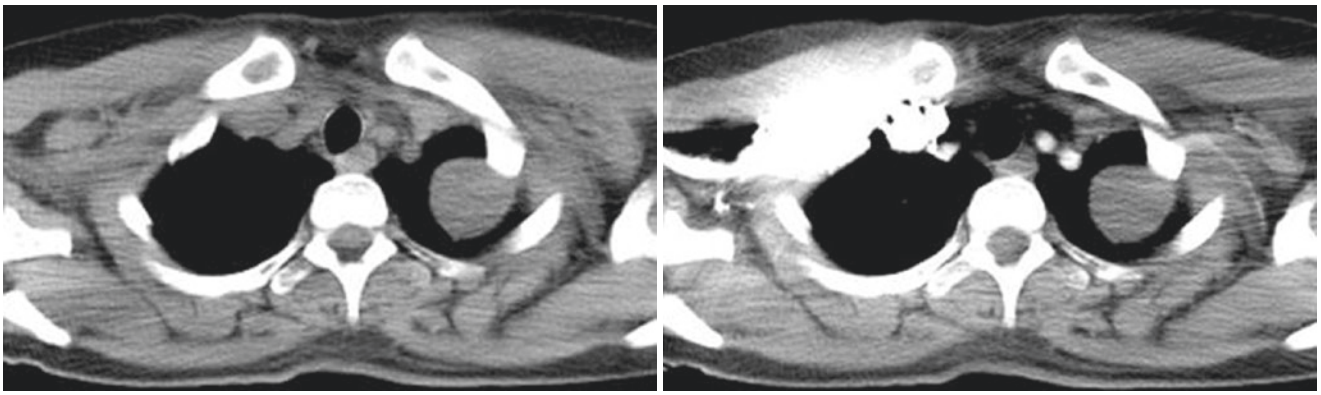

Fig. 9.16 Contrast-enhanced CT image of Neurofibromas

Ganglioneuroblastoma is a transitional stage between ganglioneuroma and neuroblastoma. It consists of neuroblasts, differently differentiated ganglion cells, proliferating Schwann cells, and glial cells. Ganglioneuroblastoma is characterized by a cellular and lobulated tumor with cordonal and pseudocarcinoid structures. Tumor cells are mainly round with pale cytoplasm and nucleated nuclei with focal atypical cells and mitotic figures.

Neuroblastoma shows tumor cells that are round and oval. They look like lymphocytes, but larger than them, with less cytoplasm, deeply stained nuclei, and mitotic figures. One characteristic feature of neuroblastoma is the formation of Homer-Wright rosettes. Rosettes are circular or ovoid columns of tumor cells arranged around a central core of neuropil. Homer-Wright rosettes are typical of Neuroblastoma, but they are not always present. There are eosinophilic nerve fiber networks around tumor cells. These fibrous substances are composed of tangled axon clumps (Fig. 9.18).

In ganglioneuroma, Schwann cells express S100. Neuroblastoma cells express neuroendocrine markers including chromogranin and synaptophysin. They are cytokeratin, HMB45, and CD99 negative.

Ganglioneuromas can occur at all ages, with 42–60% occurring in adolescents and young adults, more commonly found in children older than 10 years. They can originate from any location in the paravertebral sympathetic plexus or more rarely from the adrenal medulla. They are usually asymptomatic but can lead to compression symptoms according to tumor size and rarely to systemic symptoms. As these tumors may produce excessive catecholamines, patients may present with unstable hypertension and flushing. Unlike the case with neuroendocrine tumors, catecholamines are

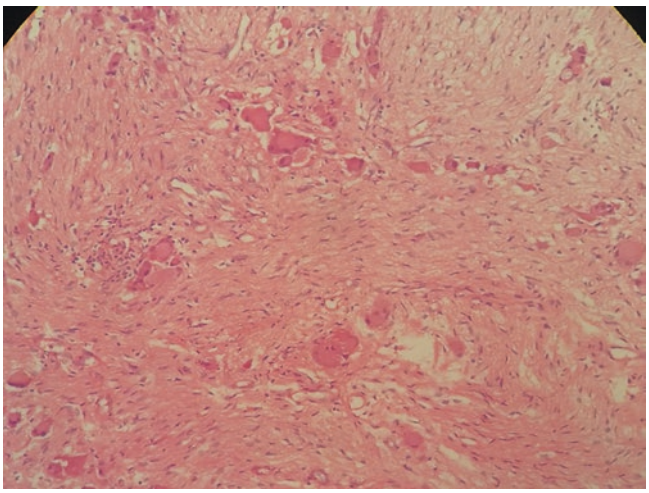

Fig. 9.17 Ganglioneuroma consists of ganglion cells, nerve sheath cells, and nerve fibers. Single or plexiform ganglion cells are found between nerve fiber

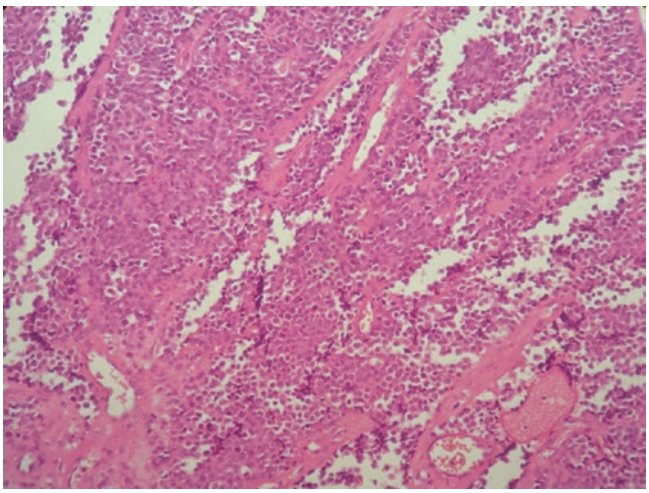

Fig. 9.18 Neuroblastoma is characterized by diffuse small round cells with hyperchromatic nuclei and numerous mitoses

metabolized in the tumor, which may be the reason for the relative lack of symptoms. Ganglioneuromas is also associated with a syndrome of chronic diarrhea, which is usually found in children and may be mediated by vasoactive intestinal peptide. As well as hypertension, this symptom resolves after removal of the tumor. Patients may also present with nonspecific chest pain or symptoms caused by compression of the tracheobronchial tree.

On CT, because ganglioneuroma originates from the neural crest cells of the sympathetic chain, thoracic ganglioneuromas are most commonly located in the posterior mediastinum (Fig. 9.19), retroperitoneum, and cervical region in decreasing order. Since the neural spinal cells will enter the cortex of the fetal adrenal gland during the embryo, there will be very few neural crest cells that differentiate into sympathetic ganglion cells, so the adrenal gland is also its prone site. Ganglioneuromas elongate and orient on a vertical axis following the direction of the sympathetic chain, thus having a craniocaudal length to major axis ratio greater than 1 (Fig. 9.20). Ganglioneuromas tend to grow embedded in the tissue gap or surround other tissues, but the lesions do not invade adjacent tissues and organs (Fig. 9.21). The tumor capsule can be shown intact or incomplete, is of equal density, and can be slightly enhanced. Pathologically, the tumor is well encapsulated, which contain different amounts of mucus-like matrix. Approximately 20% of ganglioneuromas may show calcification with a pattern that is typically fine and speckled but can be coarse in appearance (Fig. 9.22). Most calcifications are located around the lesions, which has a certain significance for qualitative diagnosis. Scattered spotty or grain-like calcification indicates benign lesions, while large patchy or irregular calcification implies malignant tendencies. Contrast-enhanced CT shows slight-to-moderate enhancement and partially delayed enhancement (Figs. 9.23 and 9.24). Owing to a large amount of mucous matrix exist in ganglioneuroma, cell components are enhanced, while mucous matrix is non-enhanced. Delayed enhancement is mainly due to blocked perfusion of contrast agent by mucus. Fatty components may appear in some ganglioneuromas (Fig. 9.25).

On MRI, ganglioneuromas were reported to be homogeneously hypointense on T1WI and heterogeneously hyperintense on T2WI. According to reports, the comparison of the signal intensity on T2WI with pathologic findings shows a good correlation. A large amount of myxoid stroma with relatively low cellularity and few collagen fibers demonstrated markedly high signal intensity, whereas the abundant cellularity and collagen fibers with relatively scarce myxoid stroma in the tumor showed intermediate to high intensity. Thus, the signal intensity on T2WI is highly influenced by the proportion of myxoid stroma, cellular components, and collagen fibers.

9.5 Neuroblastoma

Neuroblastoma is an embryonal origin tumor of the sympathetic nervous system, arising from either primitive sympathetic neural cells in the adrenal medulla or the paraspinal sympathetic ganglia. During embryonic development, neural crest cells continuously differentiate into neuroblasts, which then further differentiate into mature ganglion cells. Neuroblastoma is subtyped as undifferentiated, poorly differentiated, and differentiating types based on morphology and the mitotic-karyorrhectic index (MKI) by the International Neuroblastoma Pathology Classification (INPC). Differentiation of the neuroblastic cells indicates that they display some characteristics of mature cells (dif-

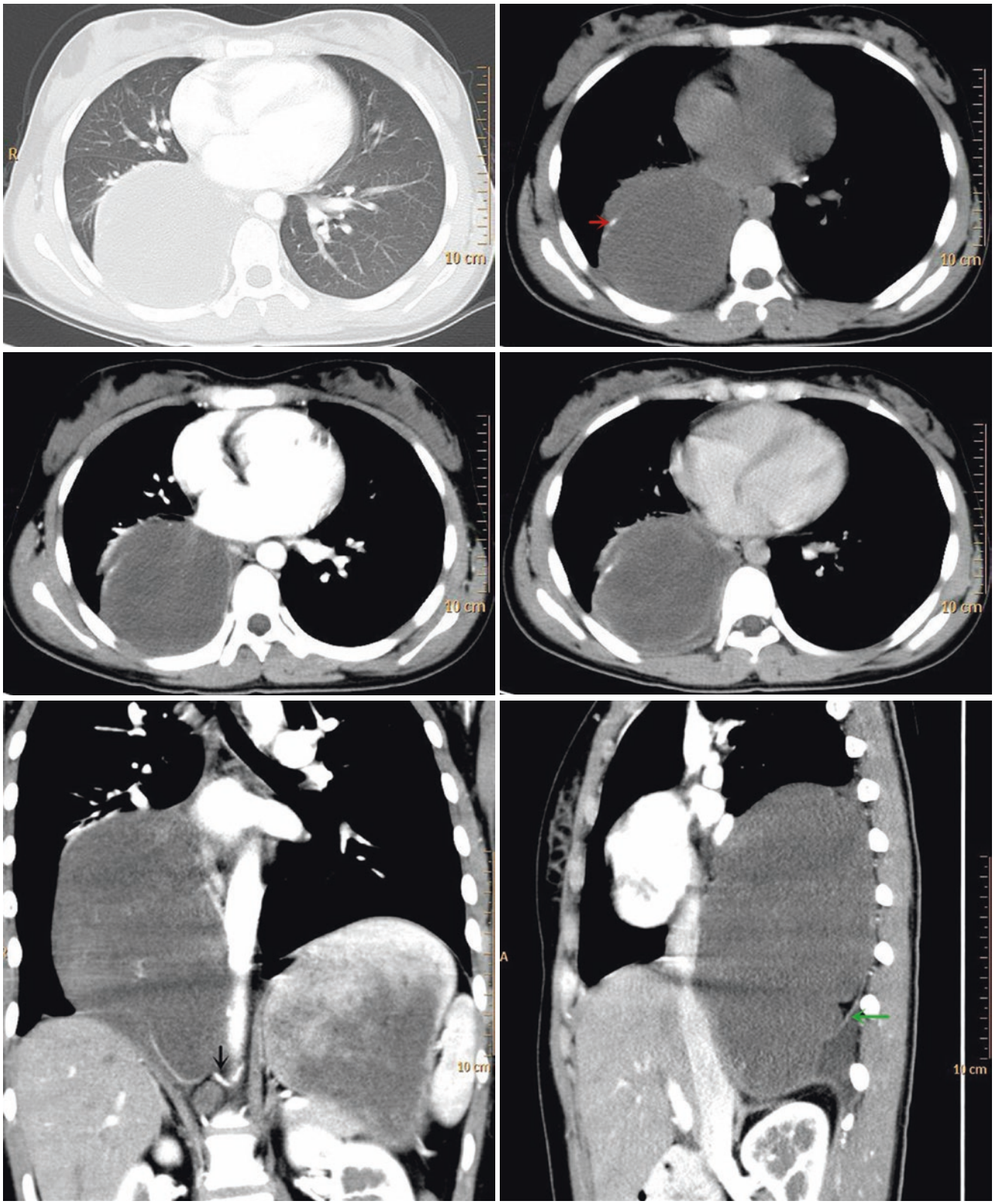

Fig. 9.19 A 14-year-old girl with ganglioneuroma. Chest CT showed an oval mass in the right paravertebral region, with calcification (red arrows) and complete capsule (green arrows). The mass was supplied by the descending aorta (black arrow), grows along the spine, and the diaphragm moved downward under pressure. The tail-like extension represents an extension of neoplasm to the adjacent extrapleural fat tissue

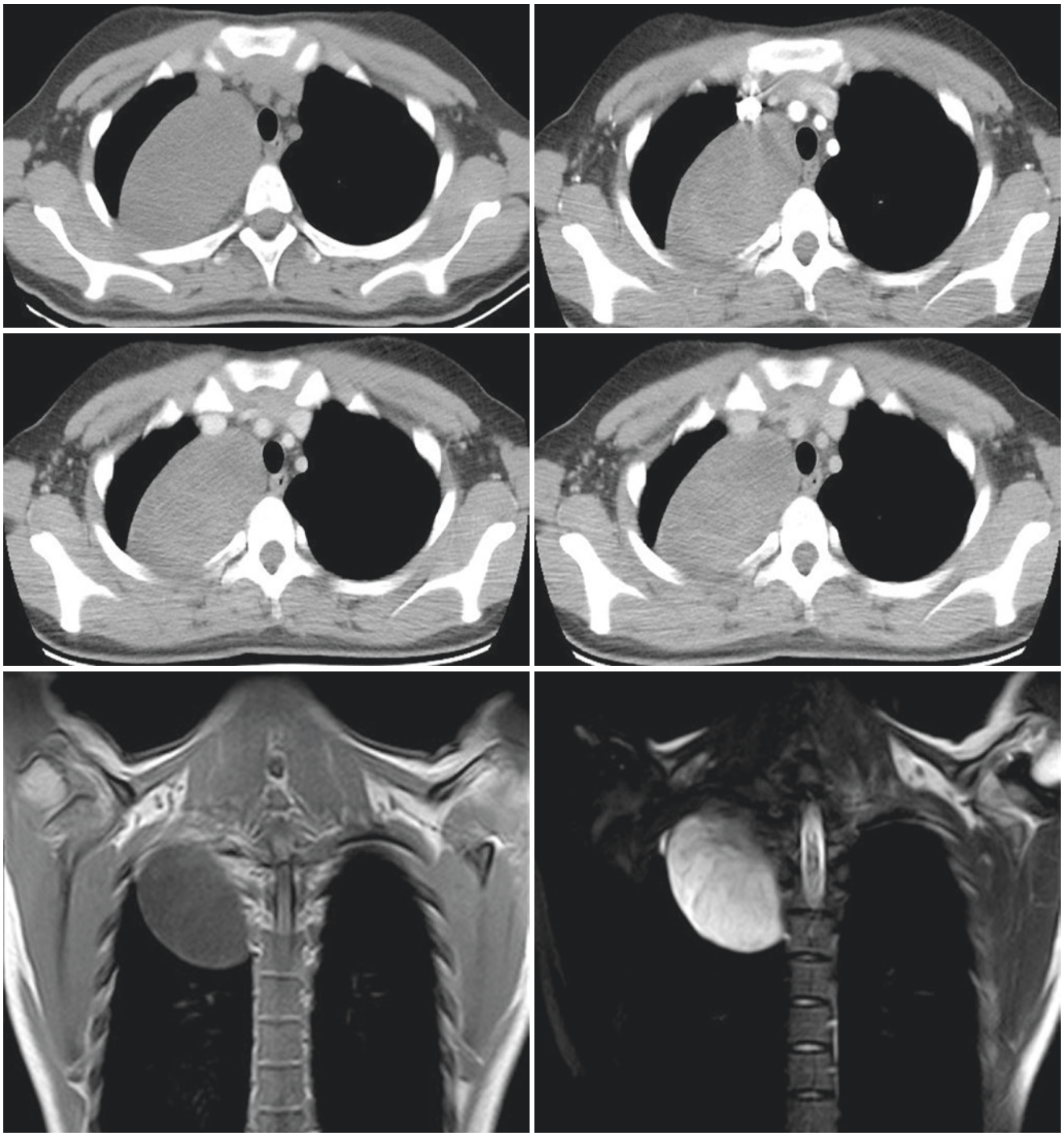

Fig. 9.20 A 14-year-old girl with ganglioneuroma. Chest CT showed well-demarcated soft tissue mass in the right posterior superior mediastinum, with mild enhancement and delayed enhancement. MRI showed that T1WI was low signal, with a little linear high signal on the inside, and T2WI was mainly high signal, with a little low signal. The linear high signal on the medial side of the lesion was connected to the parathoracic sympathetic trunk, suggesting that the lesion originated from the sympathetic nerve chain of the posterior mediastinum

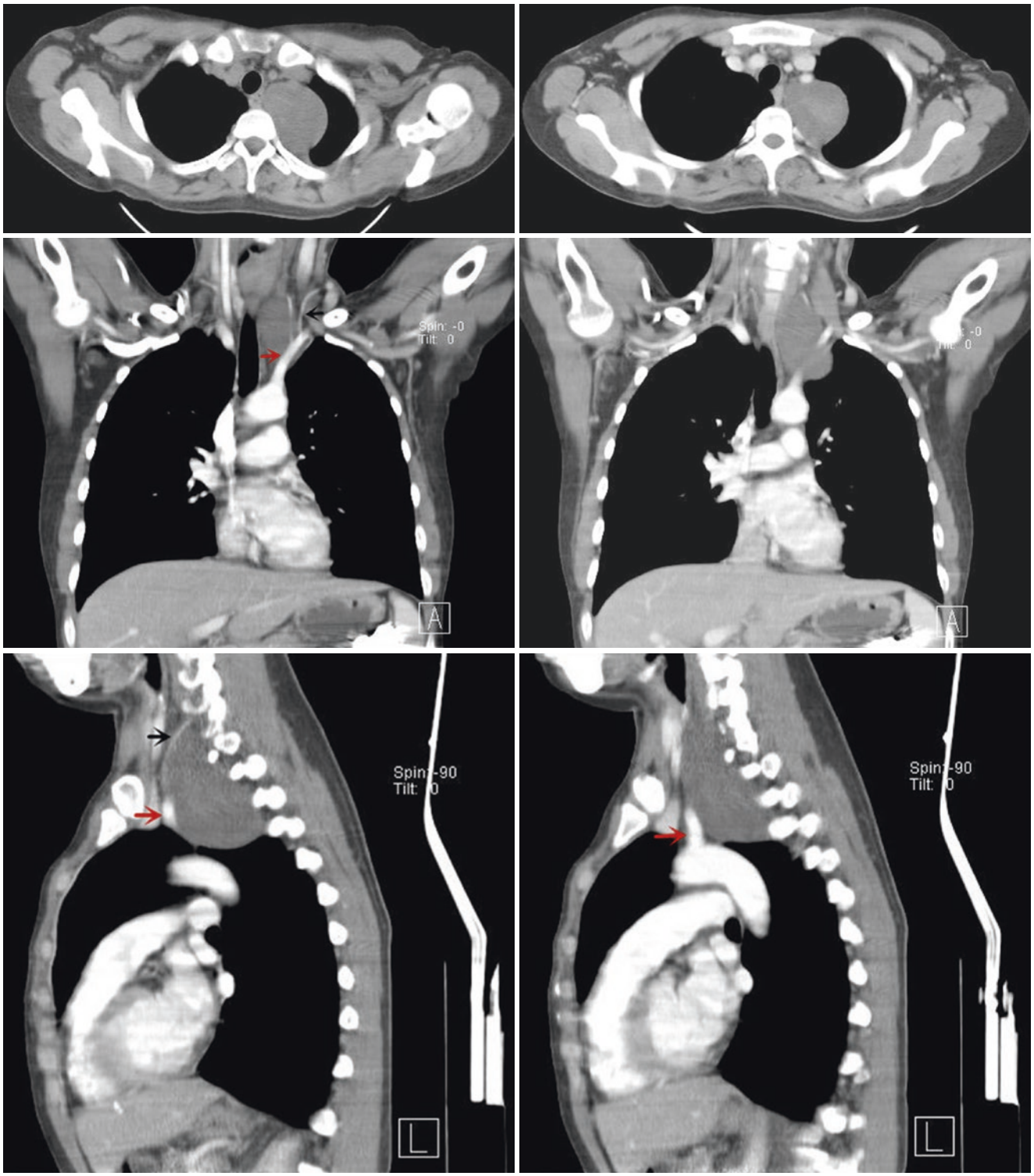

Fig. 9.21 A 30-year-old woman with mediastinal ganglioneuroma, which surrounded the left subclavian artery (red arrow). The left subclavian artery sent out two small blood vessels that run through the tumor surface (black arrow, vascular floating sign)

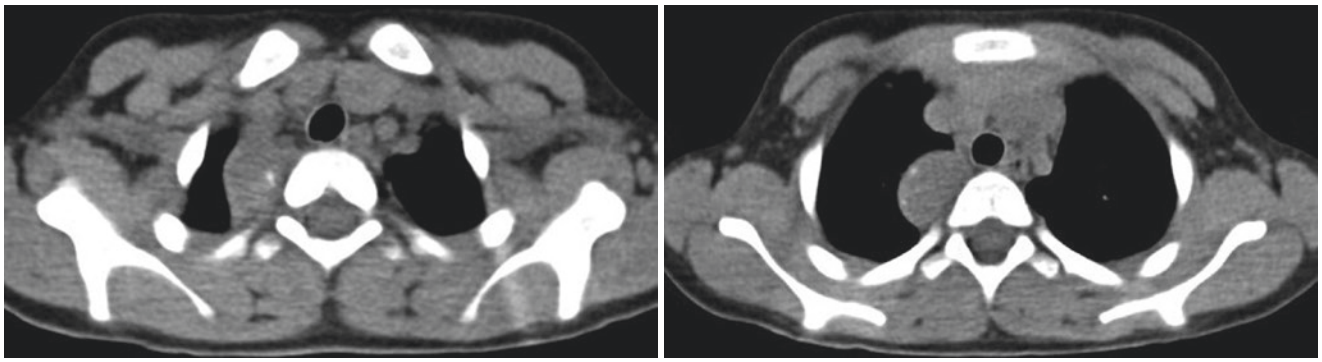

Fig. 9.22 A 8-year-old girl with paraspinal soft tissue mass of the right posterior superior mediastinum, multiple spotted calcifications can be seen at the edge of the mass

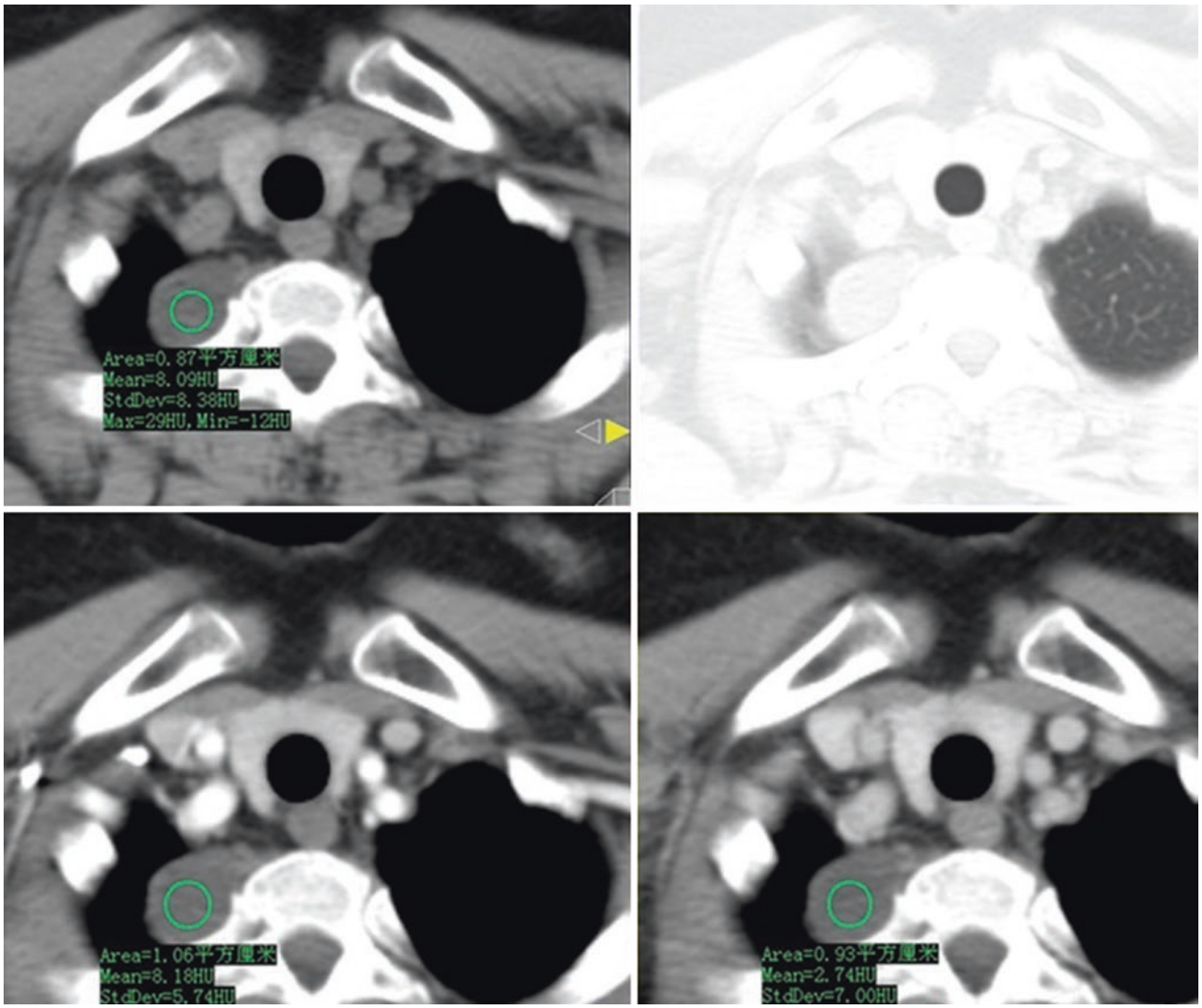

Fig. 9.23 A 56-year-old woman with ganglioneuroma in the right posterior superior mediastinum, with homogenous low density that did not show marked enhancement

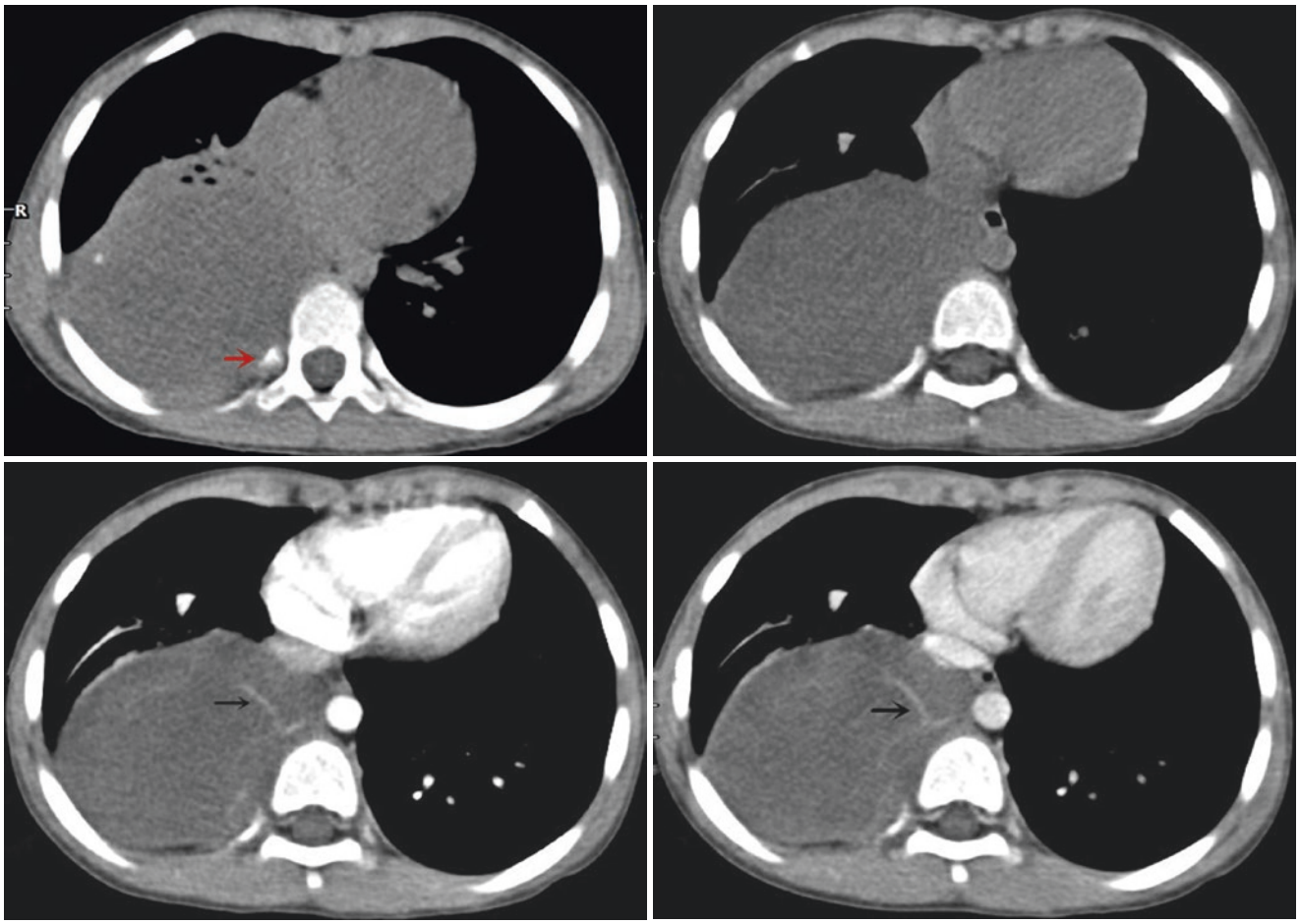

Fig. 9.24 A 6-year-old girl with round right paraspinal soft tissue mass, with spotty and massive calcifications (red arrow). The contrast-enhanced scan showed a slight progressive enhancement with visible vascular shadows (black arrows)

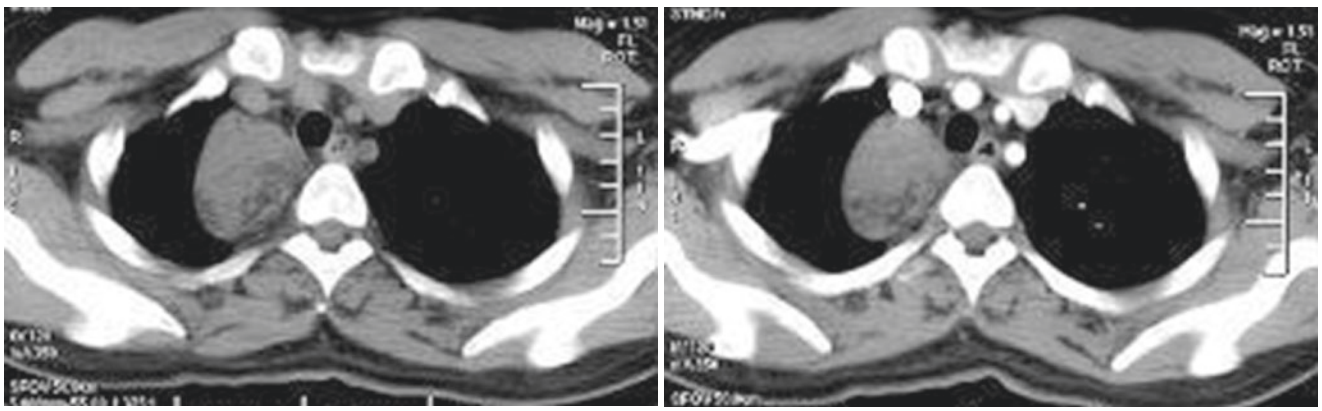

Fig. 9.25 A 46-year-old woman with ganglioneuroma. The enhancement was not obvious, and fat attenuation was visible in the tumor

ferentiating cells show nuclear enlargement, nucleoli, cytoplasmic eosinophilia and enlargement, clear cytoplasmic border, and cell processes).

Neuroblastoma is the most common extracranial solid tumor in childhood and displays a broad spectrum of clinical behavior. The median age at diagnosis is 22 months, and more than 95% of cases are diagnosed by 10 years. Although rare, there are documented cases of familial neuroblastoma. The most common sites of origin of neuroblastoma are the adrenal medulla (40%), extraadrenal retroperitoneum (30%),

and posterior mediastinum (20%). The neck (1–5%) and pelvis (2–3%) are less common sites. Unusual locations such as anterior mediastinum, thymus, lung, stomach, kidney, and cauda equina have also been described.

Primary mediastinal neuroblastoma accounts for 14% of all neuroblastomas. The common location is posterior mediastinum. Grossly, neuroblastoma does not have a capsule, and necrosis, hemorrhage, and calcification are common. Calcification is a characteristic of infantile neuroblastoma. Approximately 50% of thoracic neuroblastomas will have coarse, finely stippled, or curvilinear calcifications on CT (Fig. 9.26). The appearance can range from a homogeneous solid to a predominantly cystic or hemorrhagic mass that shows either heterogeneous or little enhancement (Fig. 9.27). MRI shows homogeneous or heterogeneous signal intensity on all sequences. MRI signals depend on whether there is bleeding, necrosis, cystic changes, and calcification in the tumor or not. High signal intensity may be seen from hemorrhage on T1-weighted images and from cystic change on T2-weighted images.

Neuroblastoma has a high degree of malignancy and is prone to early multi-site metastasis. Bone marrow (70.5%), bone (55.7%), lymph nodes (30.9%), and liver (29.6%) are common metastasis sites of neuroblastoma. Patients with tumors of abdominal origin were more likely to develop bone marrow metastasis. The bone was the second most common metastatic site in patients with neuroblastoma, and its detection may be important for tumor staging and risk stratification, as it is for other metastatic diseases.

Treatment of neuroblastoma is based on tumor stage and biological characteristics, and is mainly risk oriented. Low-risk patients with localized tumors obtain excellent results with resection alone, whereas higher-risk patients with distant disease require chemotherapy or radiotherapy combining with surgery. The goal of surgery should be to achieve the preservation of anatomy as much as the resection of tumor. The outcome is poor in high-risk cases, although rarely, spontaneous regression or differentiation has been reported. Clinically, primary thoracic neuroblastoma portends a better prognosis than neuroblastomas in other sites.

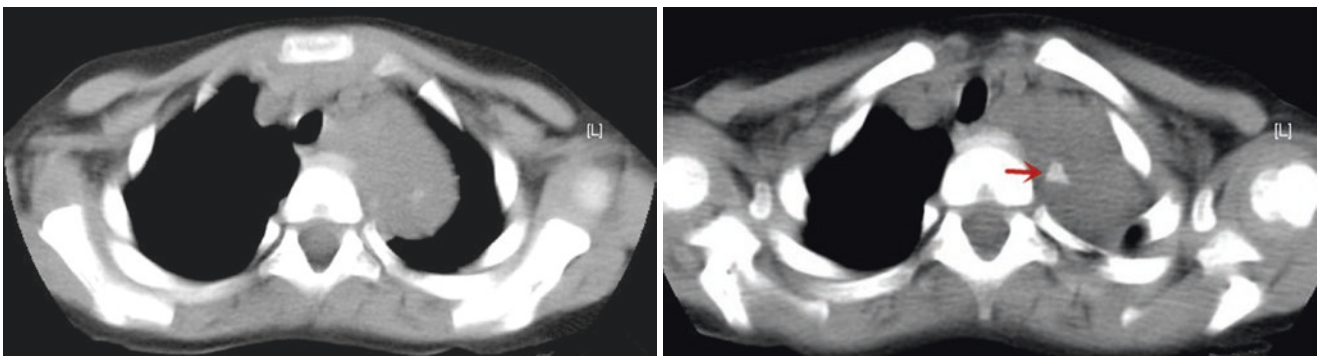

Fig. 9.26 A 3-year-old boy complained of fever and cough. Chest CT showed a soft tissue mass of the left posterior superior mediastinum with coarse calcification (red arrow)

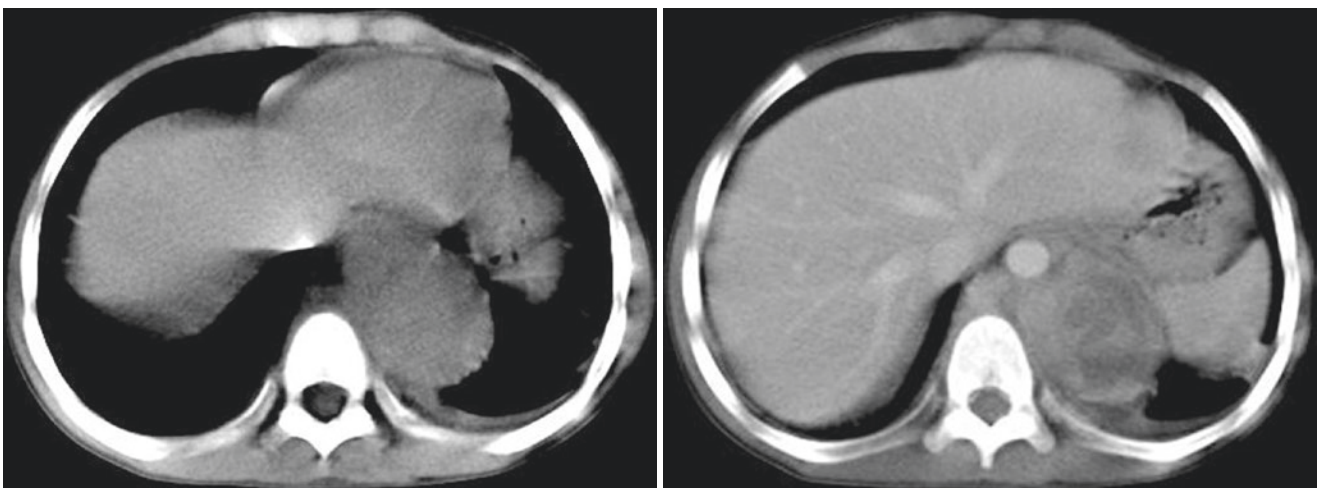

Fig. 9.27 A 13-year-old boy complained of chest and back pain for several years. Chest CT showed heterogeneous soft tissue mass in the left posterior mediastinum with mild enhancement

Screening infant urine samples can detect tumor-derived catecholamine, but this approach has nothing to do with reducing mortality, so it has not been widely used.

9.6 Paraganglioma

Pheochromocytoma and paraganglioma are rare neuroendocrine tumors, which produce catecholamines and arise from adrenal medulla chromaffin cells or from neural crest cells outside the adrenal gland. In 80% of cases, these tumors occur in the adrenal medulla and in the remaining 20% tumors appear outside the adrenal glands in the prevertebral and paravertebral sympathetic ganglia located mainly in the chest abdomen and pelvis. According to the latest WHO definitions, the term pheochromocytoma is used for tumors arising from the adrenal gland while tumors that arise outside the adrenal gland are called paraganglioma.

With only about 150 cases reported in the literature, paragangliomas occurring in mediastinum are extremely rare, accounting for only 1–2% of all paragangliomas and less than 0.3% of all mediastinal tumors. They may occur at any age, although most arise in the group of 40–50. Paraganglioma is associated with the sympathetic chain present in slightly younger patients. Vagal paraganglioma has a female predominance. According to its ability to synthesize and release catecholamines, paragangliomas are classified as either functional or nonfunctional. Most of the mediastinal paragangliomas are nonfunctional, asymptomatic, and usually found incidentally. Nonfunctional paragangliomas are usually postoperatively diagnosed and they have mediastinal, pulmonary, or endobronchial origin. They can produce a mass effect such as dysphagia, angina, or dyspnoea, due to the compression of adjacent structures. Functional mediastinal paragangliomas are rare, and most of them originate in the posterior mediastinum. Functional paragangliomas present with paroxysmal hypertension, palpitation, sweating, and headache due to increased catecholamines.

Paragangliomas have a characteristic microscopic pattern of anastomosing cords of tumor cells arranged in a trabecular pattern or a nesting pattern separated by a rich microvasculature. However, these patterns may appear in carcinoid tumors and immunohistochemical studies are needed to make a definitive diagnosis. Paragangliomas typically consist of two histologic cell types; chief cells and sustentacular cells. The chief cells have a characteristic "zellballen" pattern, with compact cell nests (Fig. 9.28). Cytoplasm can be transparent or eosinophilic, with little mitosis. Chief cells are surrounded by sustentacular cells, which are positive for the S100 protein. Paragangliomas are typically positive stain for chromogranin, synaptophysin, and neuron-specific enolase (Fig. 9.29). Paragangliomas are negative for cytokeratins and epithelial membrane antigens, an important differentiating

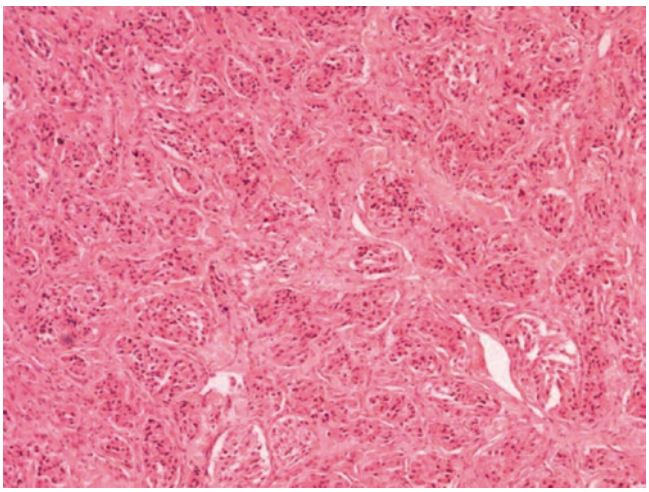

Fig. 9.28 The tumor comprised cells arranged in nests ("Zellballen") with vascular stroma

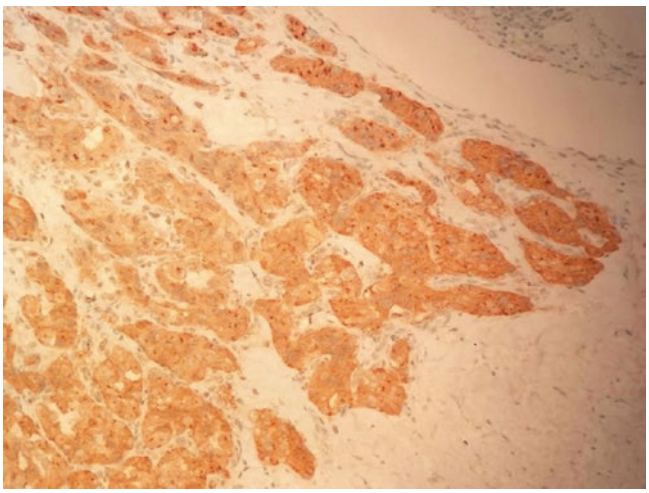

Fig. 9.29 Immunohistochemically, the chromogranin was positive

factor from carcinoid tumors. Ultrastructurally, paragangliomas contain numerous dense neurosecretory granules. They display marked variation in shape and size, differentiating them from carcinoids that demonstrate smaller and more consistent granules. However, a lack of dense-core granules is shown in the surrounding sustentacular cells. Angiosarcomas should be considered because of the similarity in the striking vascular pattern seen in paragangliomas. Angiosarcomas can be distinguished immunohistochemically from paragangliomas by staining for vascular markers CD31 and CD34, both of which are negative in paragangliomas.

Paragangliomas can be located in any of the three mediastinal compartments: chemoreceptor tissue along the paravertebral area or around the aortic arch, vagus nerves, and sympathetic nerves within the middle and superior mediastinum and within the anterior mediastinum from the pericardium of the heart, within the interatrial septum, or within the

left atrial wall. Thoracic paragangliomas tend to be quite vascular, and their malignancy rate is higher than that of primary paragangliomas in other locations.

CT and MRI of thoracic paragangliomas show a soft-tissue mass with marked enhancement due to increased vascularity (Fig. 9.30). Some tumors may have extensive hemorrhage or cystic degeneration, which results in areas of low attenuation on CT (Fig. 9.31). The signal intensity on MRI in a large mass may be heterogeneous due to hemorrhage or necrosis. The MRI feature of paragangliomas is the presence of multiple curvilinear and punctate signal voids, which reflect high-velocity flow in the intratumoral vessels. The adjacent high- and low-signal-intensity areas in the tumor on T2-weighted images have been described as having a "salt-and-pepper" appearance. Representing high-signal-intensity regions the salt component is owing to slow flow within tumor vessels or hemorrhage, and the pepper component corresponds to high flow within tumor vessels. However, this finding is not specific to paraganglioma and may be seen in other hypervascular tumor.

Paraganglioma is mostly a benign clinical process, and about 10% is malignant. It can invade the capsule and blood

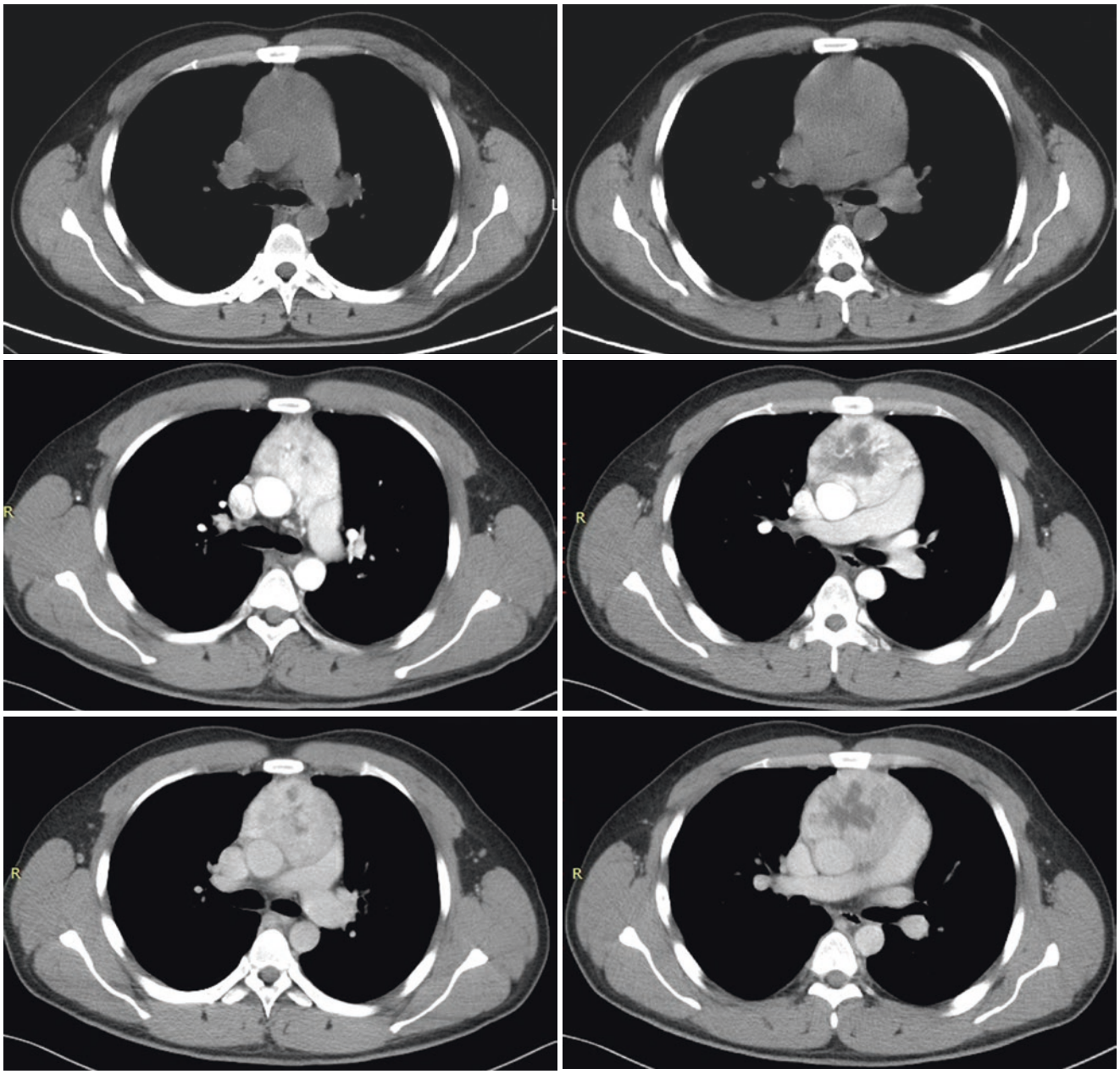

Fig. 9.30 A 29-year-old man with anterior mediastinal paraganglioma showed obvious enhancement in the arterial phase and the enhancement amplitude in the venous phase, which was consistent with that of large vessels

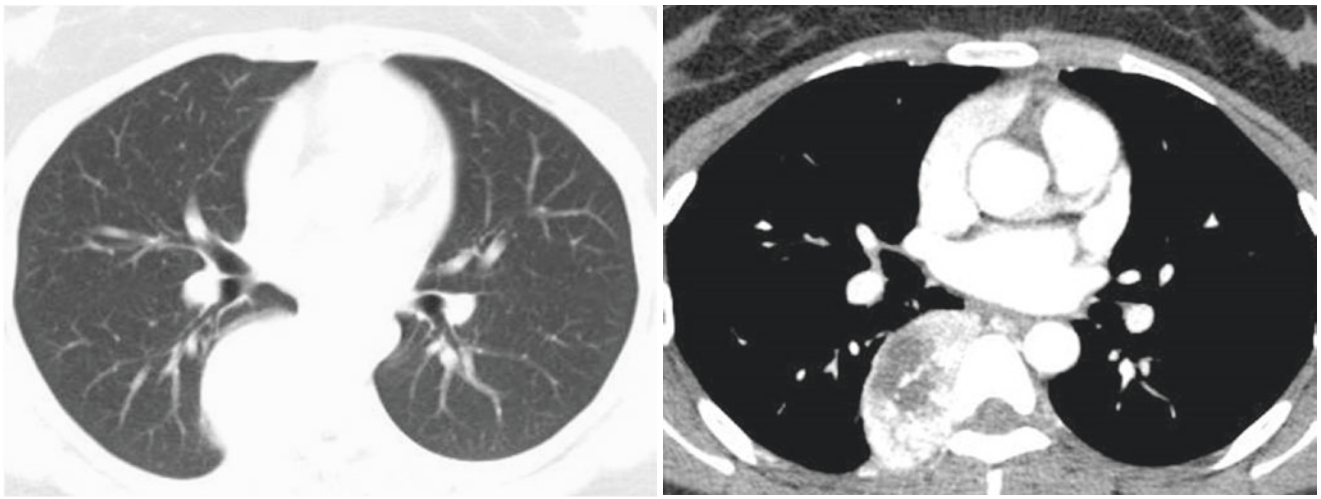

Fig. 9.31 A 23-year-old woman with right posterior mediastinal paraganglioma, with obvious enhancement and low-density areas without enhancement

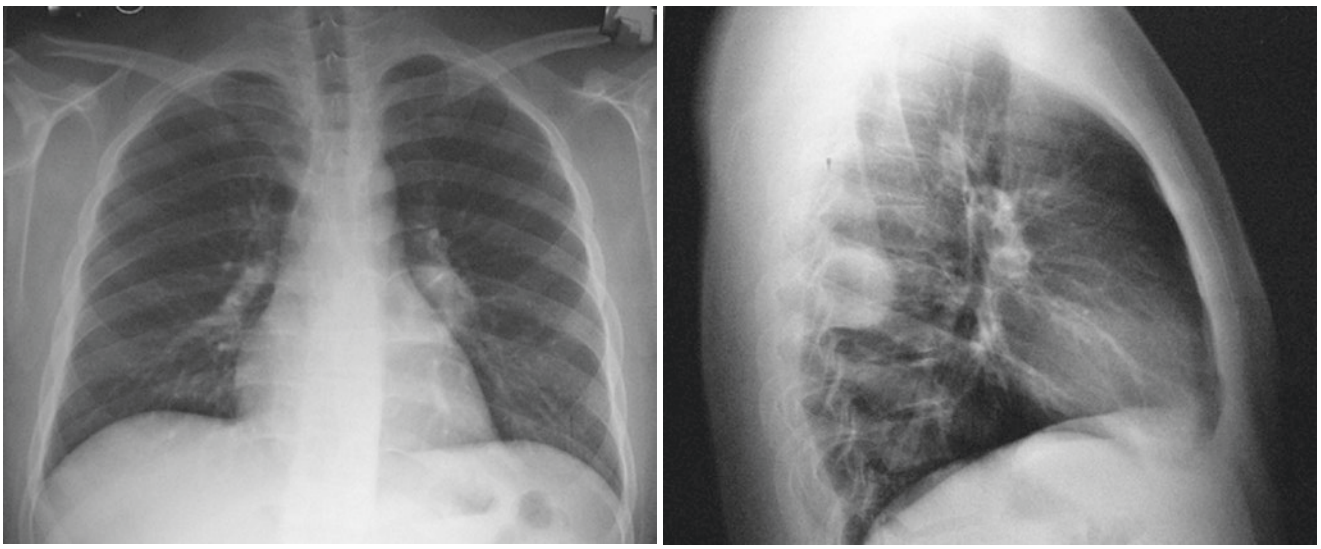

Fig. 9.32 X-ray of a 21-year-old man found a posterior mediastinal mass for 10 days

vessels, and can metastasize to lymph nodes, lungs, bones, and other organs. It is difficult to distinguish benign tumors from malignant ones histologically. Metastasis is the only exact malignant criterion.

9.7 Case Analysis

9.7.1 Case 1

A 21-year-old man found a posterior mediastinal mass for 10 days.

Radiograph: The circular mass of the left posterior mediastinum, with smooth edges and a size of 4 cm × 4 cm (Fig. 9.32).

Chest CT: A dumbbell-shaped soft tissue mass projected from the spinal canal, protruding into the chest cavity, and the left T7-8 intervertebral foramen enlarged (Fig. 9.33).

MRI: Abnormal signal lesions in the left posterior mediastinum spinal canal, which pressed the spine, after injection of GD-DTPA, the lesions were obviously heterogeneous enhancement (Fig. 9.34).

[**Diagnosis**] Schwannoma

[**Diagnosis basis**] The posterior mediastinal dumbbell-shaped mass is closely related to the spinal canal and is consistent with the performance of schwannomas. Intraoperatively, the tumor measured 4.5 × 3.5 × 2.5 cm located in the subdural space, and the intervertebral foramen enlarged significantly. The tumor was completely

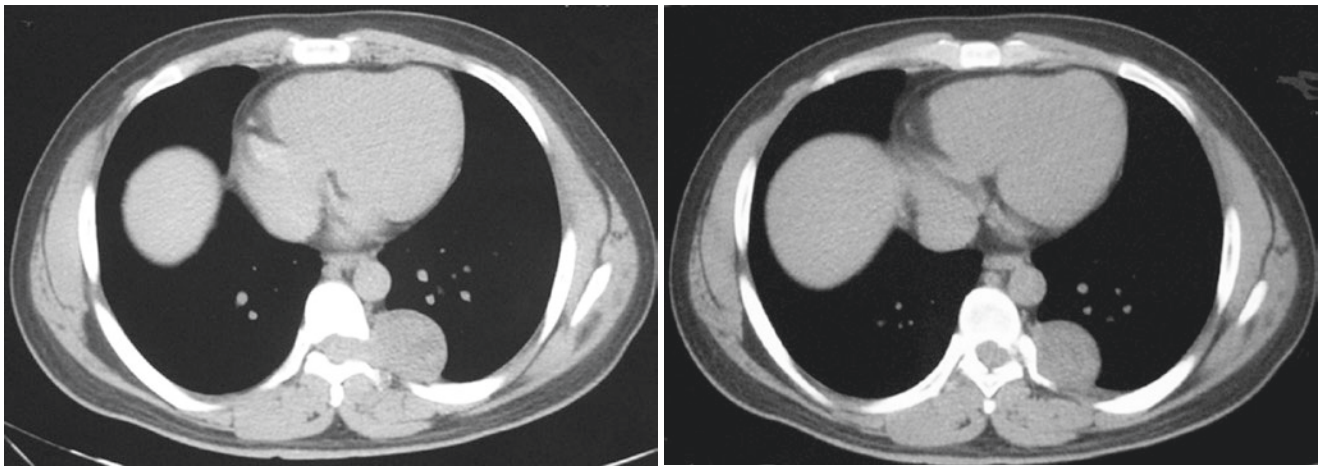

Fig. 9.33 Chest CT images of a 21-year-old man found a posterior mediastinal mass for 10 days

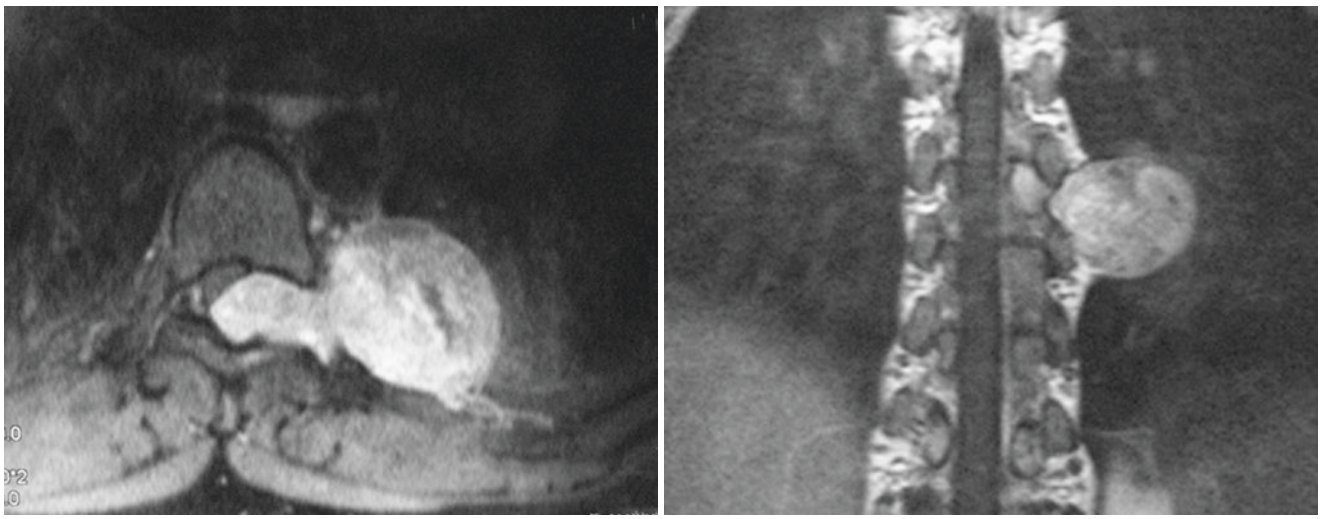

Fig. 9.34 MRI of a 21-year-old man found a posterior mediastinal mass for 10 days

resected. Pathology showed schwannomas with bleeding and cystic changes.

[Analysis] The tumor showed an intraspinal extension, the so-called dumbbell type. Mediastinal dumbbell tumors are rare and most are benign. The differential diagnoses of posterior mediastinal dumbbell-shaped tumors include neurogenic tumors (schwannomas, neurofibromas), hemangiomas, and meningiomas. Few cavernous and capillary hemangiomas also present as dumbbell-shaped lesions. A total of 19 tumors from the period 1989–1994 was retrospectively evaluated by Isoda et al. [1] that exhibited dumbbell configuration. Eleven benign tumors, 9 neurogenic tumors, and 8 malignant tumors are included. A statistically significant difference was noticed in the short/long axis ratios (minimum tumor diameter divided by maximum tumor diameter) in the vertebral canal components between benign and malignant tumors. All malignant tumors in this study were found to be extradural and paraspinal type. Most benign tumors had regular margins and enlarged intervertebral foramina, while most malignant tumors had irregular margins. Many neurogenic tumors had cystic lesions (77.8%) and a string-of-beads structure (44.4%). Abnormal signal intensities were found in those tumors that surrounded the thecal sac in the vertebral canal and whose adjacent vertebral bodies, showing infiltrating and malignant. MRI is useful in diagnosing dumbbell-shaped spinal tumors, especially those of neurogenic origin, and aids in distinguishing benign from malignant tumors.

Dumbbell-shaped posterior mediastinal neurogenic tumors are mostly schwannomas and neurofibromas, which develop from the intervertebral foramen and grow bidirectionally along the affected nerve, including a larger posterior mediastinal tumor and a smaller inner part of the spinal canal. Symptoms debut with medullary or spinal compres-

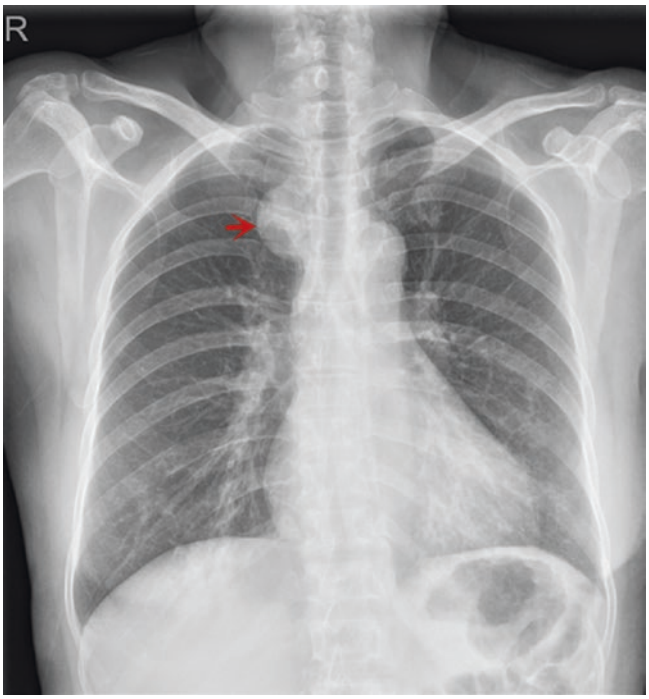

Fig. 9.35 X-ray of a 61-year-old woman complained of cough and sputum for 1 week

sion. Mediastinal dumbbell-type neurogenic tumors are usually encapsulated, without obvious invasion, and surgical procedures can be formulated according to specific circumstances.

9.7.2 Case 2

A 61-year-old woman complained of cough and sputum for 1 week.

Radiograph: Right posterior mediastinal hemispherical smoothly marginated mass (Fig. 9.35).

Chest CT: A spherical soft tissue mass in the right posterior mediastinum with heterogeneous enhancement, low-density areas could be seen at the edges, and bone windows showed no damage to the bone (Fig. 9.36).

MRI: T1-weighted fat-saturated MRI scan showed equal signal of the mass. Mass had a thin low-signal-intensity rim (red arrow) in periphery (Fig. 9.37). T1-weighted equal signal areas were slightly high signal (white arrow) in the T2-weighted fat-saturated MRI scan, T1-weighted low-signal areas were high-signal (green arrow) in T2-weighted MRI scan, the overall signal was heterogeneous (Fig. 9.38). Contrast-enhanced T1-weighted fat-suppressed MRI scan showed that the solid area was obviously heterogeneous enhancement (white arrow), the low signal area was not obvious enhancement (green arrow), and the edge of the mass could also be seen to be evenly enhancement (yellow arrow) (Fig. 9.39).

[**Diagnosis**] Schwannoma

[**Diagnosis basis**] A right posterior superior mediastinum spherical soft tissue mass with clear border, contrast-enhanced scan showed mild enhancement (Fig. 9.36b) and delayed enhancement (Fig. 9.36c), low-density areas (blue arrows) were visible at the edge (blue arrow). Bone windows showed no bone destruction areas around the mass (Fig. 9.36d). MRI revealed a mixed-signal intensity lesion in the right paraspinal region of the posterior mediastinum. Combining Radiograph, CT, and MRI manifestations, schwannoma is the first diagnosis. The patient underwent right-sided video-assisted thoracoscopic surgery (VATS). Grossly, the mass had a complete envelope and was completely excised. Histologically, the tumor contained spindle cells with strong positivity for S100 protein and was diagnosed as schwannoma.

[**Analysis**] Schwannoma, also called neurilemmoma, perineural fibroblastoma, Schwann cell tumor and lemmoma, is a benign nerve sheath tumor derived from Schwann cells. Initially described as "neurinoma" by Verocay in 1910, this entity is subject to frequent misdiagnosis clinically. Microscopically, schwannoma is made up of spindle cells that give rise to dense cellular areas (Antoni A) and hypocellular areas (Antoni B). The cystic appearance is the result of necrosis, mucinous degeneration, hemorrhage, and microcysts formation. MRI is the technique of choice for evaluating peripheral nerve tumors in the paraspinal region. The multiplanar capability and high-contrast resolution of MRI can accurately determine the location and extent of intrathoracic neurogenic tumors, especially intracanalicular and intraspinal extension in paraspinal regions. The solid part of the schwannoma shows mostly equal signal on T1-weighted images (T1WI), and shows equal signal or slightly high signal onT2-weighted images (T2WI). In the necrotic cystic area, the T1WI signal is low and the T2WI signal is high due to more water contents. If subacute hemorrhage is combined, both T1WI and T2WI show high signal changes. The T2WI sequence of schwannoma is conducive to the display of tumor pathological changes and tissue characteristics. The specific manifestations are the low signal on the center of T2WI and the high signal on the periphery, so-called target sign, which has been described to be 100% specific for as schwannoma. The appearance of this sign is related to a large number of closely arranged tumor cell components in the center of the lesion, and the surrounding structure is loose mucus-like tissue. This case is fully consistent with this sign.

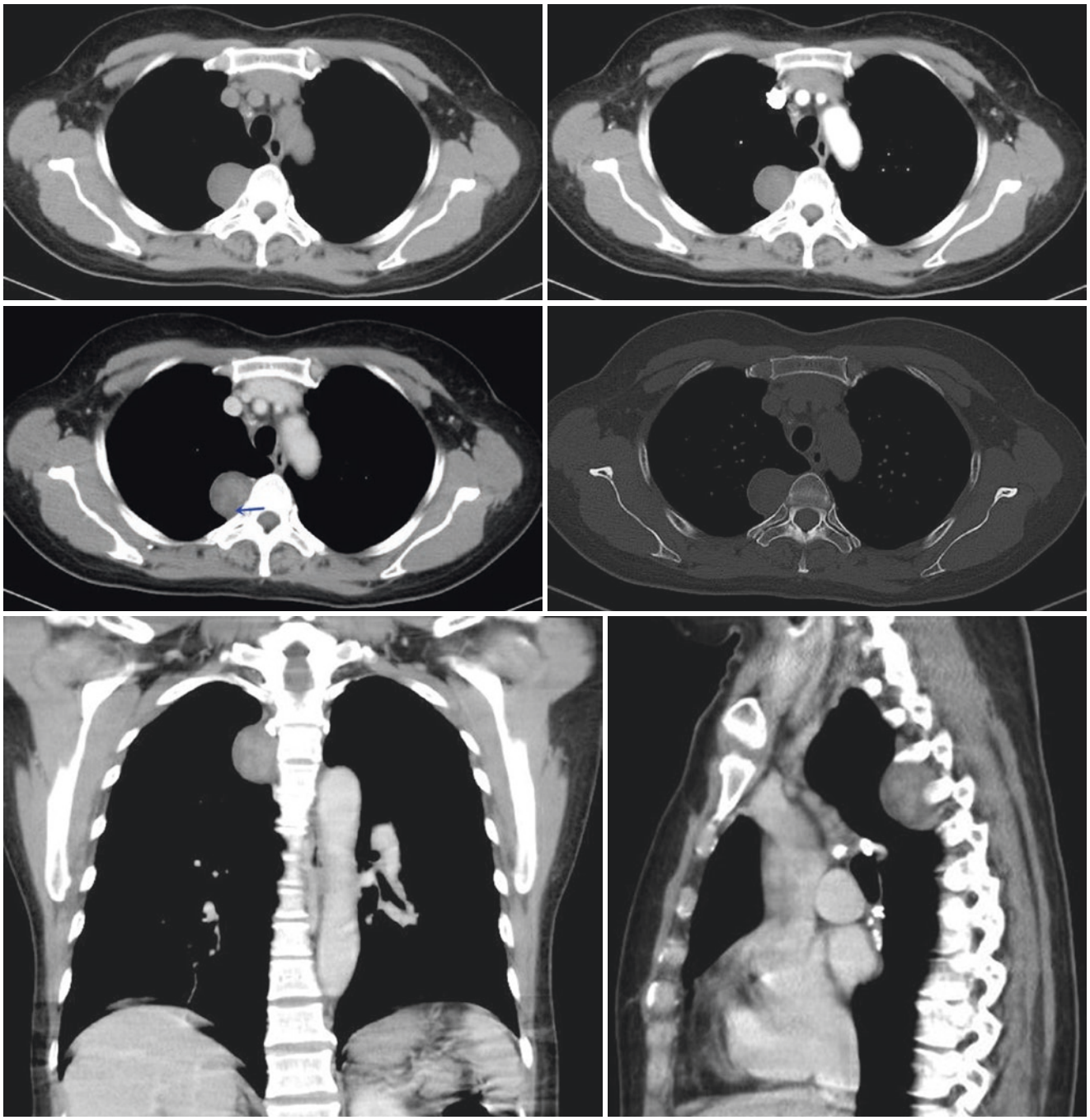

Fig. 9.36 Chest CT images of a 61-year-old woman complained of cough and sputum for 1 week

9.7.3 Case 3

A 39-year-old man complained of chest tightness for 1 month.

Chest CT: A spherical soft tissue mass next to the left spine with necrotic or cystic components. The solid part of the mass was enhanced (Fig. 9.40).

[**Diagnosis**] Schwannoma

[**Diagnosis basis**] A huge mass located in the left posterior mediastinum with complete envelope (white arrow), the lesion presses adjacent rib showing compression destruction and hyperplasia (red arrow). Contrast-enhanced CT image shows heterogeneous enhancement. An extensive unenhanced area with a reticular septum is seen within the mass. The above characteristics are consistent with schwannoma. Intraoperatively, the mass had a complete

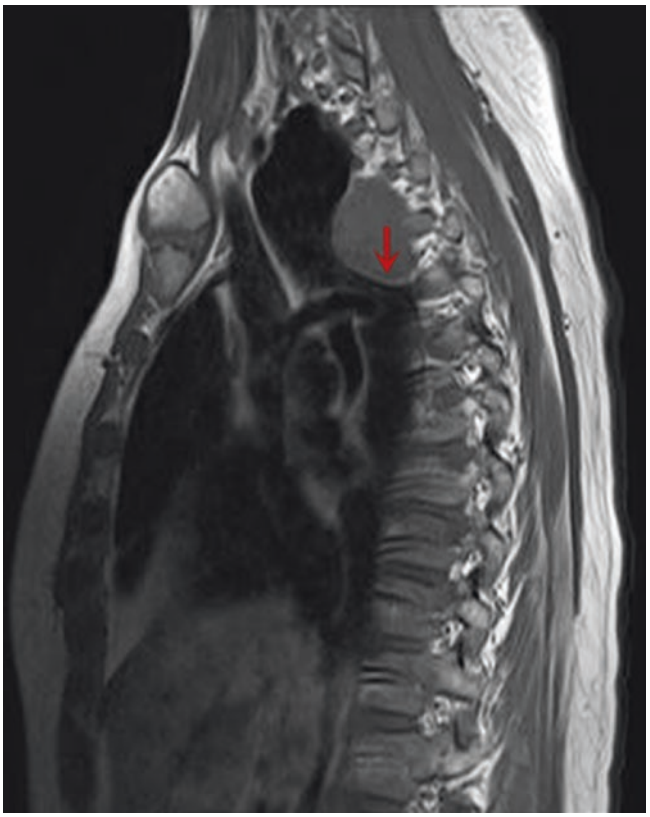

Fig. 9.37 MRI of a 61-year-old woman complained of cough and sputum for 1 week

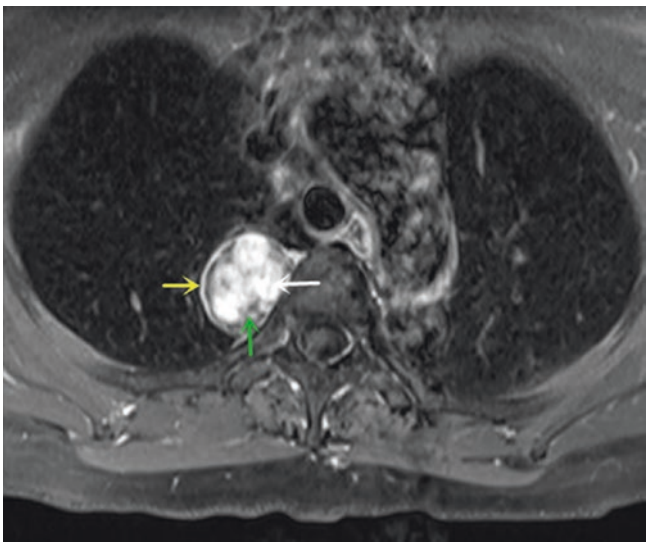

Fig. 9.39 Contrast-enhanced T1-weighted fat-suppressed MRI scan showed that the solid area was obviously heterogeneous enhancement (white arrow), the low signal area was not obvious enhancement (green arrow), and the edge of the mass could also be seen to be evenly enhancement (yellow arrow)

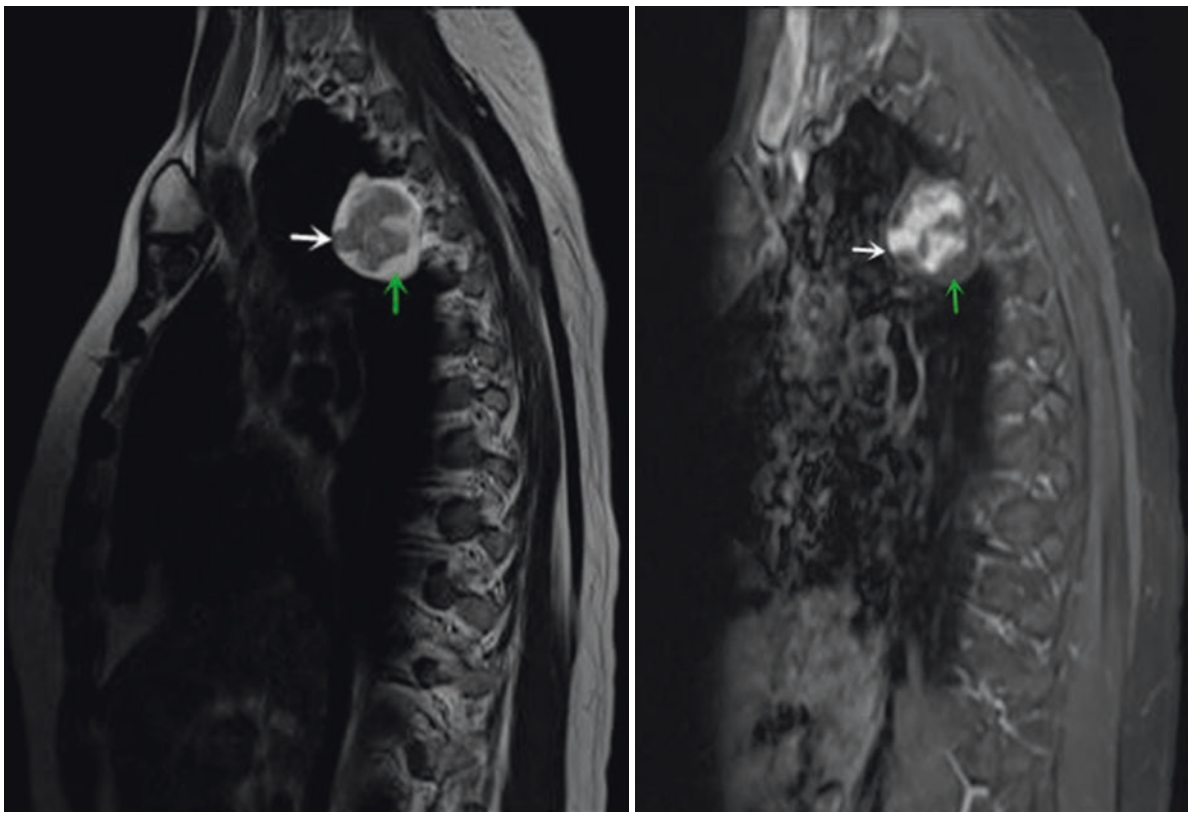

Fig. 9.38 Overall signal was heterogeneous

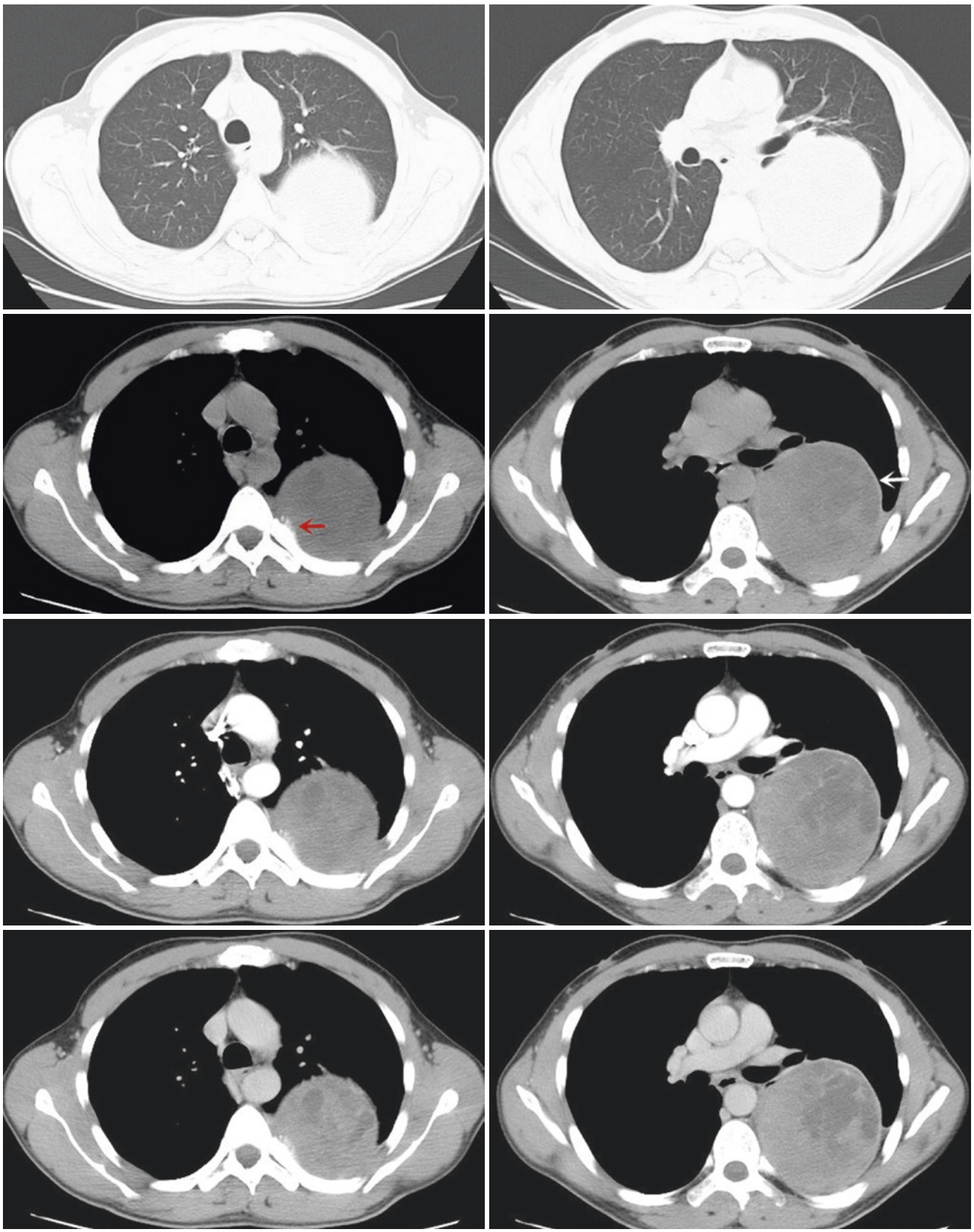

Fig. 9.40 Chest CT images of a 39-year-old man complained of chest tightness for 1 month

envelope and a large number of capillaries on the surface of the tumor. The postoperative pathological diagnosis was a schwannoma.

[**Analysis**] Schwannoma is a type of benign nerve sheath tumor, which is often located in the head, neck, and extremities, and mostly asymptomatic. Occasionally, schwannoma may present with symptoms of compression of the neighboring structures or intraspinal invasion of the tumor. Radiologically, as a spherical paraspinal mass with clean lobular margins, schwannoma involves one or two posterior intercostal spaces, and can grow to large dimensions. In 50% of cases, they result in benign erosions and deformities of the ribs, vertebral bodies, and nerve foramina. CT sometimes appears dots of calcification and areas of hypodensity corresponding to the zones of hypocellularity, which are cystic and hemorrhagic and are full of myelin lipids. After contrast medium infusion, schwannoma can show homogeneous, heterogeneous, or with peripheral enhancement.

This case needs to be distinguished from pleural solitary fibrous tumors. Pleural solitary fibrous tumors have obvious enhancement when the tumor is large, and most of them are map-like enhancement, which is easy to identify.

9.7.4 Case 4

A 20-year-old man revealed a left mediastinal mass for 1 week.

Chest CT: A clear boundary mass in the left posterior mediastinum with necrotic or cystic component. The contrast-enhanced CT scan showed slight enhancement and delayed enhancement in the periphery. Adjacent rib is compressed to be sunken (Fig. 9.41).

MRI: Coronal T2-weighted fat-saturated (Fig. 9.42) and axial T2-weighted fat-suppressed (Fig. 9.43) MRI scan showed high signal. Contrast-enhanced T1-weighted fat-

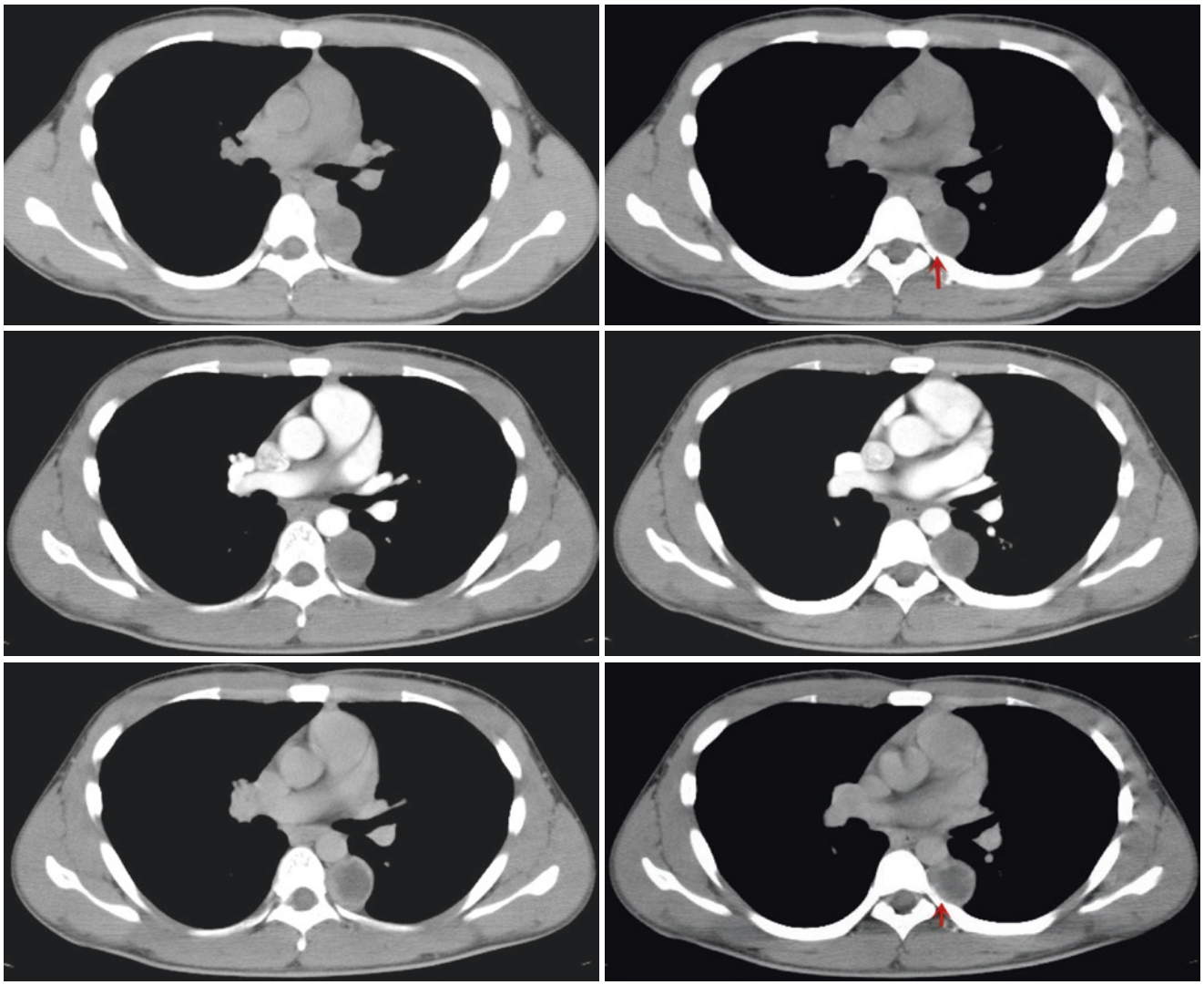

Fig. 9.41 Chest CT images of a 20-year-old man revealed a left mediastinal mass for 1 week

Fig. 9.42 Coronal T2-weighted fat saturated

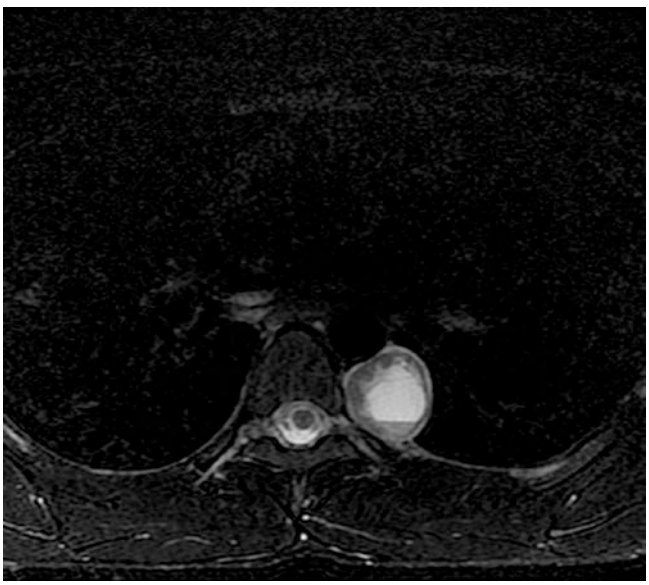

Fig. 9.43 Axial T2-weighted fat suppressed

suppressed MRI scan showed circular enhancement in the periphery (Fig. 9.44).

[**Diagnosis**] Schwannoma with cystic change

[**Diagnosis basis**] A left posterior mediastinal soft tissue mass had a low-density area, which was not enhanced in the contrast-enhanced scan, suggesting cystic change and necrosis. There was a well-corticated margin at the site where the mass was invading the vertebral body (red arrow), suggesting a chronic pressure-type remodeling process. MRI examination further supports necrosis and cystic change inside the mass. Intraoperatively, the tumor was encapsulated and the wall thickness was 1 cm. The postoperative pathological diagnosis was a schwannoma with cystic change.

[**Analysis**] On CT scan, well-circumscribed masses are shown in schwannomas that are heterogeneous after intravenous contrast administration, with hypodense regions likely representing cystic degeneration. On MRI, schwannomas appear heterogeneous with T2 hyperintensity, which represent cystic degeneration. When the cystic change becomes obvious, it is easy to be misdiagnosed as encapsulated effusion and mediastinal cyst. Cystic neurogenic tumors usually have a thicker and more irregular wall than true cysts. Posterior schwannomas generally have sharp margins due to their interface with the lung and erode off the ribs. The encapsulated effusion showed a water-like density, but no enhancement in the enhanced scan. The mediastinal cyst wall can be enhanced, but the adjacent vertebral bodies or ribs are normal.

9.7.5 Case 5

A 58-year-old woman complained of chest tightness for 1 week.

Chest CT: There a quasi-circular solid mass in the left posterior mediastinum with a left pleural effusion On May 19, 2015 (Fig. 9.45).

Chest CT: After CT-guided puncture, the pleural effusion increased on May 21, 2015 (Fig. 9.46).

[**Diagnosis**] Schwannoma

[**Diagnosis basis**] Chest CT shows a heterogeneous posterior mediastinal mass with a mild degree of enhancement and a necrotic or cystic component. The pathological diagnosis was benign schwannoma.

[**Analysis**] When the schwannoma is small, the density is uniform, and when it is large, it can cause cystic degeneration, necrosis, calcification, and pleural effusion. It is often difficult to distinguish it from malignant tumors. Pleural effusion is often associated with inflammatory lesions or malignant tumors, rarely caused by benign tumors. It has been reported that benign schwannoma can cause bloody pleural effusion, which is caused by the internal rupture of the tumor and stimulation of the pleura. The patient's pleural effusion increased significantly after diagnostic puncture and the possibility of tumor bleeding should be considered. Malignant lesions often show unclear boundaries, invasion of adjacent tissues, and some signs of distant metastasis. Schwannoma with pleural effusion should be distinguished from malignant pleural mesothelioma. Malignant mesothelioma mostly shows irregular thickening of the pleura. Patients often complained of chest pain, but pain symptoms were in remission with the increase of pleural effusion.

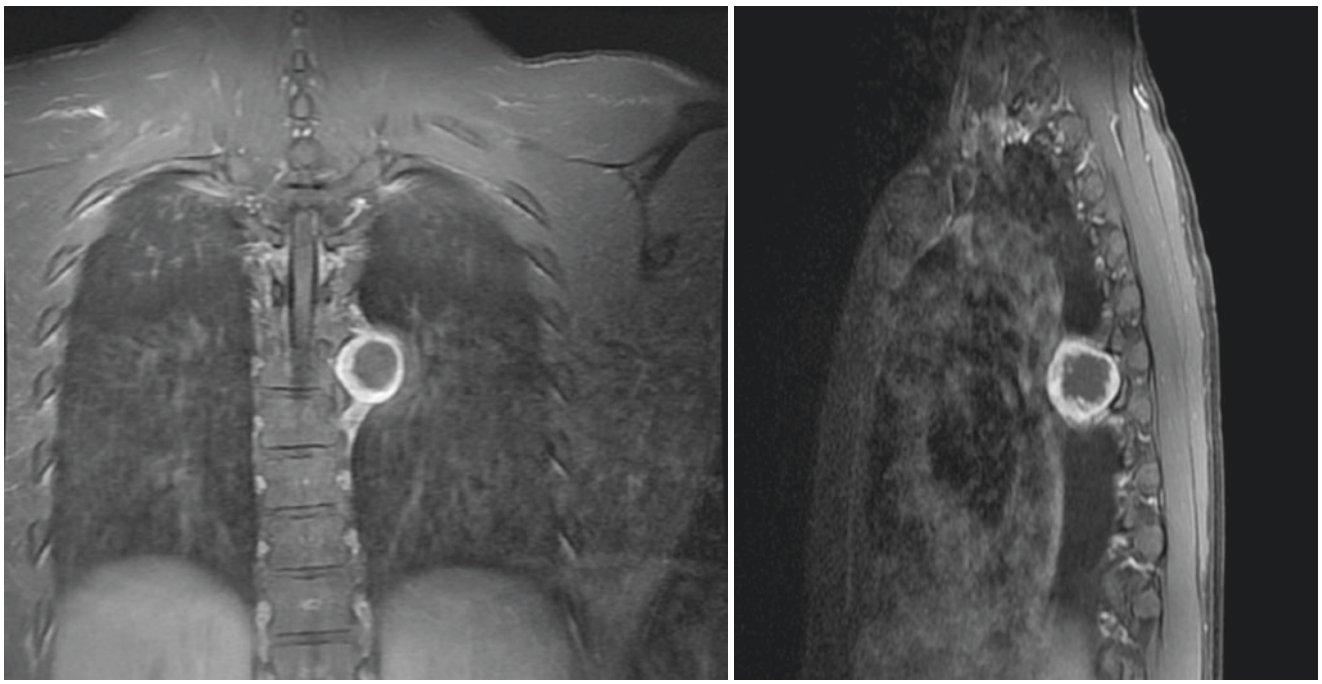

Fig. 9.44 Contrast-enhanced T1-weighted fat-suppressed MRI scan showed circular enhancement in the periphery

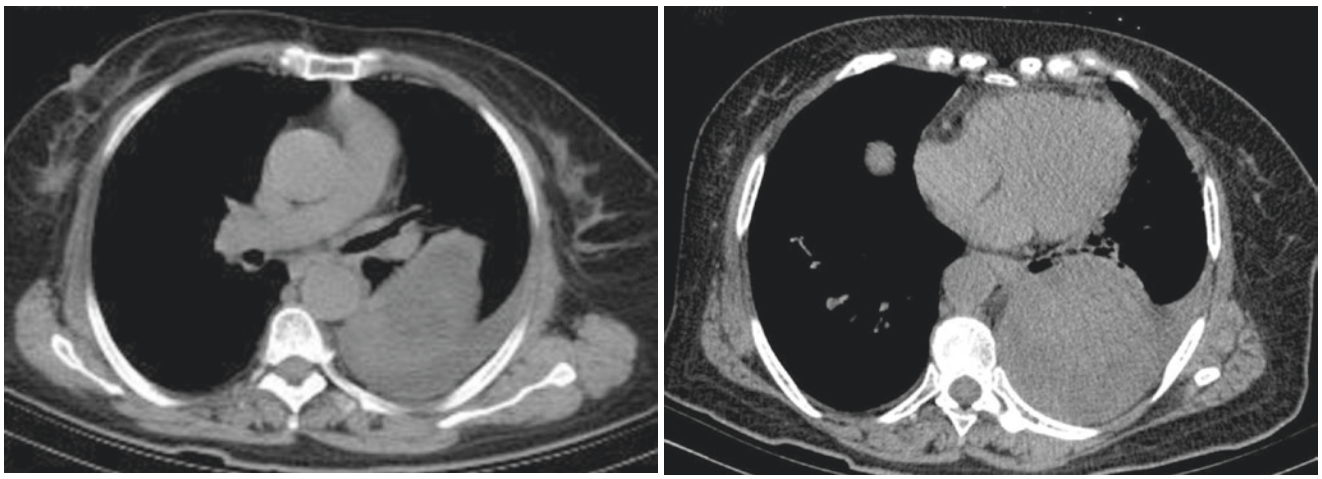

Fig. 9.45 Chest CT images of a 58-year-old woman complained of chest tightness for 1 week

9.7.6 Case 6

A 44-year-old man's physical examination revealed lung lesions.

Chest CT: Soft tissue masses were seen in the left thoracic entrance and the right chest wall. The contrast-enhanced scan showed slight enhancement (Fig. 9.47).

[**Diagnosis**] Multiple schwannoma

[**Diagnosis basis**] Two pleural-based masses protruding into the lungs were seen in the corresponding intercostal space between the right chest wall and the left thoracic entrance, and the adjacent ribs showed arc-shaped concave impressions without bone destruction. The lesions were slightly enhanced, and there are multiple cystic changes in the left thoracic entrance lesion, which is characteristic of schwannoma. The location, morphology, density, and bone resorption of the two lesions were similar, and multiple schwannomas were considered. The postoperative pathological diagnosis was schwannoma.

[**Analysis**] Intrathoracic schwannomas are generally solitary, and multiple lesions are rare (Fig. 9.48). Schwannomas usually arise from a spinal nerve root, most

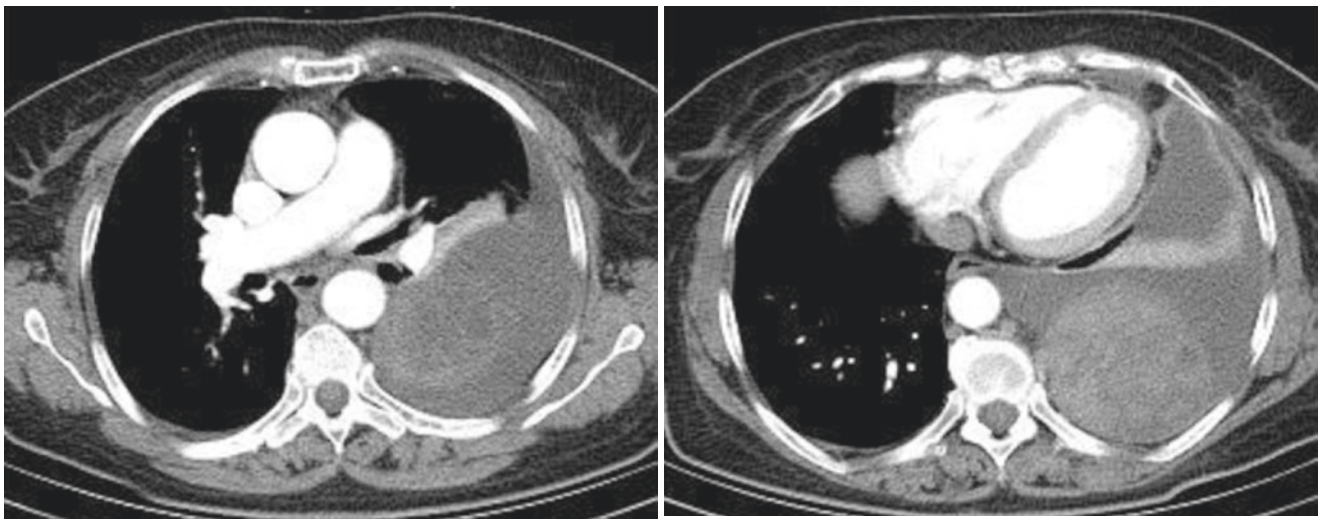

Fig. 9.46 The pleural effusion increased

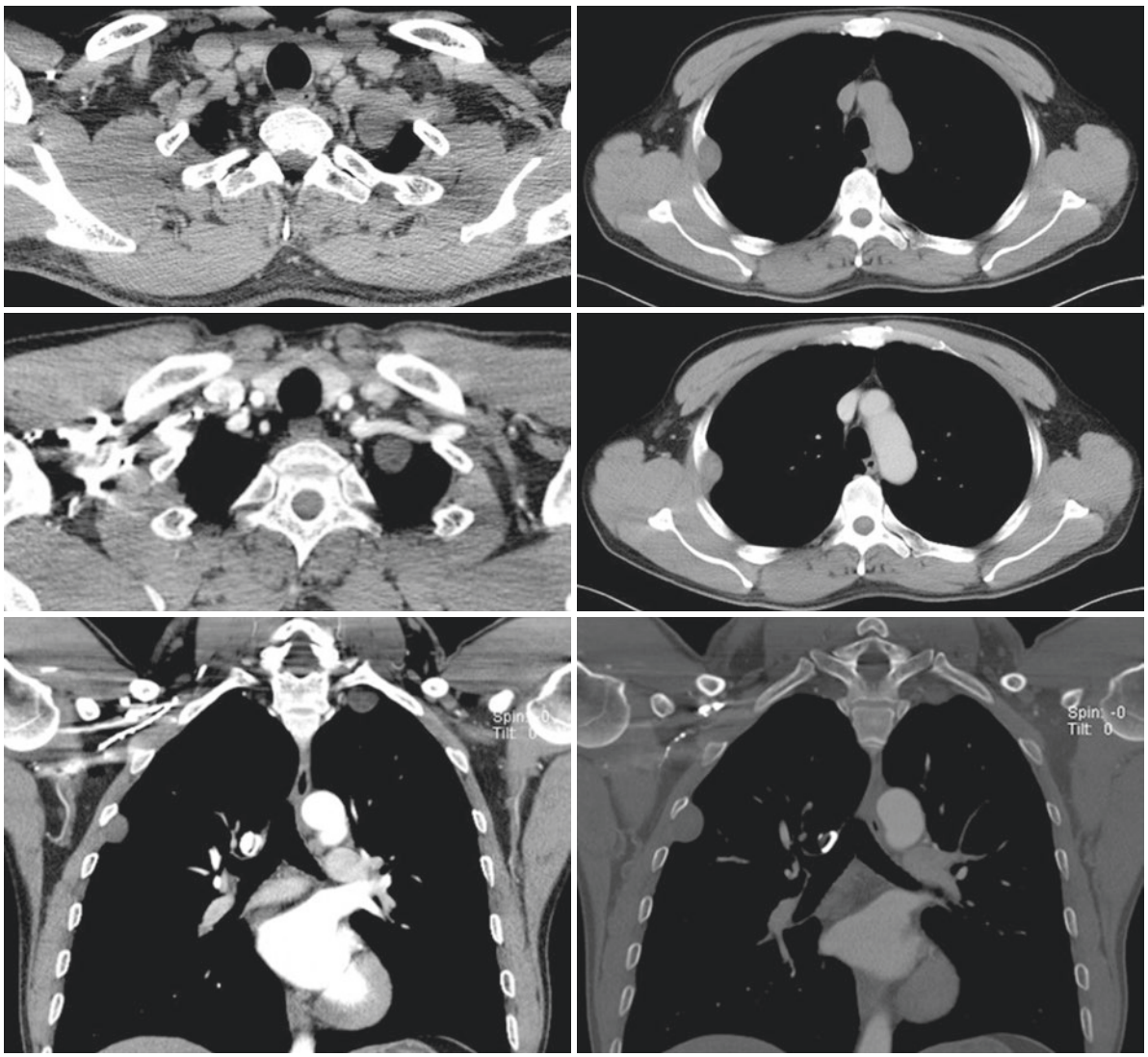

Fig. 9.47 Chest CT images of a 44-year-old man's physical examination revealed lung lesions

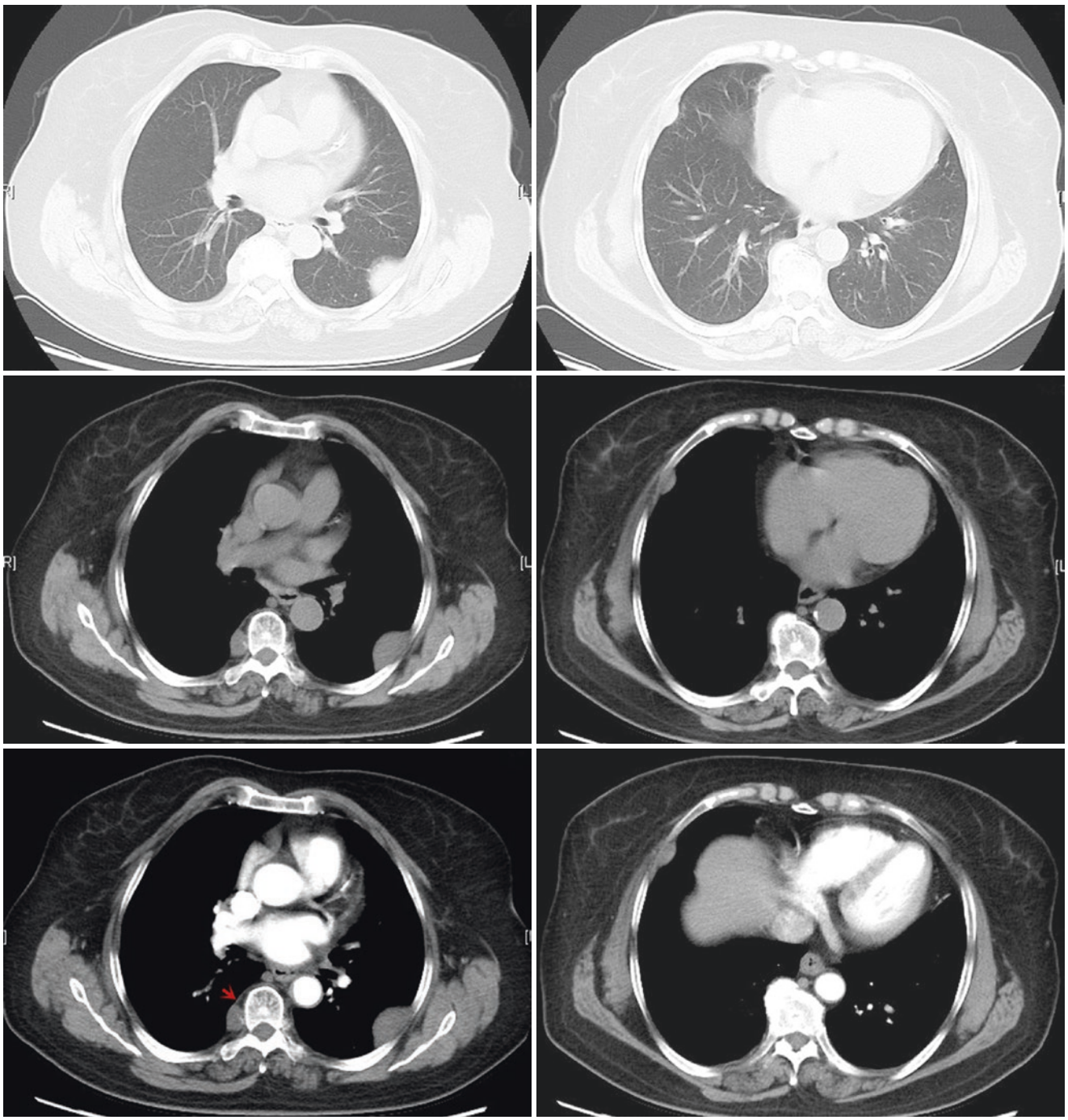

Fig. 9.48 A 68-year-old woman complained of chest pain for more than 2 months. CT showed three hemispherical soft tissue lesions on the bilateral chest wall. The lesion near the right posterior mediastinal intervertebral foramen was clearly located outside the pleura (red arrow), and the contrast-enhanced scan was slightly enhanced. The tumors were removed and the postoperative pathological diagnosis was schwannoma

commonly arising from the proximal intercostal nerves. Each spinal nerve passed through the intervertebral foramen and immediately divided into the anterior and posterior rami at the distal point of the spinal ganglion. The posterior rami ran in the posterolateral direction. The posterior rami ran laterally and bifurcated into two major branches, that is, medial and lateral branches. The back muscles are innervated by the posterior rami of the spinal nerves. The anterior rami include the intercostal nerve and the subcostal nerve. The intercostal nerves originate from the T1–T11 spinal nerve anterior rami and the subcostal nerve originates from the T12 spinal nerve anterior ramus.

The largest intercostal nerve branch is the lateral cutaneous nerve, which is located in the lateral thoracic wall. The intercostal nerve ends in the anterior cutaneous branch, which appears in either the parasternal region or the paramedian abdominal wall. Schwannoma may occur in any of the above regions. Although thoracic schwannoma runs along the nerve, it can grow away from the nerve root. Therefore, the clinical symptoms of such tumors are often not obvious. A few patients only show chest discomfort or hidden pain. When intercostal nerves are involved, they can cause corresponding intercostal neuralgia.

9.7.7 Case 7

A 47-year-old woman complained of chest pain and chest tightness for 3 months.

Chest CT: The circumscribed mass was identified in the left superior mediastinum with punctate calcifications, the CT attentions of solid components in unenhanced scan, arterial phase, and venous phase were 55HU, 65HU, and 76HU, respectively. The CT attention of the surrounding low-density area was no enhancement with 31HU (Fig. 9.49).

[**Diagnosis**] Schwannoma

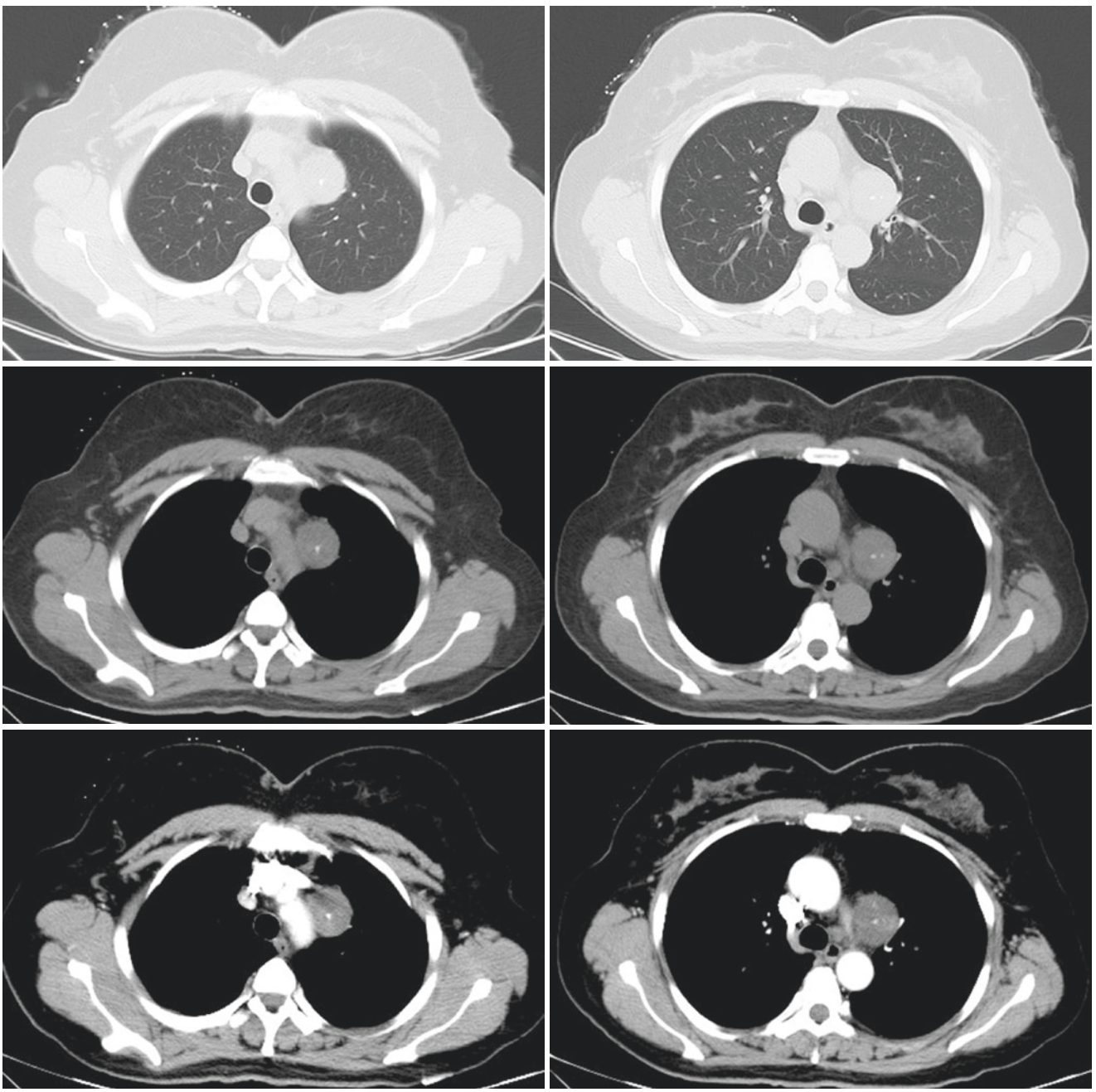

Fig. 9.49 Chest CT images of a 47-year-old woman complained of chest pain and chest tightness for 3 months

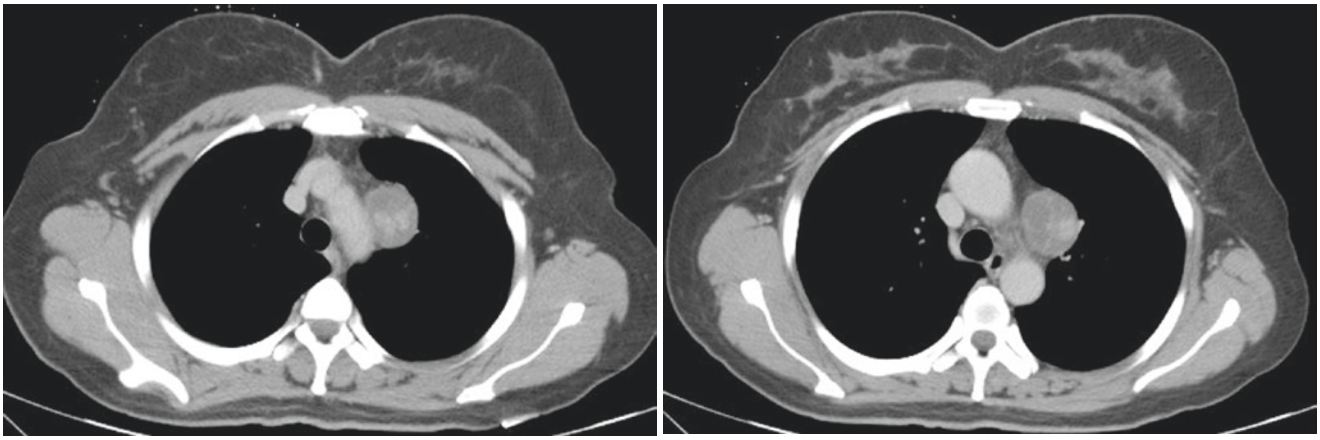

Fig. 9.49 (continued)

[**Diagnosis basis**] The mass is located in the left aortic arch, with clear boundaries. The patient's age, lesion location, enhancement method, and calcification characteristics support the diagnosis of schwannoma. Intraoperatively, the tumor extended along the left common carotid artery, the left subclavian artery to the base of the neck, and adjacent to the left brachiocephalic vein. Tumor involved the left vagus nerve and the recurrent laryngeal nerve. The postoperative pathological diagnosis was schwannoma.

[**Analysis**] Schwannomas originating from the vagus nerve within the mediastinum are rare, comprising only 1.4% of intrathoracic schwannomas. In 1935, Stout first named vagal tumors of nerve sheath origin as "neurilemmomas." The vagus nerve originates from the medulla oblongata, and exits the cranium via the jugular foramen. At this point, the vagus nerve courses between the internal and the external carotid arteries and enters the carotid sheath. In the chest, the left and right vagus nerves have different movements and positions. On the left, leaving the carotid sheath, the vagus nerve passes between the left common carotid and the left subclavian arteries as it approaches the lateral aspect of the aortic arch. Here, the nerve lies posterior to the left superior intercostal vein and phrenic nerve. After passing posterior to the left hilum, the vagus nerve contributes branches to the pulmonary plexus before dividing into the esophageal plexus. Just before reaching the esophageal hiatus, the nerve coalesces to form the anterior vagal trunk, which lies along the anterior wall of the esophagus, passing into the abdomen. On the right, after passing anterior to the proximal right subclavian artery, the vagus nerve courses posterior to the right brachiocephalic vein and superior vena cava through the middle mediastinum along the right lateral margin of the trachea. At the level of the hilum, the pulmonary plexus are formed by branches along the distal trachea and main-stem bronchi. Then, travelling posteriorly, the nerve divides into the esophageal plexus along the mid and distal esophageal surface. Near the level of the diaphragm, the branches coalesce into the posterior vagal trunk, which passes through the esophageal hiatus along the posterior wall of the esophagus to enter the abdomen.

Mediastinal vagus nerve schwannomas are almost twice on the left than on the right, as the recurrent laryngeal nerve arises lower in the thoracic cavity on the left side and the left nerve trunk is thicker. The tumor may occur at any age and does not show a gender preference. Schwannoma is asymptomatic in the majority of cases; however, a number of symptoms, including chest pain, dysphagia, cough, and hoarseness, to varying degrees, may occur due to compression of the neighboring organs. When the lesion is located in the area of the left (Fig. 9.50) and right vagus nerves (Fig. 9.51), and the calcification and enhancement methods are consistent with typical schwannoma, the diagnosis should be considered. Originating from the intrathoracic vagus nerve, the management of these tumors is primarily surgical excision to prevent a mass effect or loss of the host nerve function. Even though it is not a common entity, clinicians should consider schwannoma of the vagus nerve in the differential diagnosis of a middle mediastinal tumor.

9.7.8 Case 8

A 52-year-old woman's physical examination revealed diaphragm mass.

Chest CT: Oval soft tissue density mass located between the left diaphragm and the heart, with low-density areas inside, contrast-enhanced scan with mild enhancement and delayed enhancement, and low-density areas without enhancement (Fig. 9.52).

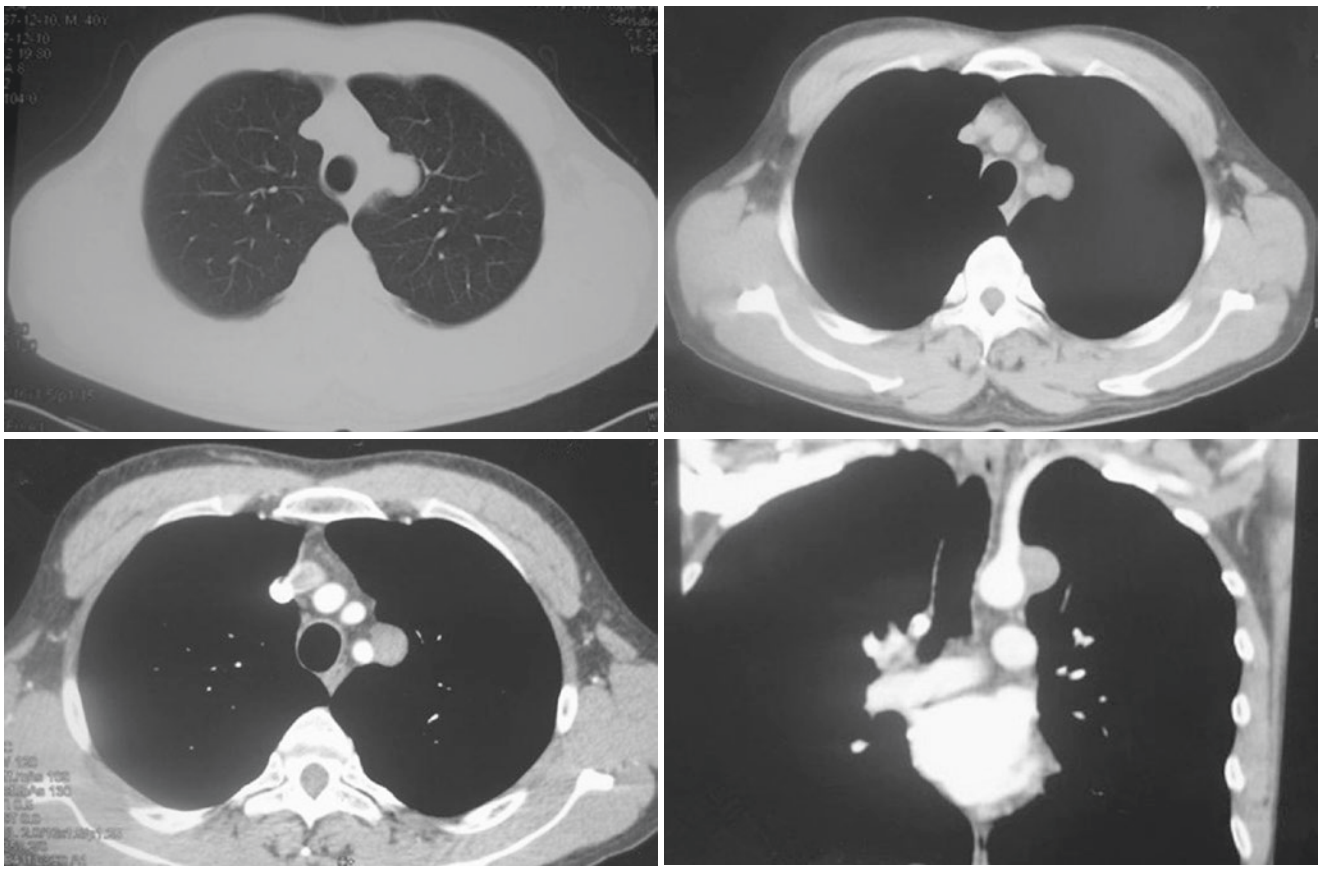

Fig. 9.50 A 40-year-old man with a mass in the left superior mediastinum with a smooth and clear margin. The CT attentions in unenhanced scan and the arterial phase were 16.1HU and 26.9HU, respectively. Intraoperatively, the tumor was found to be arising from the vagus nerve. Histopathology confirmed the diagnosis of vagus nerve schwannoma

[**Diagnosis**] Schwannoma of the left diaphragm with cystic change

[**Diagnosis basis**] The sagittal (Fig. 9.52g) and coronal (Fig. 9.52h) reconstructions showed that the lesion originated from the diaphragm (red arrow). CT showed an approximately 4 cm, well-circumscribed, delayed-enhanced round tumor in a peridiaphragmatic portion (Fig. 9.52e,f). Diaphragmatic schwannoma with cystic change was considered. Intraoperatively, the tumor was completely encapsulated located on the left diaphragm. The phrenic nerve entered the tumor. The tumor and 0.5 cm of the phrenic nerve were removed. Histopathologically, the tumor was well-demarcated, which consisted of a proliferation of spindle cells in a loose myxoid pattern or with some clear palisading. In addition, a few mitotic figures were seen in tumor cells. As a result, the tumor was diagnosed as a benign schwannoma with cystic changes.

[**Analysis**] Diaphragm tumors are clinically rare, and most of them originate from the central tendon or anterior muscle of the diaphragm. A primary tumor of the diaphragm was first reported in 1868 when Grancher discovered a fibroma of the diaphragm during an autopsy study. Wiener and Chou in 1965 [2] reviewed 85 cases of primary diaphragmatic tumors and showed 52 cases to be benign and 33 cases malignant. The most popular benign tumor was the cystic tumor (34%).

Primary benign tumors of the diaphragm include lipomas, hemangiomas, lymphangiomas, fibrohemangiomas, neurogenic tumors, teratomas, and dermoid cysts, and most benign lesions being cystic or lipomatous. Primary malignant diaphragm tumors mostly originate from muscle fibers, such as fibrosarcoma and fibrovascular endothelial tumor. Fibrosarcoma is the most common malignant tumor. Patients usually present symptoms of dyspnea, cough, chest pain, or finger clubbing. About 20% of patients are asymptomatic.

Primary neural tumors of the diaphragm are rare, representing approximately 10% of the neoplasms of the diaphragm. Primary schwannoma of the diaphragm is extremely rare, with less than 10 cases reported so far. Primary neuro-

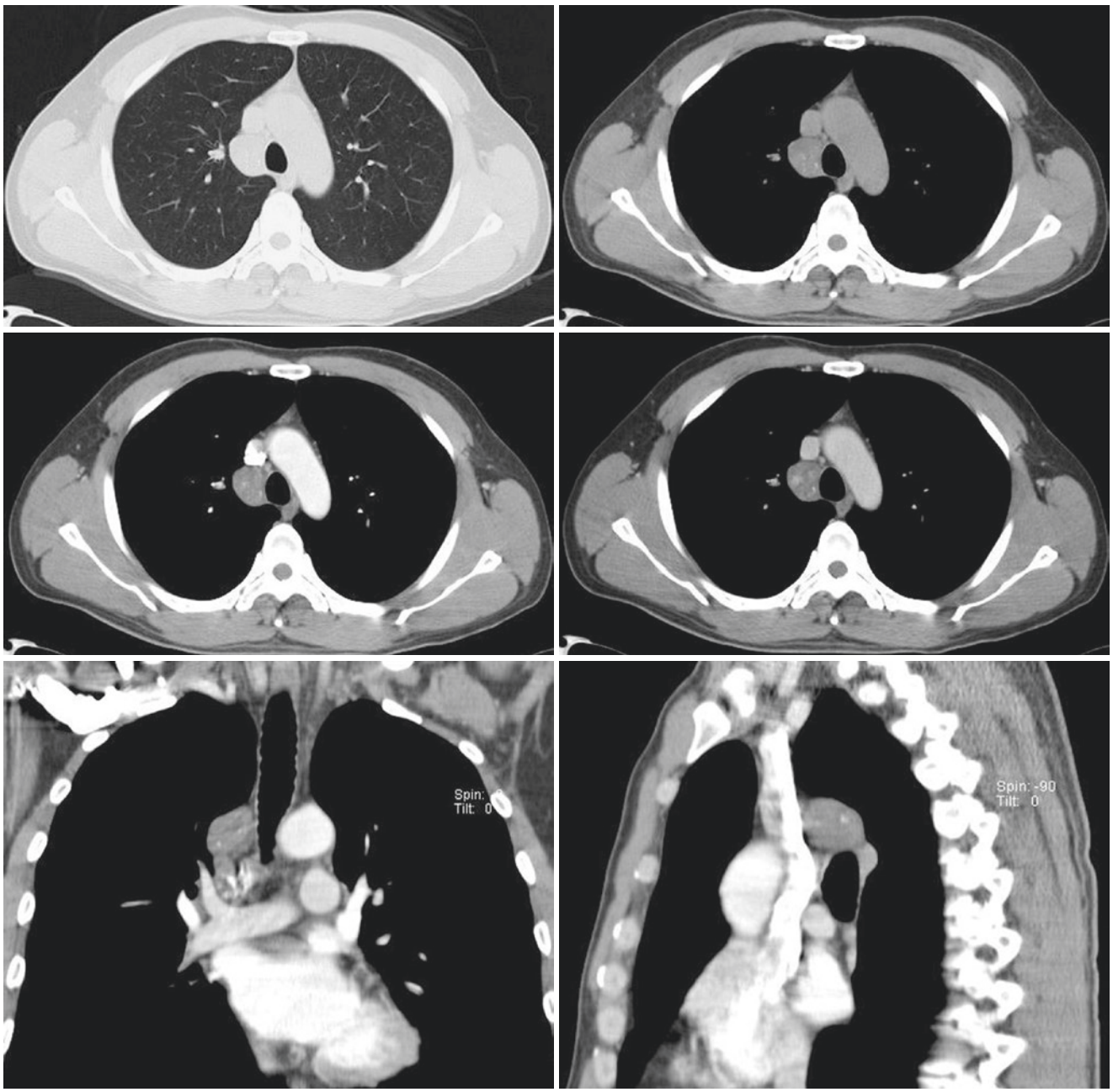

Fig. 9.51 A 42-year-old man complained of chest pain and chest tightness for 3 months. The pathological diagnosis was schwannoma with extensive bleeding, necrosis, and calcifications

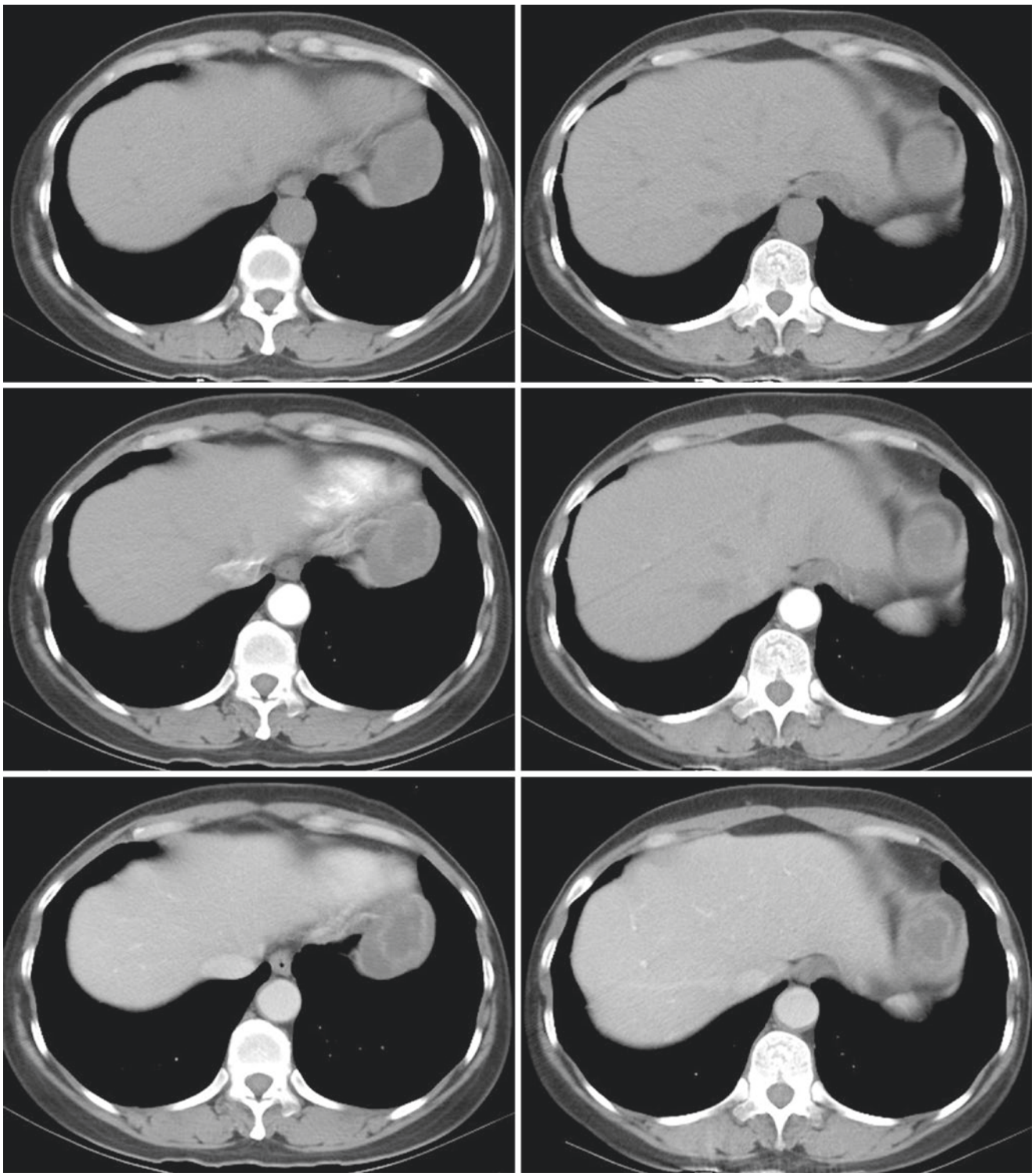

Fig. 9.52 Chest CT images of a 52-year-old woman's physical examination revealed diaphragm mass

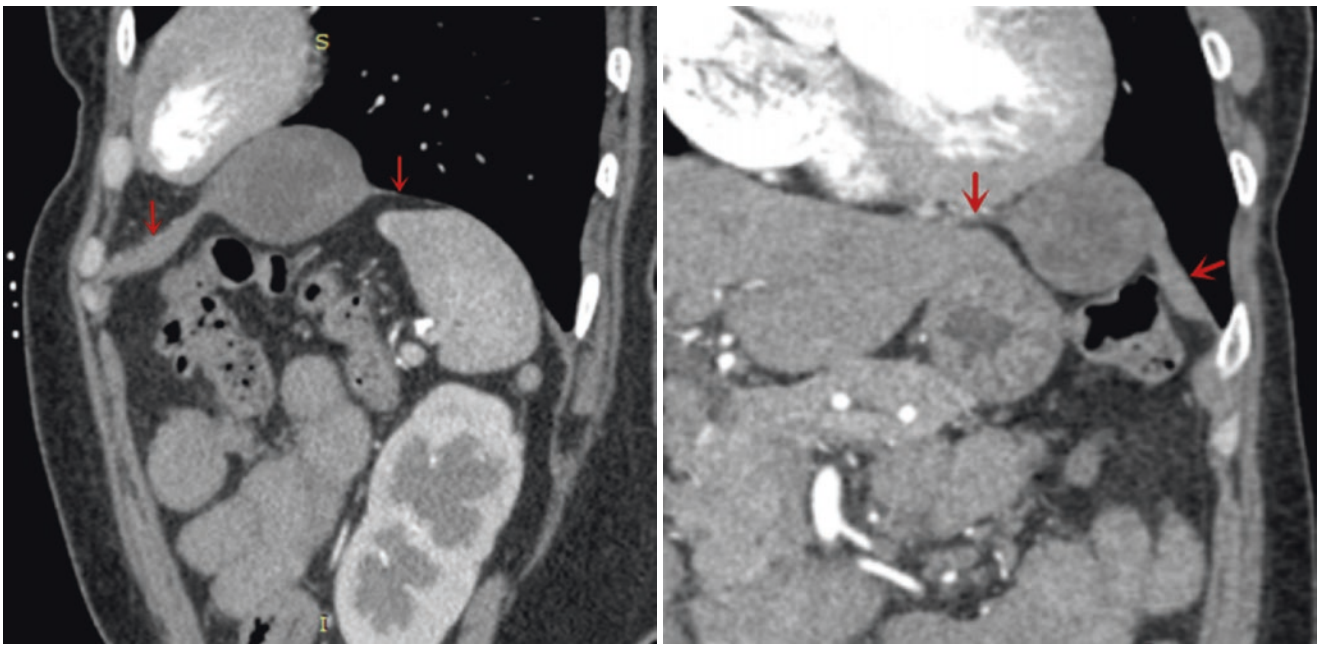

Fig. 9.52 (continued)

genic tumors of the phrenic nerve are most commonly benign neurogenic tumors including schwannomas or neurofibromas, with most reported schwannomas appearing sporadically and neurofibromas typically occurring in neurofibromatosis type 1. Malignant peripheral nerve sheath tumors of the phrenic nerve are exceedingly rare.

With contributions from the ventral rami of C3 and C5, the phrenic nerve is formed predominantly from the ventral ramus of the fourth cervical nerve (C4). Immediately coursing to the anterior surface of the anterior scalene muscle near its origin from a lateral approach, the nerve descends to the thoracic inlet along this muscle. The phrenic nerve is the sole motor innervation to the diaphragm in addition to providing sensory innervation to pericardium, the mediastinal pleura, central portion of the diaphragm, and diaphragmatic peritoneal surfaces.

Successful imaging diagnosis of such tumors of the diaphragm has been difficult. In addition to the identification of tumors from above and below the diaphragm, the heart or mediastinal lesions should be distinguished. Complete surgical removal of this benign tumor should be the most effective method of diagnosis and treatment, and no recurrence has been reported.

9.7.9 Case 9

A 28-year-old woman complained of intermittent hemoptysis for 2 months. Chest CT: right middle bronchial spherical lesion with obstructive pneumonia (Fig. 9.53).

[**Diagnosis**] Tracheal schwannoma

[**Diagnosis basis**] The patient underwent bronchoscopy, and the lesion was located in the right middle bronchi, almost completely occluding the lumen. Bronchial biopsy pathology showed fascicles of spindle-shaped cells with indistinct cytoplasm and oval nuclei displaying nuclear palisading, consistent with schwannoma. Intraoperatively, the tumor grew from the opening of the proximal lobe to the opening of the basal segment and the size was 2.2 cm × 2 cm × 1.8 cm. The lower lobe has atelectasis and partially consolidation, and the middle lobe has atrophy. The patient underwent right middle and lower lobe resection and bronchoplasty. The diagnosis of schwannoma was confirmed.

[**Analysis**] Primary tracheal tumors are uncommon, and account for only 1% of all tumors. Malignant squamous cell carcinoma and adenoid cystic carcinoma (intermediate malignant) account for approximately 75% of the tumors. The other quarter of the tumors consists of multiple histological subtypes that include benign, intermediate, and malignant tumors. Neurogenic tumors of the tracheobronchial tree are extremely rare and include schwannoma and neurofibroma, accounting for less than 0.5% of primary tracheal tumors. Schwannomas are extremely rare in the trachea, being more frequently reported in the lungs and bronchi. Primary neurogenic tracheal tumors (neurofibroma and schwannoma) can occur in any age, with a majority of cases occurring after the age of 20. This type of tumor arises from nerves located inside the tracheal wall. Neurofibroma has been reported only in male patients, while schwannoma has a predilection for female patients.

Tracheal schwannoma, first reported by Straus in 1951 [3], is usually solitary, well-encapsulated lesion that is

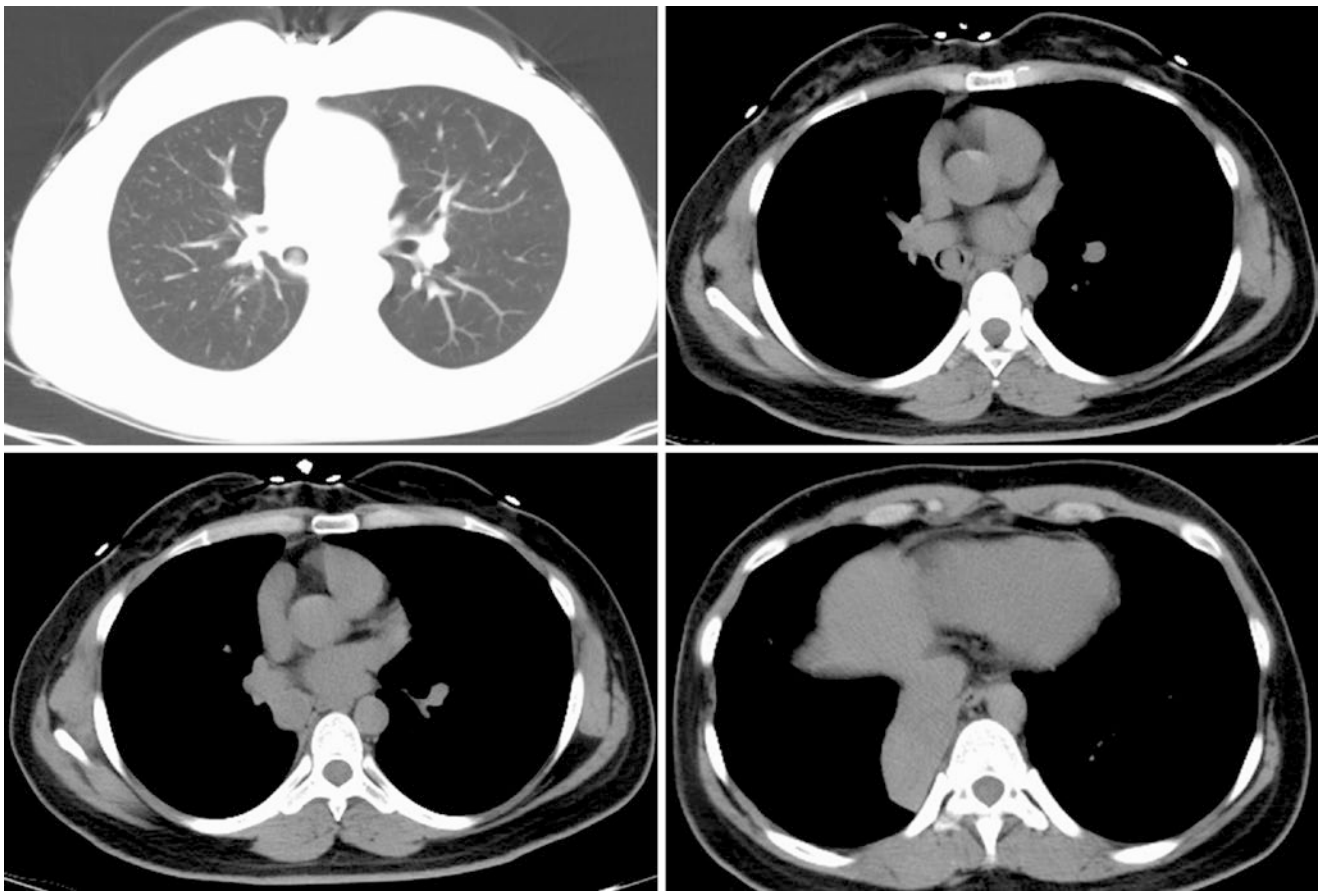

Fig. 9.53 Chest CT images of a 28-year-old woman complained of intermittent hemoptysis for 2 months

attached to the nerve sheath and sometimes covered with several small, discrete vessels. It is rarely associated with von Recklinghausen disease and malignant transformation.

A classification of the pulmonary schwannomas was proposed by Kasahara et al. [4]. If the lesion is located in the trachea or proximal bronchi, and can be found by bronchoscopy, it can be divided into central type; if the lesion cannot be detected by bronchoscopy, but can be detected by chest X-ray or computed tomography as a nodule, it is divided into peripheral type. The central type is also divided into two subtypes: (1) tumors that exist only in the intraluminal space and (2) tumors that occur in both intraluminal and extraluminal spaces (combined type or dumbbell tumor). Tracheal schwannoma most commonly found in the distal third of the trachea, followed by the proximal, and then middle thirds.

The clinical manifestations of intraluminal schwannomas of the trachea depend on the site, size, and the extent of obstruction produced by the tumor. Because of the flexibility of trachea, patients with intratracheal tumors usually have no symptoms in the early stage of disease. Only when the trachea is occupied more than 50%, patients will present some nonspecific symptoms such as shortness of breath and dry cough, symptoms of upper airway obstruction, and less frequently with hemoptysis and hoarseness. Due to the rarity of the primary tracheal schwannoma and its nonspecific clinical feature, the average delay in diagnosis is 17 months from the onset of symptoms.

Tracheal primary neurogenic tumors usually have a long natural history, causing symptoms only after they have reached a significant size. Preferred diagnostic method for tracheal primary neurogenic tumors should be rigid bronchoscopy, which helps to measure the true size of the tumor, size of the tumor-free trachea that could be needed for the reconstruction after surgery, and to control bleeding that could occur after biopsy. Additionally, multislice computerized tomography is used to delineate tumor size, site, and extratracheal extension (Fig. 9.54). Pulmonary function tests aid early diagnosis especially flow-volume curves which demonstrate upper airway obstruction.

Endoscopic excision, sleeve excision, or tracheal resection, are all commonly accepted treatment modalities. The choice of treatment is affected by the clinical presentation of the tumor (pedunculated vs. sessile), the risk of tracheal resection, and the presence or absence of an extratracheal component. Small intraluminal tumors can be treated with

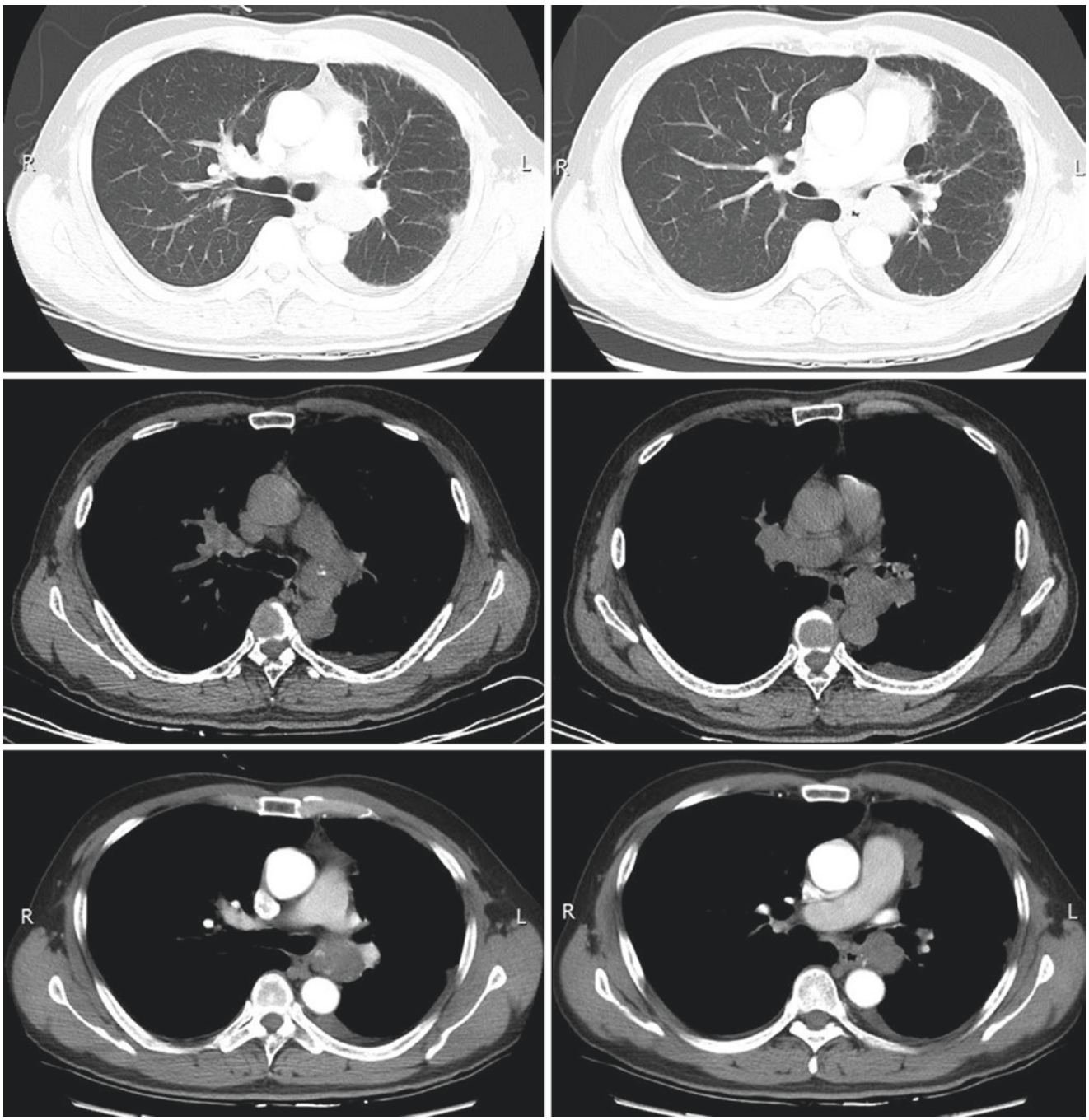

Fig. 9.54 A 52-year-old man with tracheal schwannoma

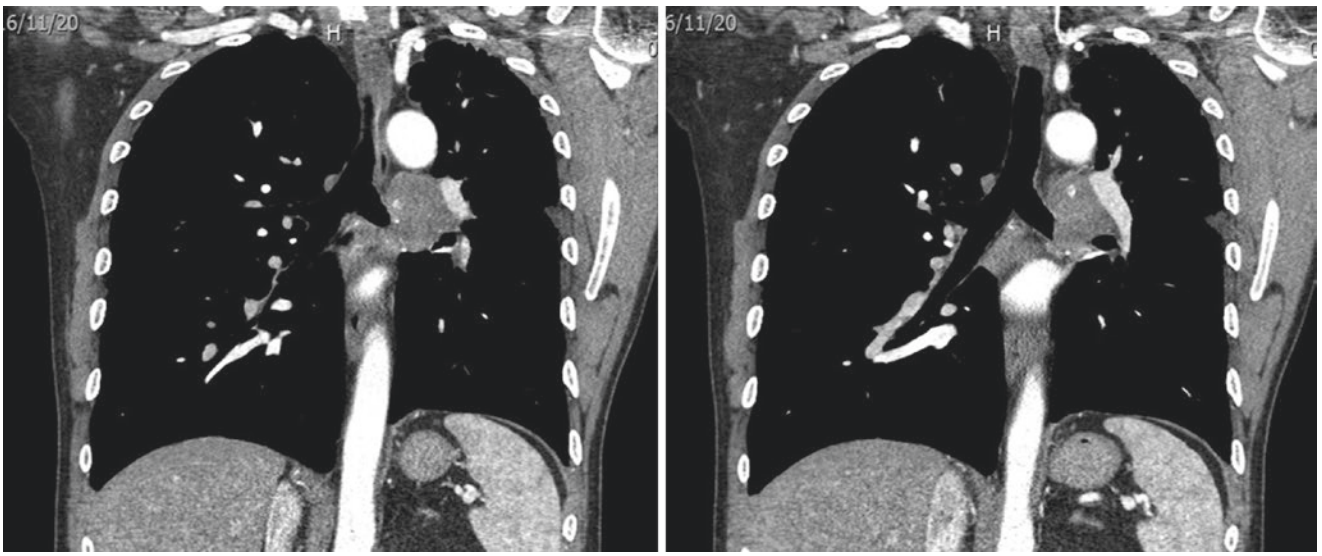

Fig. 9.54 (continued)

endoscopic resection. However, the majority require an open resection for curative intent. The prognosis for patients with schwannomas who are either removed surgically or by endoscopic treatment methods is excellent.

9.7.10 Case 10

A 34-year-old woman complained of chest tightness for 2 months.

Chest CT: A soft tissue mass in the lower part of the right chest wall, with visible calcification and heterogeneous enhancement (Fig. 9.55).

[**Diagnosis**] Malignant schwannoma

[**Diagnosis basis**] There are calcification, cyst, necrosis, and heterogeneous enhancement in this lesion, supporting the diagnosis of schwannoma. The tumor was surgically removed and the pathological diagnosis was malignant schwannoma.

[**Analysis**] In 2002, the WHO nervous system tumor classification referred to neurosarcoma, neurofibrosarcoma, malignant Schwann cell tumor, and malignant schwannoma as malignant peripheral nerve sheath tumors (MPNST), accounting for 5–10% of all soft tissue sarcoma and 13–20% of neurogenic tumors. MPNST can be diagnosed when the soft tissue sarcoma meets one of the following criteria: (1) The tumor originates from the peripheral nerve; (2) The tumor originates from an existing benign nerve tumor; (3) The tumor shows histological features differentiated by Schwann cells or peripheral nerves confirmed by immunohistochemistry or electronmicroscopy.

MPNST tends to occur in the arms and legs and trunk of the body, with mediastinal occurrence in only a few cases. MPNST is often thought to arise from benign peripheral nerve sheath tumors, usually neurofibromas. Approximately 50% of them are Neurofibromatosis Type I associated, 10% associated with prior therapeutic irradiation, and the remainder sporadic.

Intrathoracic MPNST may involve mediastinum, lung, and chest wall; mediastinal and chest wall tumors are often elongated masses along the course of nerves. The imaging manifestations of MPNST include high attenuation and necrosis/hemorrhage on CT, isointense on T1 and hyperintense on T2 on MRI, heterogeneity on T1-weighted images (Fig. 9.56).

Treatment of MPNST relies primarily on surgical resection. Neoadjuvant chemoradiation is often used for initially unresectable tumors with an intention to downstage the mass pre-resection. In addition to surgical resection, radiotherapy can also be performed to improve local control. Chemotherapy is typically reserved for aggressive cases, and also applied to tumor rupture, positive margins, or metastases, although there is no evidence of improved survival.

Regardless of exact site or origin, thoracic MPNST shows aggressive behavior and poor outcome, even with aggressive multimodality treatment. The 5-year survival rate for MPNST is 34%–43.7%. Localized recurrence after excision is 46%–65%, with the distal metastasis rate considered 40%–68%. Factors in poor prognosis include large tumor diameter, age at onset of 30 or lower, occurrence inside the trunk, complicated by nerve fiber tumor type 1, and incomplete excision.

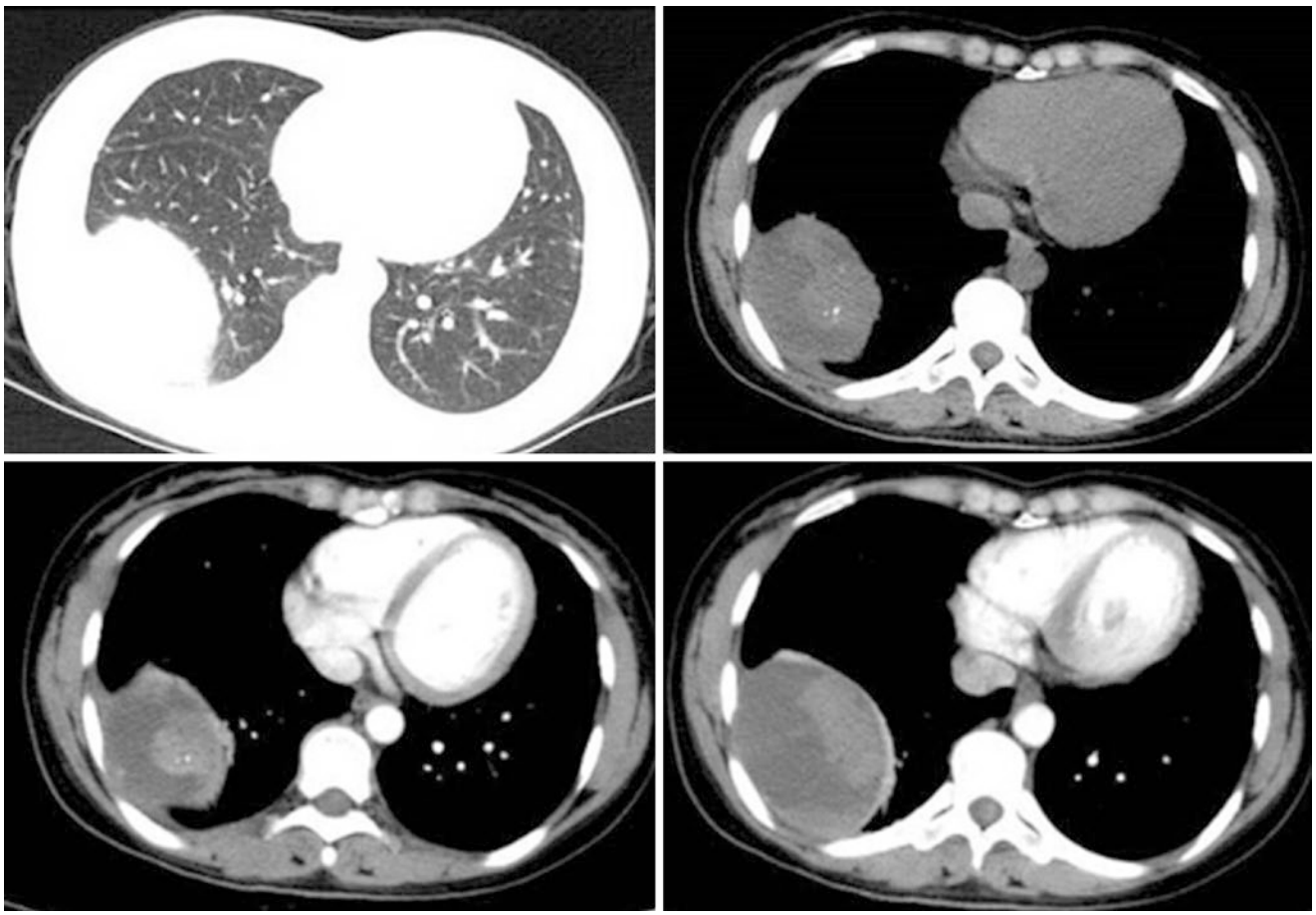

Fig. 9.55 Chest CT images of a 34-year-old woman complained of chest tightness for 2 months

9.7.11 Case 11

A 17-year-old woman complained of cough repeatedly for 3 months.

Chest CT: A heterogeneously enhancing mass occupied the anterior mediastinum (Fig. 9.57).

[**Diagnosis**] Epithelioid malignant peripheral schwannoma

[**Diagnosis basis**] The pathology of the patient's puncture revealed a malignant tumor of mesenchymal tissue. Immunohistochemistry demonstrated positivity for Vim, CD99, and S100, and negativity for CK, SMA, TTF-1, CR, MC, CD34, AFP, PLAP, and HMB45, and the staining index for Ki-67 was about 80%, supporting neural origin, considered epithelioid malignant peripheral nerve sheath tumor.

[Analysis] Epithelioid MPNSTs are rare tumors with substantial clinical and histologic overlap with epithelioid schwannoma. The fact that epithelioid MPNSTs arise more often in conventional schwannomas than in their epithelioid counterparts raises the question of epithelioid malignant change.

Histologically, epithelioid MPNSTs are composed of epithelioid cells of eosinophilic cytoplasm, large nuclei with vesicular chromatin, and prominent nucleoli. Cells are often arranged in clusters and nests within a variably myxoid background. Mitotic rate is usually elevated (>10/10 HPF). Epithelioid MPNSTs are generally highly cellular, may have focal or geographic necrosis, and can exhibit tumor cell spindling. Epithelioid MPNSTs differ from conventional malignant peripheral nerve sheath tumor by showing diffuse S100 protein and SOX10 positivity, infrequent association with NF1, and occasional origin in a schwannoma. Approximately 40% of them show diffuse loss of INI-1. GFAP and keratin expression is variable.

The differential diagnosis of epithelioid MPNST includes clear cell sarcoma, melanoma, epithelioid sarcoma, and carcinoma. Lack of expression of melanocytic markers (e.g., Melan-A, MITF, and HMB45) is very helpful in distinguishing epithelioid MPNST from clear cell sarcoma and melanoma, and absence of cytokeratin expression distinguishes them from epithelioid sarcoma and carcinoma. A loss of SMARCB1/INI1/BAF47 protein expression may be shown in both epithelioid MPNST and epithelioid sarcoma, a potential diagnostic pitfall in the differential diagnosis with malignant rhabdoid tumor. Myoepithelial carcinoma may be a consideration given epithelioid morphology, myxoid

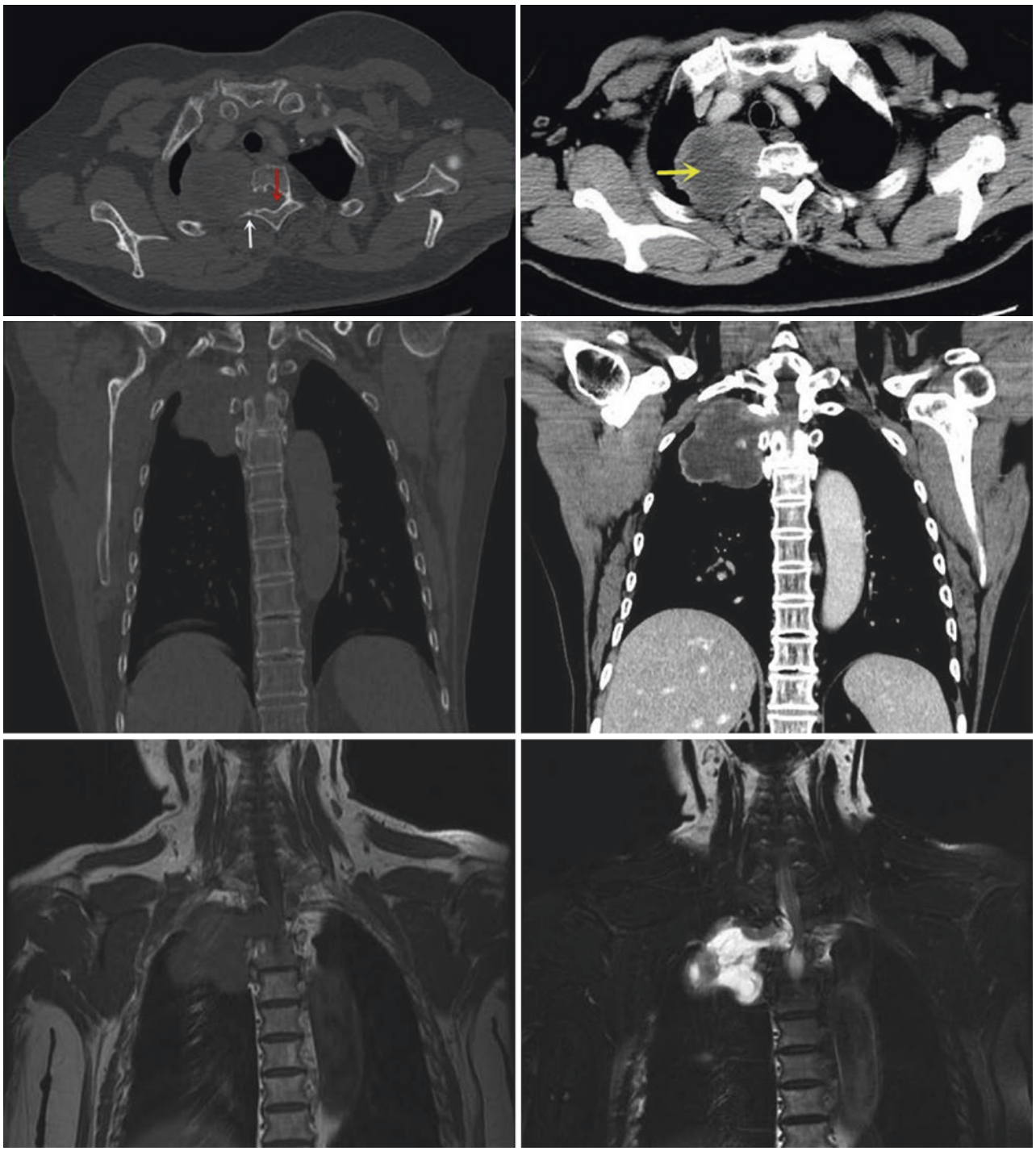

Fig. 9.56 A 61-year-old woman with irregular soft-tissue mass in the right posterior superior mediastinum. Chest CT showed enlarged intervertebral foramen (red arrow), adjacent bone compression (white arrow), necrosis and cystic change (yellow arrow), and peripheral enhancement (Fig. 9.56a–d). MRI showed isointense on T1 (Fig. 9.56e) and hyperintense on T2 (Fig. 9.56f). Pathology was low-grade malignant peripheral schwannoma

background, GFAP, S100 protein, and keratin positivity, and the potential for INI-1 loss. Myoepithelial tumors tend to be less diffusely S100 positive and, outside of the salivary gland, are rarely SOX10 positive. In this histologic and immunophenotypic setting, the finding of *EWSR1* rearrangement is highly specific for myoepithelial carcinoma but not sensitive.

The majority of patients diagnosed with epithelioid MPNSTs are cured by their first surgery. Jo et al. [5] identified sixty-three cases in consultation files. There were

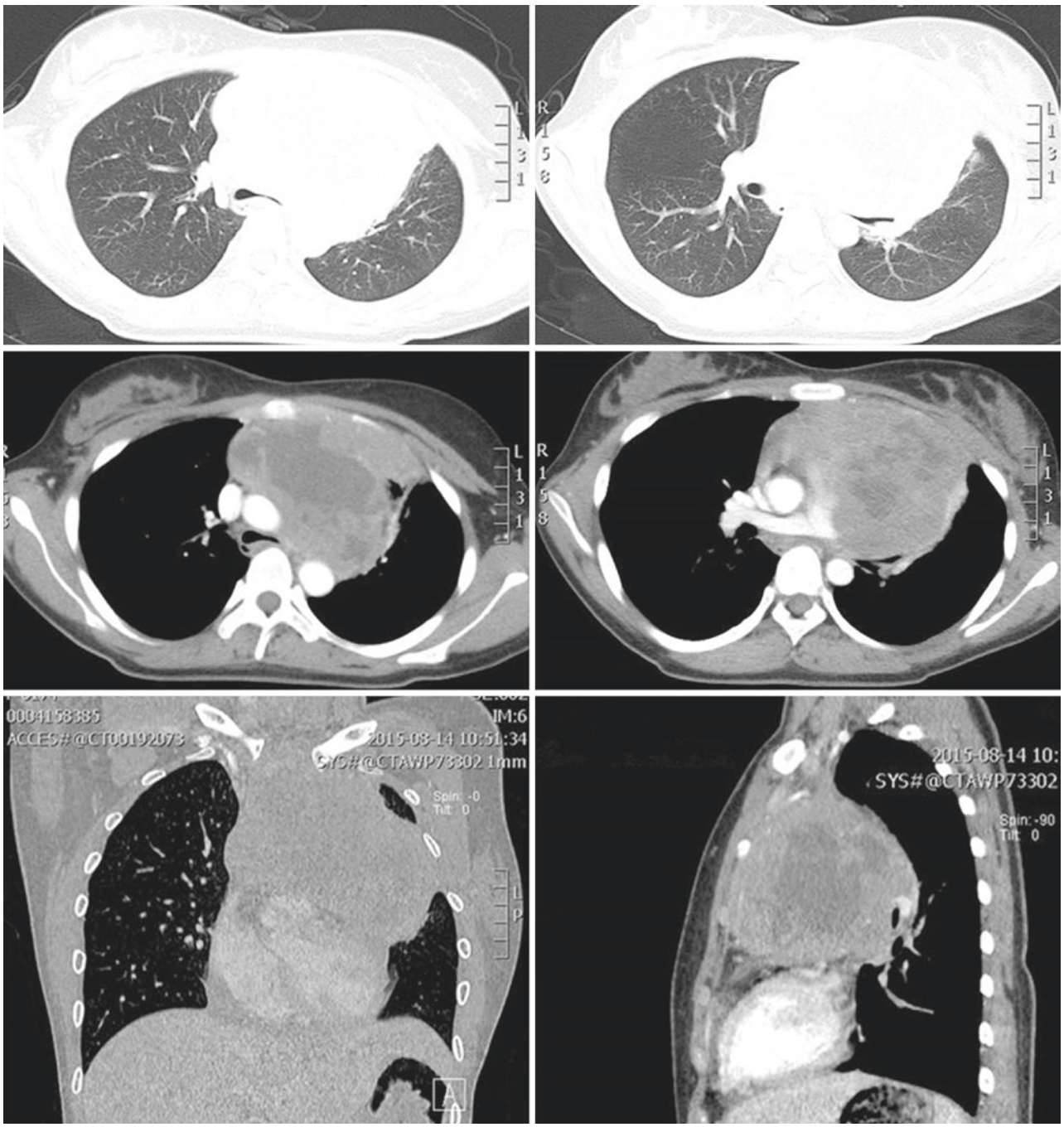

Fig. 9.57 Chest CT images of a 17-year-old woman complained of cough repeatedly for 3 months

nine recurrences resulting in two deaths from local disease and five metastases resulting in two deaths. There is a comparatively low risk for recurrence and metastasis, irrespective of tumor depth.

9.7.12 Case 12

A 45-year-old man complained of cough and suffocation for 2 months.

Chest CT: There was a huge mass in the anterior superior mediastinum, and a few spot calcifications could be seen in the front of the lesion. The CT attentions of unenhanced scan, arterial phase, and venous phase were 24HU, 46HU, and 65HU, respectively (Fig. 9.58).

[**Diagnosis**] Anterior mediastinum malignant tumor

[**Diagnosis basis**] Intraoperatively, the mass measured 26 cm × 20 cm × 18 cm located in the anterior mediastinum, up to the base of the neck, down to the pericardium, extending to both sides of the chest cavity, infiltrating the left bra-

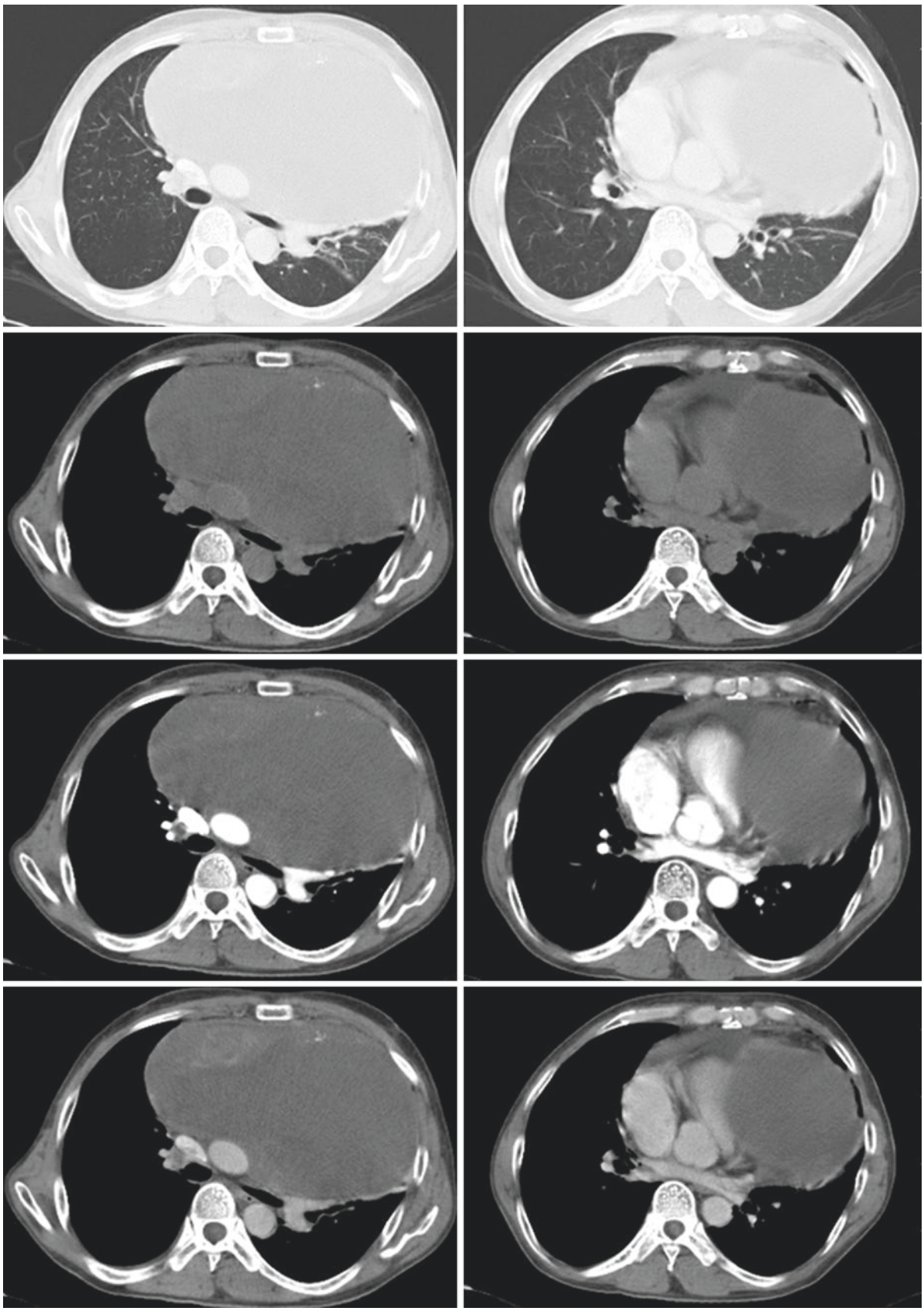

Fig. 9.58 Chest CT images of a 45-year-old man complained of cough and suffocation for 2 months

chiocephalic vein, left subclavian artery, diaphragm nerve, left vagus nerve, aortic arch and left pericardial layer, there was also sheet infiltration in front of the left hilum. Histologically, the tumor was mainly composed of spindle cells, some cells are epithelial (Fig. 9.59), some cells are long spindle, arranged in whorls (Fig. 9.60), and cartilage (Fig. 9.61) and glandular (Fig. 9.62) differentiation can be seen in the tumor. Immunohistochemistry demonstrated positivity for CD99, Bcl-2, and CK8/18, and negativity for S100, MBP, NF, EMA, GFAP, CD34, and Desmin. Pathological diagnosis was malignant peripheral nerve sheath tumor with chondrosarcoma-like differentiation and glandular differentiation, invading the pericardial wall.

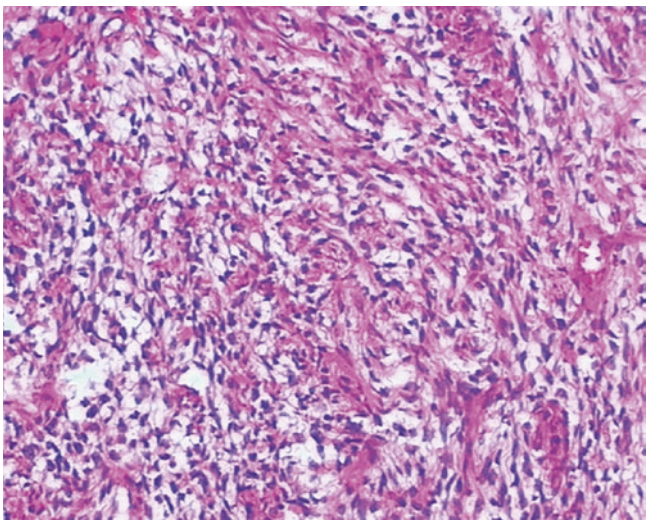

Fig. 9.59 The tumor was mainly composed of spindle cells, and some cells were epithelial

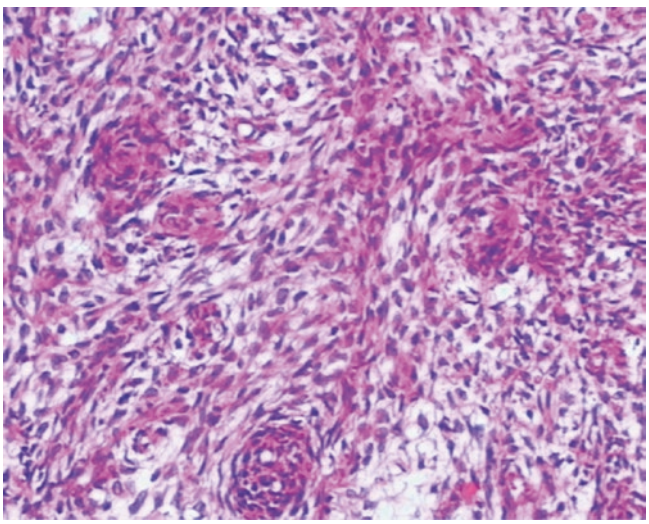

Fig. 9.60 The tumor was mainly composed of spindle cells, arranged in whorls

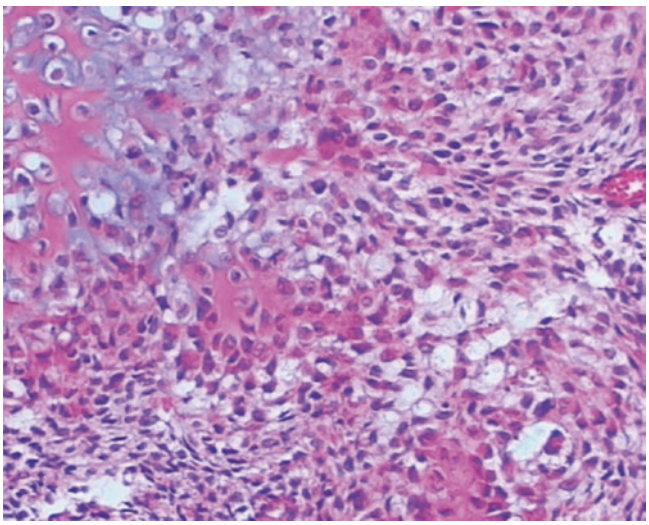

Fig. 9.61 Cartilage differentiation can be seen in the tumor

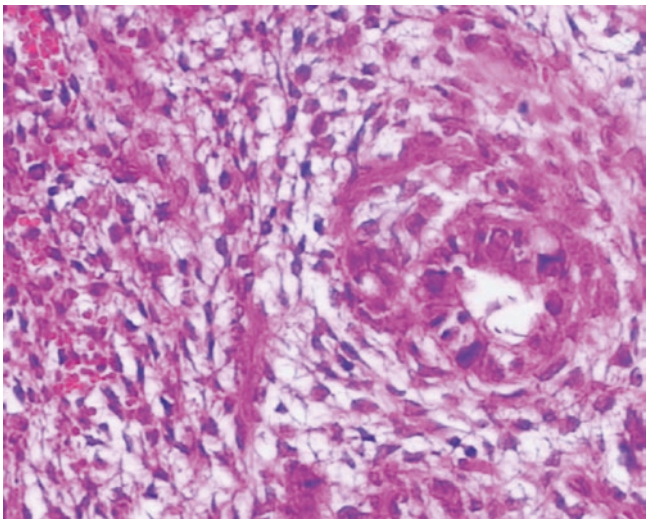

Fig. 9.62 Glandular differentiation can be seen in the tumor

[**Analysis**] Although neurogenic tumors located in the anterior and middle mediastinum only account for 10% of the total, the incidence of malignancy is much higher than that of the posterior mediastinum.

Remarkable developmental plasticity, including divergent differentiation, may be shown in MPNSTs. Although not entirely specific, frequent histologic findings include fascicles of alternating cellularity, palisades, whorls, or rosette-like arrangements, perineural/intraneural spread when associated with nerve, subendothelial accentuation of tumor cells, and large areas of geographic like necrosis. Heterologous differentiation in the form of cartilage and bone, or less commonly smooth muscle, skeletal muscle (so-called malignant triton tumor), angiosarcoma, and even well-formed glands occur on occasion, particularly in patients with NF1.

According to the 2007 WHO classification criteria for nervous system tumors, malignant schwannoma was divided into Epithelioid MPNST, MPNST with glandular differentiation, and MPNST with mesenchymal differentiation (also known as malignant tritontumor, MPNST with rhabdomyosarcoma differentiation). The 2016 version of the new classification added a subtype of perineurial MPNST. Special histological structures such as MPNST with glandular differentiation and MPNST with mesenchymal differentiation were classified into the subtype of MPNST with divergent differentiation. The pathology of this case is in accordance with the new classification of MPNST with divergent differentiation.

MPNST needs to be distinguished from synovial sarcoma, particularly its monophasic variant. Synovial sarcomas usually involve nerves and may even grow in a multinodular or plexiform growth pattern. Although glandular differentiation may be shown in both synovial sarcoma and MPNST, glandular MPNST tends to show glands similar to enteric epithelium with frequent endocrine differentiation, whereas those of synovial sarcoma are lined by cuboidal cells. It is often accompanied by intraluminal eosinophilic necrotic debris. Obviously, a history of NF1 and/or a coexisting neurofibroma precursor indicate the diagnosis of MPNST. By immunohistochemistry, low molecular weight cytokeratins and EMA may be expressed in both synovial sarcoma and MPNST, although the expression of high molecular weight cytokeratins is seen only in synovial sarcoma. S100 may express in both tumors, but CD34 express only in MPNST. Although typically diffuse and strong in synovial sarcomas, transducin-like enhancer protein (TLE1) expression may also be present in a somewhat weaker, more variable pattern in some MPNST. Given the limited discriminatory power of histology and immunophenotype in the differential diagnosis of MPNST and synovial sarcoma, a definitive diagnosis of intraneural synovial sarcoma may require demonstration of *SS18-SSX1* or *SS18-SSX2* gene fusions, usually resulting from a characteristic t(X;18) translocation, because these gene fusions are limited to synovial sarcoma.

9.7.13 Case 13

A 20-year-old woman found a mediastinum mass.

Chest CT: Contrast-enhanced CT image showed a heterogeneous mass in the right posterior mediastinum with regular contour and a slight degree of enhancement (Fig. 9.63).

[**Diagnosis**] Neurofibroma

[**Diagnosis basis**] The posterior mediastinal paraspinal lesion exhibits dilated growth rather than invasive growth. Visible compression of the thoracic spine and ribs can be seen, considering benign neurogenic tumors. Intraoperatively, the tumor was solid and yellowish. Microscopically, it contained cells with long, narrow nuclei as well as wavy bands of spindle-shaped cells with myxomatous interstitial tissue in the background. The histopathological diagnosis was neurofibroma.

[**Analysis**] Neurofibroma was first reported by Verocay in 1908. The disease can occur at any age and there is no obvious gender difference. CT shows sharply marginated, smooth, or lobulated mass with possible split fat sign. Osseous pressure erosion of adjacent ribs and calcification may be seen. CT scan is low density, the CT attention is 20–25HU, mainly due to lipid-rich nerve sheath cells, adipocytes and mucoid degeneration, the central necrosis and cystic change of large tumors are another reason for low density. On MRI, homogeneous low to intermediate signal

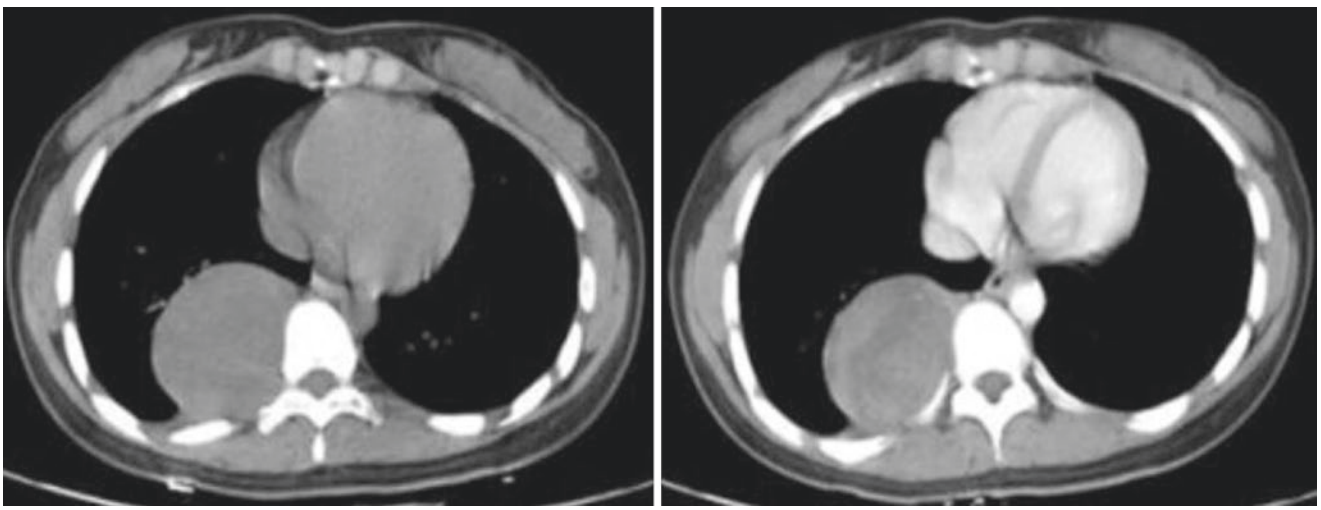

Fig. 9.63 Chest CT images of a 20-year-old woman found a mediastinum mass

intensity on T1-weighted images were shown in neurofibroma. On T2-weighted images, the peripheral region sometimes appears higher signal intensity than the central region (target sign). Corresponding to myxoid degeneration, there are high-intensity regions in the periphery of a neurofibroma on T2-weighted images, whereas nodular areas of low signal intensity correspond to collagenous fibrous tissue. The pattern was absent in lesions with cystic, hemorrhagic, or necrotic degeneration. Varma et al. [6] reported that this target sign on T2-weighted MR images was seen in 52% of cases, and proved helpful in differentiating neurofibroma from malignant peripheral nerve sheath tumors. A target pattern was not visible in malignant lesions. MRI cannot distinguish schwannoma from neurofibroma, and benign tumor may mimic malignant nerve sheath tumors when cystic, hemorrhagic, and necrotic degeneration is present.

9.7.14 Case 14

A 76-year-old man complained of chest pain for 1 month.

Chest CT: A dumbbell-shaped soft tissue mass could be seen on the right chest wall intercostal space, the density was lower than the muscle, and contrast-enhanced CT image showed a slight degree of enhancement during the venous phase (Fig. 9.64).

[**Diagnosis**] Neurofibroma

[**Diagnosis basis**] The lesion grows in a dumbbell shape across the intercostal space, and the adjacent rib is compressed. The diagnosis first considers schwannomas or neurofibromas. The density of the lesion is uniform, no enhancement in the arterial phase, and mild enhancement in the venous phase, which is more in line with the characteristics of neurofibroma. Pathology showed fusiform tumor cells, bland nuclei with inky chromatin, no mitosis, and loose

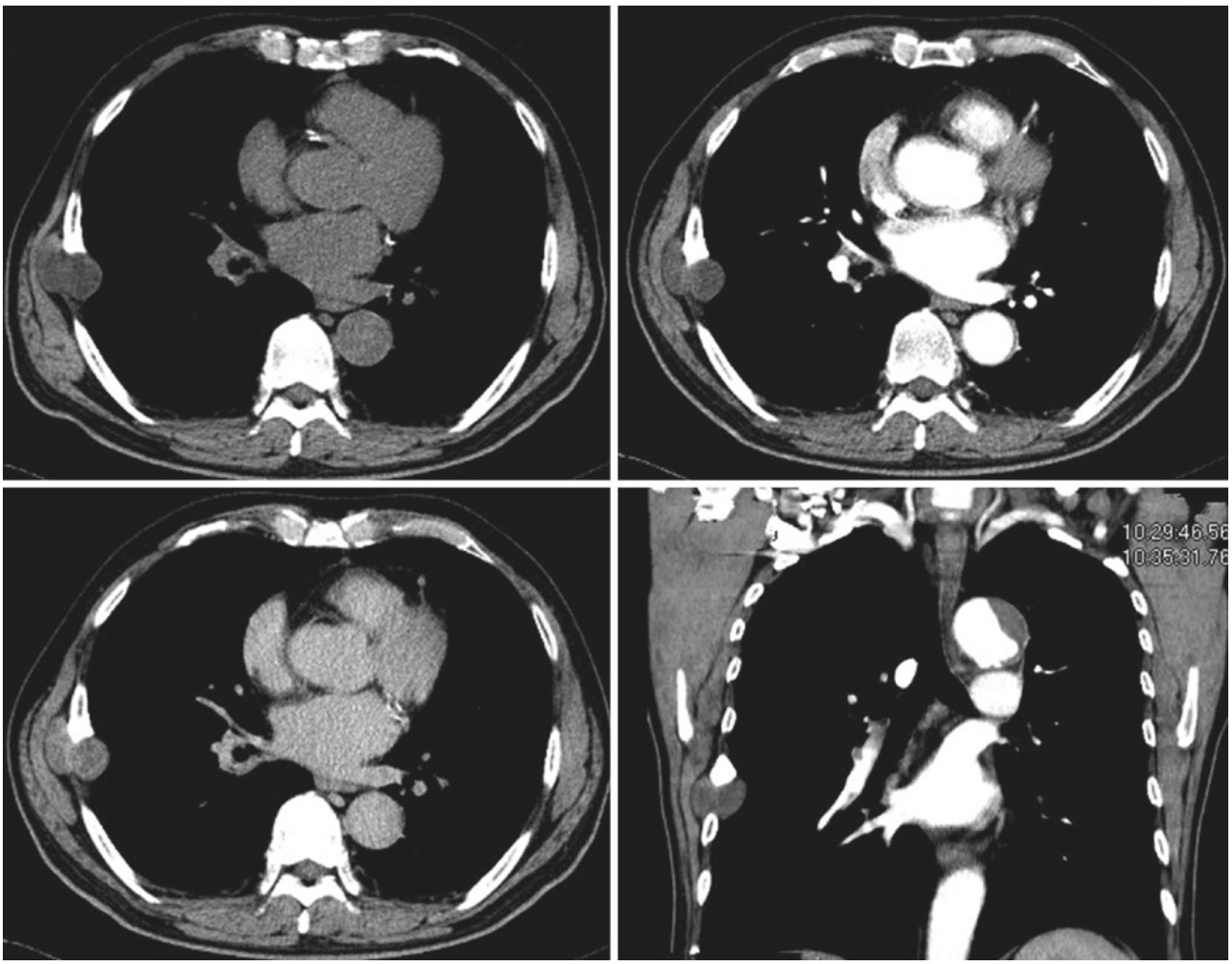

Fig. 9.64 Chest CT images of a 76-year-old man complained of chest pain for 1 month

interstitial. Immunohistochemistry showed S100 positive, and Calretin and CD68 negative. The diagnosis considers neurofibroma.

[**Analysis**] Neurofibroma consists of a proliferation of thick wavy collagen bundles with varying degrees of myxoid degeneration. Neurofibroma also incorporates a mixture of nonneoplastic peripheral nerve components, including axons, fibroblasts, perineurial cells, and variable inflammatory elements, such as mast cells and lymphocytes. By immunohistochemistry, all forms of neurofibroma are positive for S100, SOX10, and CD34. CD34 often has a characteristic "thumbprint" pattern. In contrast to neurofibroma in other localizations, mediastinal neurofibroma is pseudoencapsulated. Pseudoencapsulation was considered to be a host reaction toward the tumor and not a well-defined fibrous capsule.

Some neurofibromas exhibit unusual features such as degenerative cytological atypia (atypical neurofibroma, neurofibroma with ancient change) and/or increased cellularity (cellular neurofibroma), often resulting in the differential diagnosis with MPNST. Immunohistochemistry and genetics play no role in these distinctions. Neurofibromas with atypical features harbor genetic changes that are seen in MPNSTs but not typical neurofibromas, namely loss of CDKN2A/p16, p53, SMARCA2, and others, especially on the 9p2 locus. The term "atypical neurofibroma" should be avoided as it confuses ordinary neurofibromas with degenerative atypia and neurofibromas with true atypical features and premalignant genetic changes. Neurofibromas with atypical features usually develop within a plexiform neurofibroma, which are typically located along major nerves and are not amenable to resection without substantial morbidity. Therefore, despite the increased risk of MPNST in NF1 patients, care should be taken not to over-diagnose malignancy or atypia.

Schwannomas are encapsulated lesions derived from nerve sheaths, which grow from the formation of a lateral mass on the parent nerve, often making the nerve easier to recognize. Schwannomas do not involve the nerve fibers themselves, so they can be resected without sacrificing the nerve, if necessary. On the contrary, it is often impossible to completely resect the neurofibroma while preserving the original nerve, because neurofibromas are nonencapsulated tumors comprising all nerve elements, i.e., axons, sheath cells, and connective tissues.

9.7.15 Case 15

A 17-year-old man complained of right chest pain for 3 months.

Chest CT: There were multiple soft tissue lesions on the right anterior chest wall, right posterior spinal wall, and mediastinum, and the contrast-enhanced scan showed mild and delayed enhancement in the center of the lesions. Low-density lesions were seen behind the bilateral psoas major muscle and there were multiple soft subcutaneous small tumors (Fig. 9.65).

[**Diagnosis**] Neurofibromatosis

[**Diagnosis basis**] A young man with low-density lesions in chest wall, mediastinum, bilateral posterior psoas major muscle, and subcutaneous tissue, the diagnosis first considers neurofibromatosis. The patient underwent biopsy. Microscopically, the tumor was composed of spindle-shaped cells with narrow nuclei without atypia. Edematous interstitial tissue was seen in the background. The histopathological diagnosis was neurofibroma.

[**Analysis**] Neurofibromatosis is a heterogeneous group of hereditary cancer syndromes that result in tumors of the central and peripheral nervous systems. By far neurofibromatosis type 1 (NF1, 96%) is the most common form, followed by neurofibromatosis type 2 (NF2, 3%), and the lesser-known form of schwannomatosis. There is no gender or racial predilection in neurofibromatosis.

NF2 is an autosomal dominant disorder caused by mutations to the *NF2* tumor suppressor gene on chromosome 22q12.2, characterized by a variety of nonmalignant nervous system tumors, including schwannomas, ependymomas, meningiomas, and gliomas, with vestibular schwannomas being the hallmark lesion, affecting 95% of individuals and typically appearing bilaterally. Ocular and cutaneous manifestations also occur.

As the name implies, schwannomatosis is a syndrome characterized by the development of multiple peripheral nerve schwannomas, without concomitant involvement of the vestibular nerve. Schwannomatosis is caused by a mutation in the *SMARCB1*gene, also known as the *INI1*, *BAF47*, or *hSNF5* gene, located on chromosome 22q11.2, centromeric to the *NF2* gene. Unlike NF1 patients with characteristic dermatological findings and NF2 patients with eighth cranial nerve dysfunction at a young age, patients with schwannomatosis have nonspecific symptoms that may delay presentation or imaging time. The majority of the cases of schwannomatosis are caused by de novo mutations, though familial cases exist with an autosomal dominant inheritance pattern. Even in the familial forms, a germline *SMARCB1* mutation is only identified in 40– 50% of cases, indicating that other genetic loci yet to be identified are involved.

The hallmark peripheral nerve sheath tumor in NF1 is neurofibroma. Neurofibromas can be deep, involving single or multiple nerves. These are termed plexiform neurofibromas. There are also cutaneous neurofibromas that involve the skin thickness and cases in which neurofibromas are diffuse and involve both the skin thickness and the deep nerves. Plexiform neurofibromas are estimated to occur in up to 50%

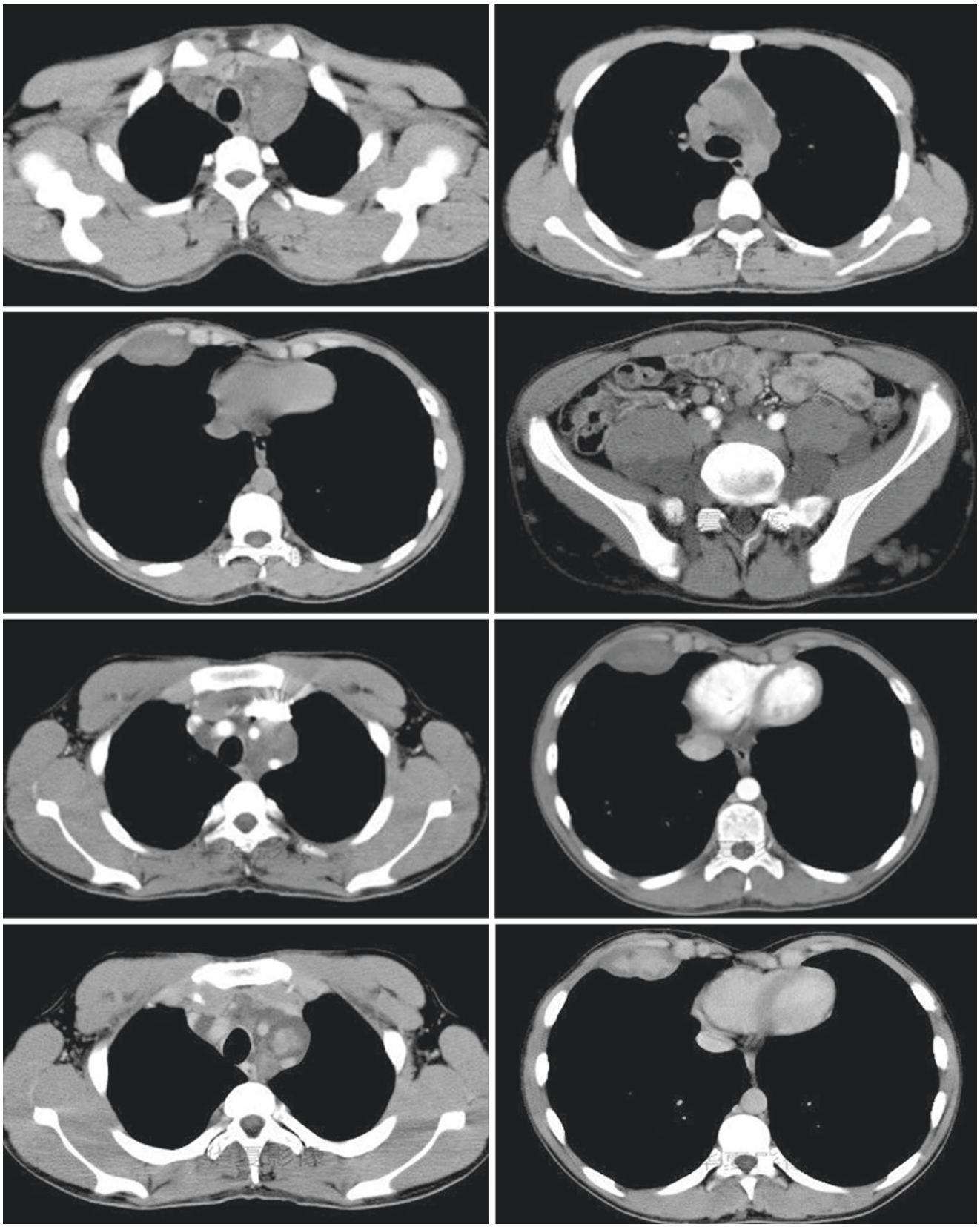

Fig. 9.65 Chest CT images of a 17-year-old man complained of right chest pain for 3 months

of people with NF1. Cutaneous neurofibromas impact up to 99% of adults with NF1. More rarely, there are atypical neurofibromas and malignant peripheral nerve sheath tumors.

Multiple neurofibromas and plexiform neurofibromas should prompt consideration of NF1. Plexiform neurofibromas are characteristic of NF1 and extend along one or multiple nerves and their branches. Most commonly seen in the paraspinal regions, they may also affect the brachial plexus or extremities. The identification of positive family history for NF1, intercostal neurofibromas, café-au-lait spots, or some combination of those factors would help the diagnosis of plexiform neurofibromatosis of the chest. A plexiform neurofibroma by definition involves multiple fascicles of a nerve and is composed of a proliferation of cells extending along the length of the nerve. Usually poorly circumscribed and locally invasive, these tumors contain a heterogeneous mix of Schwann cells, fibroblasts, and other cell types. The nerve is thickened and frequently some surrounding soft-tissue hypertrophy is seen. Although plexiform neurofibromas are considered benign, there is a risk of malignancy in approximately 2–5% of cases. Plexiform neurofibromas usually appear as smooth, well-delimited, round, or elliptical masses in the paravertebral region or along the path of the vagus, recurrent laryngeal, phrenic, or intercostal nerve. Plexiform neurofibromas are usually extensive fusiform or infiltrating masses that tend to surround mediastinal vessels with loss of normally visible fat planes and can cause diffuse mediastinal widening. They show variable contrast material enhancement and may calcify. Both types can remodel, erode, invade, or even destroy adjacent bone structures, thereby simulating more aggressive lesions. It is important to note that these lesions can exert pressure to mediastinal structures, such as the trachea, esophagus, blood vessels, or nerves. The symptoms are mainly those of compression, with chest pain and cough being the most frequent. In rare cases, digestive and other respiratory symptoms, or even superior vena cava syndrome, can also be present. The clinical, imaging, and pathological characteristics of the case are consistent with plexiform neurofibroma.

NF1 recommends various examinations, such as X-ray examination of the chest and long bones, CT scan of the brain and orbit, and MRI of the brain and orbit. Gliomas have a typical fusiform appearance with kinking in MRI. Genetic testing can be helpful when prenatal or preimplantation diagnosis is desired.

9.7.16 Case 16

A 52-year-old man complained of abdominal pain for 4 days. He and his father have a history of neurofibromatosis.

Chest CT: Multiple nodules and masses in both lungs and a large number of pedunculated tumors on the skin surface (Fig. 9.66).

[**Diagnosis**] NF1

[**Diagnosis basis**] A middle-aged male with multiple nodules and masses in both lungs, multiple pedunculated tumors on the skin surface (Fig. 9.67), and a family history of neurofibromatosis, all of them are consistent with the diagnosis of NF1. The patient underwent a needle biopsy, most of which were degeneration and necrotic fibrous connective tissue under the microscope, with small focal neurofibrous tissue and active growth. The pathological diagnosis was neurofibroma.

[**Analysis**] Also known as von Recklinghausen disease or peripheral neurofibromatosis NF1 is an autosomal dominant tumor predisposition syndrome that is most easily characterized by the development of multiple neurofibromas of the peripheral nerves. Malignancies associated with NF1 include malignant PNSTs, leukemia, pheochromocytomas, gastrointestinal stromal tumors, and others. The incidence of NF1 is approximately 1 in every 2500–3000 births. Though about 50% have new mutations, inheritance is autosomal dominant with irregular penetrance and variable expressivity with the gene locus on 17q11. Each child of a parent with NF1 has a 50% risk of developing the disorder. It has a high rate of penetrance and the mutation rate of the NF gene is high with 80% being of paternal origin. The NF1 gene protein product, neurofibromin, is a tumor suppressor expressed mainly in neurons, Schwann cells, glial cells, and melanocytes. A central region of neurofibromin is structurally and functionally homologous to GTPase-activating proteins, which promote the hydrolysis of p21Ras-GTP (the active form) to p21Ras-GDP (the inactive form) by stimulating intrinsic p21Ras-GTPase activity. Because p21Ras proteins play central roles in cell differentiation and growth, inactivation of the *NF1* gene is conducive to the active state (p21Ras-GTP), leading to the permanent stimulation of a cascade of signals and excessive cell division owing to nonregulated activation of the MAP kinase pathway. This pathway could play a role in the development of benign neurofibroma-type tumors, malignant PNSTs, pulmonary hypertension with hyperplasia of pulmonary artery smooth-muscle cells, and interstitial disease, such as hyperplasia/metaplasia of interstitial pulmonary fibroblastic cells.

The earliest known depiction of speculated neurofibromatosis dates back to the thirteenth century with sketches by a Cistercian monk. In 1862, Virchow mentioned the hereditary component when he described a man in which the "body was quite covered with lumps from pinhead-sized to pigeon egg-sized" and he pointed out that the "peculiarities have existed in an inherited manner already over three generations." However, in 1882, Friedrich von Recklinghausen, a student

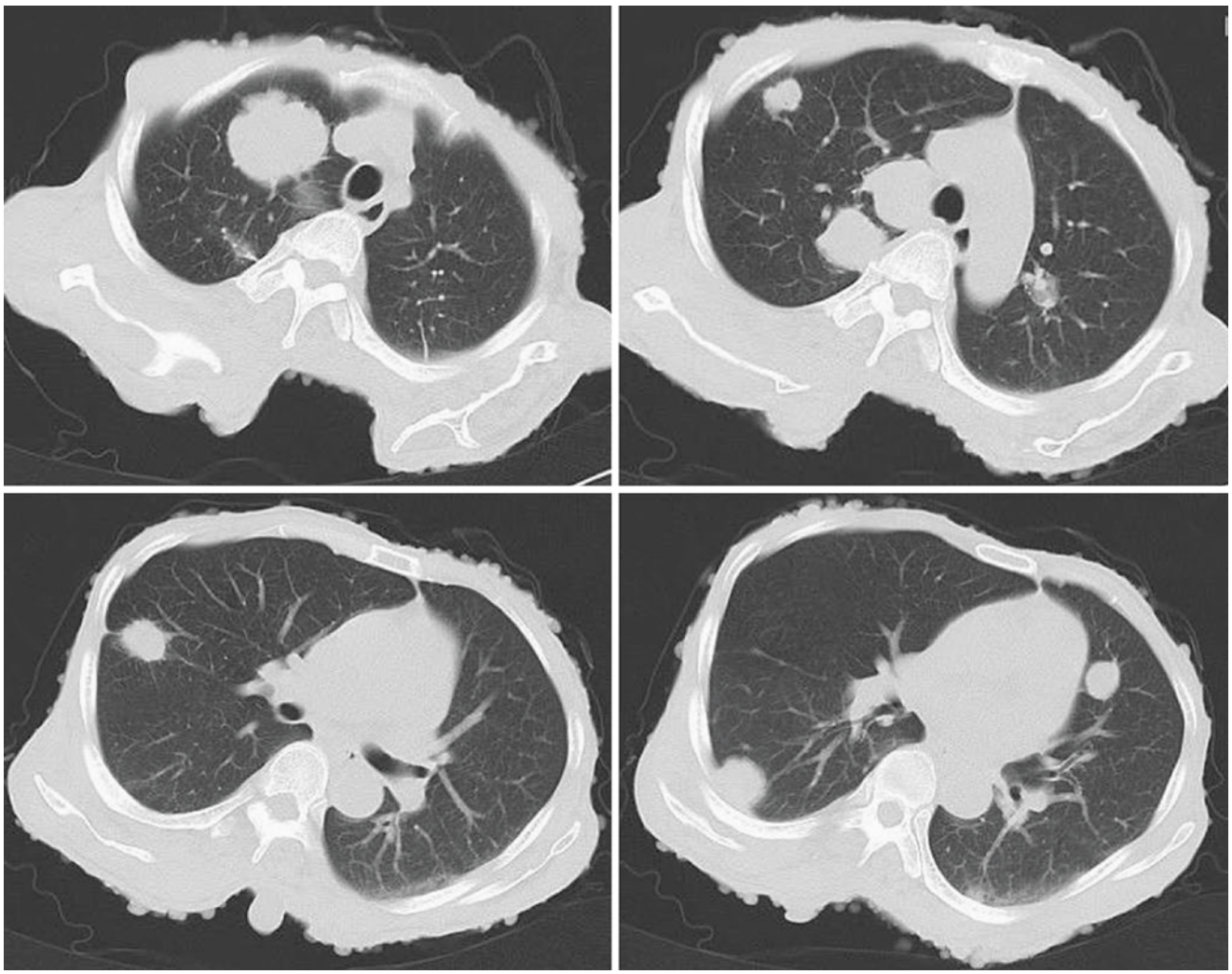

Fig. 9.66 Chest CT images of a 52-year-old man complained of abdominal pain for 4 days

Fig. 9.67 A patient has heterogeneously morphologic appearance of cutaneous neurofibromas, including sessile, globular, and pedunculated cutaneous neurofibromas

of Virchow, gave the most comprehensive clinical and histological description of the disease and coined the term "neurofibroma."

Diagnostic criteria of NF1 was developed in 1987 through the National Institutes of Health Consensus Conference and was updated in 1997. A clinical diagnosis of NF1 requires the presence of at least two of the following features: six or more café au lait macules (diameter >5 mm before puberty and >15 mm after puberty), two or more neurofibromas or one plexiform neurofibroma, freckling in the axillary or inguinal regions, optic pathway glioma, two or more Lisch nodules in the irides, a distinctive bony lesion such as sphenoid dysplasia or thinning of the long bone cortex, and a first-degree relative with NF1. Approximately 50% of patients meet the diagnostic criteria for NF-1 before the age of 1 year, 97% meet the criteria up to the age of 8 years, and virtually all patients fulfill them by the age of 20 years.

Café-au-laitmacules (CALM) are flat, hyperpigmented skin lesions that appear during infancy, and are one of the diagnostic features of NF1 (Fig. 9.68). By adulthood, about 95% of patients with NF-1 have CALM. While not completely specific for NF1, the number of CALMs at presentation is a strong predictor for the diagnosis of NF1. Therefore, greater than five CALMs in a young child highly indicate NF1. However, in the absence of a positive family history of NF1, the presence of CALMs alone is not sufficient to establish a diagnosis of NF1, and additional features are needed. Seventy percent of patients with NF-1 have freckling in the intertriginous areas of the axilla and in the inguinal region, which also can be found at the base of the upper neck, upper eyelids, and under the breasts. These freckles typically appear later in childhood and are usually used as the second diagnostic criterion. Often seen in 95–100% of adults with NF1, lisch nodules are hyperpigmented hamartomas of the iris (visualized best on slit-lamp examination). Lisch nodules usually do not cause any complication and appear as multiple pale, yellowish-brown, oval to round, and dome-shaped papules projecting from the surface of the iris. Neurofibromas may develop in many sites, and can appear as dermal, spinal, or plexiform neurofibroma subtypes. Arising in the nerves of skin, dermal neurofibromas are discrete masses and increase in number with advancing age. NF1 individuals have variable numbers of dermal neurofibromas, with some developing few and others harboring thousands of neurofibromas. Involving multiple nerve bundles, plexiform neurofibromas are complex benign nerve sheath tumors. Different from their discrete counterparts, these tumors are often congenital and grow most rapidly during the first decade of life. These tumors can appear anywhere throughout the body and may have symptoms that reflect nerve or soft-tissue compression. If the skin is overlying a plexiform neurofibroma, hyperpigmentation and fine hair growth may be exhibited in the tumor (Fig. 9.69).

Fig. 9.68 Café-au-lait macules in a region of axillary freckling with cutaneous neurofibromas

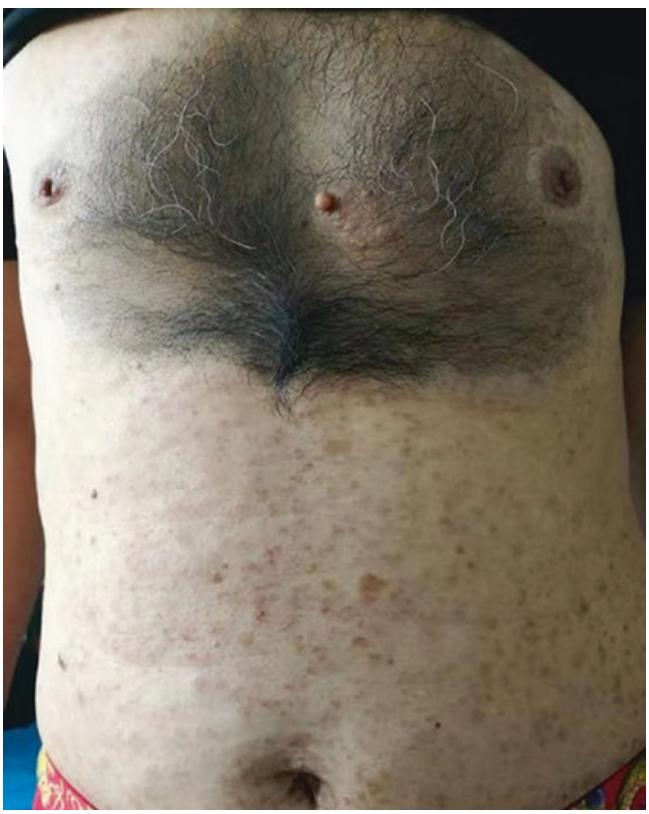

Fig. 9.69 Hyperpigmentation and hair growth

Plexiform neurofibromas are detected on clinical examination in approximately 27% of individuals with NF1. Optic pathway gliomas, seen in about 15–20% of patients with NF1, are usually low-grade astrocytomas that can grow in the optic nerve, optic chiasm, optic tract, and hypothalamus.

Almost all individuals with NF1 develop PNSTs, mainly benign neurofibromas, but about 10% of PNSTs will undergo transformation to malignant MPNSTs. Traditionally, surgical treatment of PNSTs has been considered as a standard approach. The indications for surgical resection of NF include neurologic impairment, pain, and severe disfigurement, and the purpose is to restore or protect function. However, surgery is often challenging or not feasible due to involvement of nervous system structures. The potential benefit from the use of Ras/MAPK pathway inhibitors, immunotherapy, chemotherapy or radiation therapy was underscored by latest evidence and clinical implications for new therapies of PNSTs in patients with NF1.

9.7.17 Case 17

A 60-year-old man complained of pain in bilateral lower limbs for more than a month. On examination, the power of bilateral lower limbs was 4/5, and knee and ankle reflexes were brisk with extensor plantar response. MRI of the spinal cord revealed abnormal epidural signal behind theS1 level and multiple abnormal signals in the thoracic, lumbar, and back skin, and left erector spinae muscles at the L4–5 level.

Chest CT: Multiple nodules and cystic changes in lungs, and left pleural effusion, and large number of pedunculated tumors on the skin surface (Fig. 9.70).

[**Diagnosis**] NF1

[**Diagnosis basis**] The patient's symptoms, signs, and imaging findings are consistent with NF1.

[**Analysis**] NF1 is a genetic syndrome characterized by clinical manifestations of systemic and progressive involvement that mainly affect the nervous system, skin, bones, and eyes, and can affect any other organ. Collections of neurofibromas, café-au-lait macules, axillary and inguinal freckling, and pigmented hamartomas in the iris (Lisch nodules) are the main features of NF1 and represent some of the diagnostic criteria for this disease. Less common features include bone deformities (pseudarthrosis, dysplasia), short stature, scoliosis, seizure disorders, cognitive deficits, peripheral neuropathies, and more serious manifestations, such as plexiform neurofibromas, malignant PNSTs, and optic nerve and other central nervous system gliomas. Cognitive problems are the most common neurological complications in individuals with NF1. Severe intellectual disability with an intellectual quotient <70 (mental retardation) is rare and only slightly more frequent than in the general population. Approximately 6%–7% of individuals with NF1 develop epilepsy.

The thorax and lungs can be affected in several ways, including by the development of cutaneous and subcutaneous neurofibromas on the chest wall, ribbon deformity of the ribs, kyphoscoliosis, posterior vertebral scalloping, meningoceles, intrathoracic neurogenic neoplasms, bullous lung disease (Fig. 9.71), pulmonary hypertension (PH), and interstitial lung disease (Fig. 9.72), and are reported in 10–20% of adults with the disease.

Davies [7] first described the association between neurofibromatosis and diffuse lung disease (NF-DLD) in 1963. However, the exact prevalence and reason for its association are still unclear. Zamora et al. [8] retrospectively analyzed 64 NF-DLD cases reported in 16 articles. The mean age of patients was 50 years. Males outnumbered females, and most reported dyspnoea. Twelve were ever-smokers among the 16 subjects with documented smoking histories. HRCT scan results of eight patients demonstrate ground-glass opacities (37%), bibasilar reticular opacities (50%), bullae (50%), cysts (25%), and emphysema (25%); none had honeycombing. Surgical biopsy results in a group of 14 patients showed findings of interstitial fibrosis (100%) and interstitial inflammation (93%). In conclusion, NF-DLD is a definable clinical entity, characterized by upper lobe cystic and bullous disease and lower lobe fibrosis. Its relationship with smoking remains unclear. In 2015, chest CT images of 88 patients with NF-1 were reviewed by Ueda et al. [9]; 44 (51%) were positive for subcutaneous nodules, 34 (39%) for skin nodules, 20 (23%) for scoliosis, 16 (18%) for emphysema, 13 (15%) for cysts, 13 (15%) for mediastinal masses, 8 (9%) for nodules, and 8 (9%) for ground-glass nodules. No patient had interstitial pneumonia. An upper-lobe-dominant distribution of cysts was shown in this series, in agreement with all previous reports. There was no significant difference in the rate of cysts between smoking and nonsmoking patients, suggesting that smoking does not affect the appearance of cysts in patients with NF1. Furthermore, it showed an upper- and peripheral-dominant distribution of emphysema. It is still unclear about the association between smoking and emphysema in patients with NF1.

Interstitial lung disease in patients with NF1 is pathologically similar to other diseases that produce interstitial fibrosis. In its initial stages, its characteristics are thickening and lymphoplasmocytic cellular infiltration of the alveolar wall, with enlargement and desquamation of alveolar lining cells. Subsequently, this cellular response is replaced by fibrosis, leading to destruction of the alveoli, confluence of air spaces, formation of bullae, and obliteration of blood vessels. Caused by the expansion of the alveolar septa by lymphocytic inflammatory cells, with variable and increased amounts of interstitial smooth muscle and fibrosis, this histopathology is

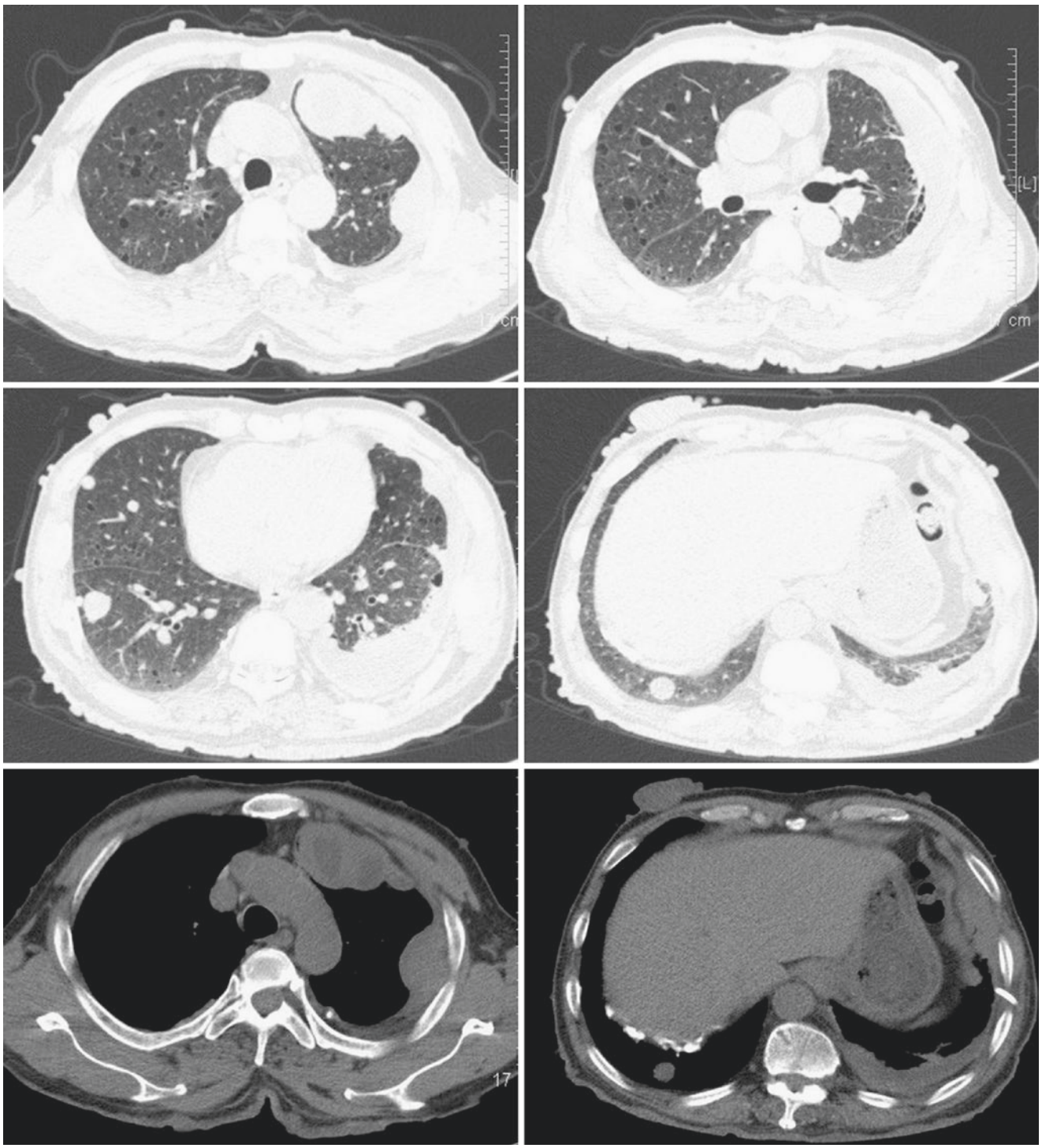

Fig. 9.70 Chest CT images of a 60-year-old man complained of pain in bilateral lower limbs for more than a month

consistent with a nonspecific interstitial pneumonia pattern. Increased numbers of intra-alveolar eosinophils and desquamated pneumocytes was also reported by Massaro and Katz [10], rather than pigmented macrophages, as would be expected in desquamative interstitial pneumonia or respiratory bronchiolitis, entities linked to smoking. Therefore, these findings support the hypothesis that NF-DLD (interstitial/cystic) is a distinct manifestation of NF1, rather than a pure smoking-related disease. However, NF1 may increase the sensitivity of the lungs to cigarette smoke, thereby

Fig. 9.71 A 60-year-old man with NF1. CT images showed numerous large subpleural bullae and emphysema with predominance in the upper lobes. Multiple cutaneous neurofibromas were visible in the thoracic wall (red arrow)

increasing the severity of NF-DLD in smokers and leading to early development of emphysema-like changes in these patients.

Centrilobular nodules and parenchymal cysts show an apical predominance, and some subpleural cysts can simulate paraseptal emphysema. In the advanced stages of NF1, damage from diffuse cystic disease may progress to chronic respiratory failure, and may even result in more serious complications, such as spontaneous pneumothorax or PH, mostly secondary to hypoxemia.

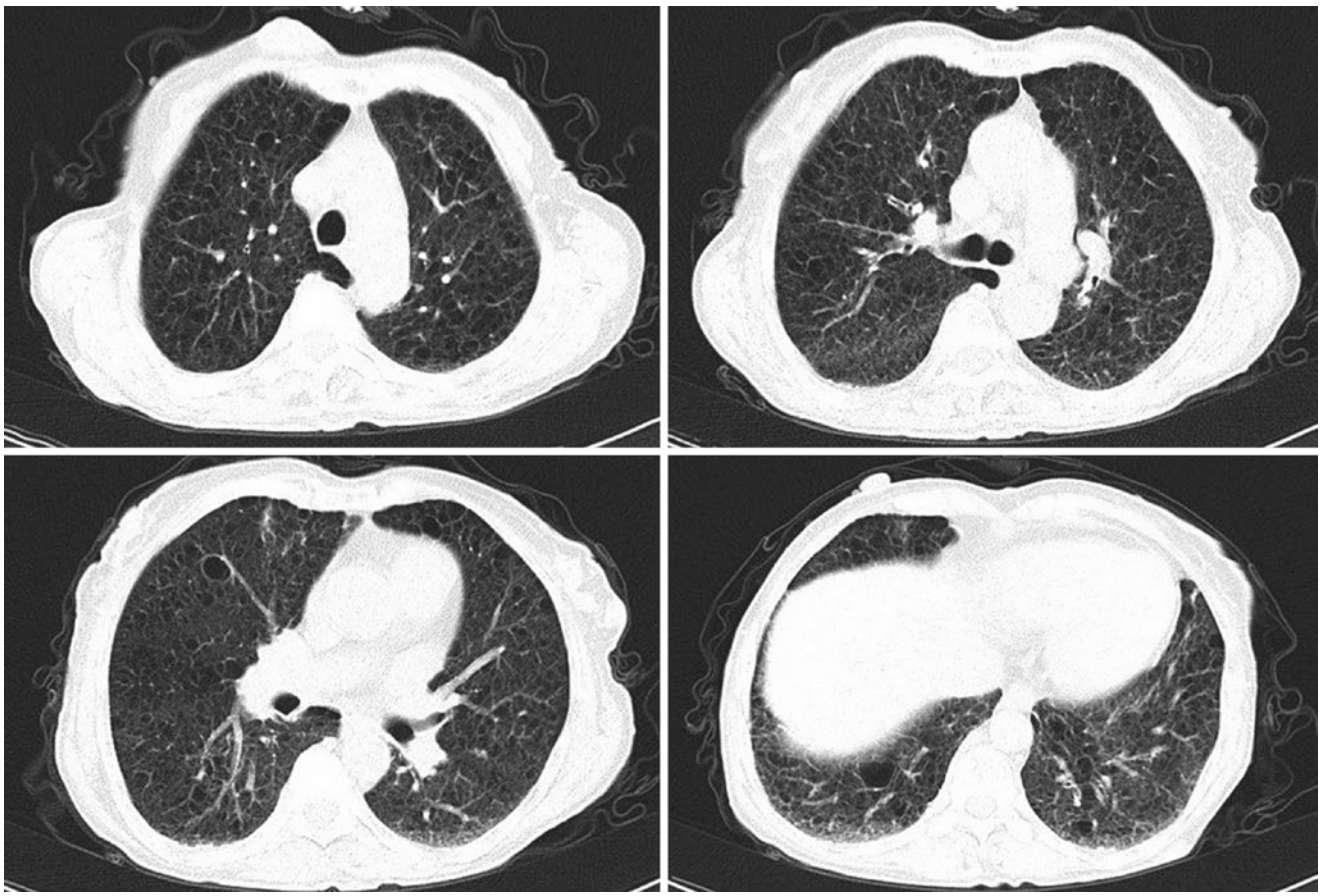

Fig. 9.72 A 64-year-old woman with NF1. CT images showed interstitial lung disease. Multiple cutaneous neurofibromas were visible in the thoracic wall

PH associated with NF1 (PH-NF1) is a rare but severe complication of NF1 and is classified as Group 5 PH, defined as "PH with unclear and/or multifactorial mechanisms." PH-NF1 was characterized by a female predominance, an advanced age at diagnosis, an association with parenchymal lung disease in two out of three cases and poor long-term prognosis. Parenchymal lung disease is absent in one-third of PH-NF1 cases, and the severity of PH is disproportionate to the degree of NF-DLD in other cases, which supports the hypothesis of a specific vascular disease, rather than disease secondary to hypoxemia. There is no data available on the efficacy of specific pulmonary arterial hypertension treatment in PH-NF1. Therefore, these patients should be assessed in expert PH centers and referred for lung transplantation at an early stage.

It is pivotal to recognize the various clinical and imaging features of NF-DLD in making a presumptive associative diagnosis, as well as defining the extent of pulmonary involvement; it also aids decision making about disease management.

9.7.18 Case 18

A 27-year-old man's physical examination revealed a mediastinal mass.

Chest CT: A craniocaudally oblong-shaped mass in the right posterior upper mediastinum, the density was lower than the muscle tissue, and showed no marked enhancement (Fig. 9.73).

MRI: T1WI showed equal signal (Fig. 9.74), T2WI showed slightly higher signal (Fig. 9.75), T2WI fat-suppressed scan showed intermediate signal intensity mass with somewhat whorled appearance (Fig. 9.76), and axial contrast-enhanced T1WI showed slightly enhancement (Fig. 9.77).

[**Diagnosis**] Ganglioneuroma

[**Diagnosis basis**] Intraoperatively, a solid gray-white mass was seen, and histologically, the tumor contained hyperplastic nerve fiber tissue and scattered ganglion cells. The pathological diagnosis was ganglioneuroma.

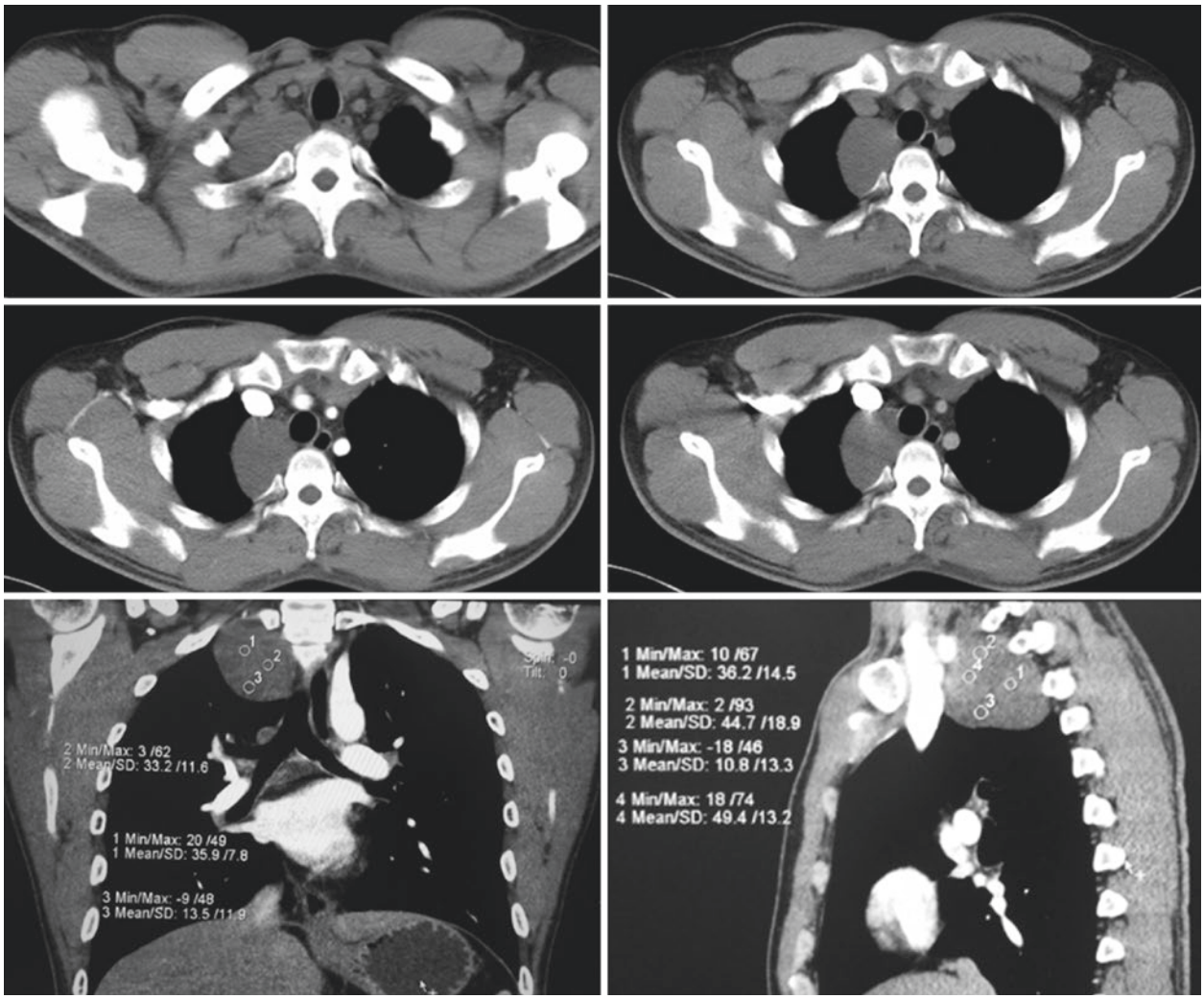

Fig. 9.73 Chest CT images of a 27-year-old man's physical examination revealed a mediastinal mass

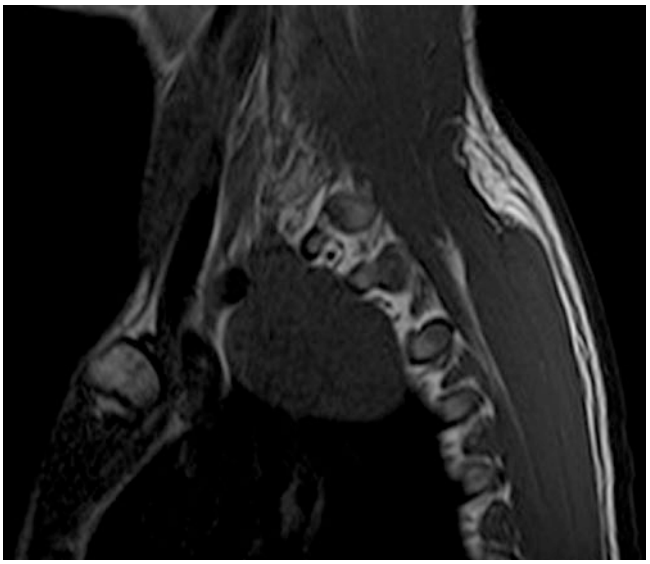

Fig. 9.74 T1WI showed equal signal

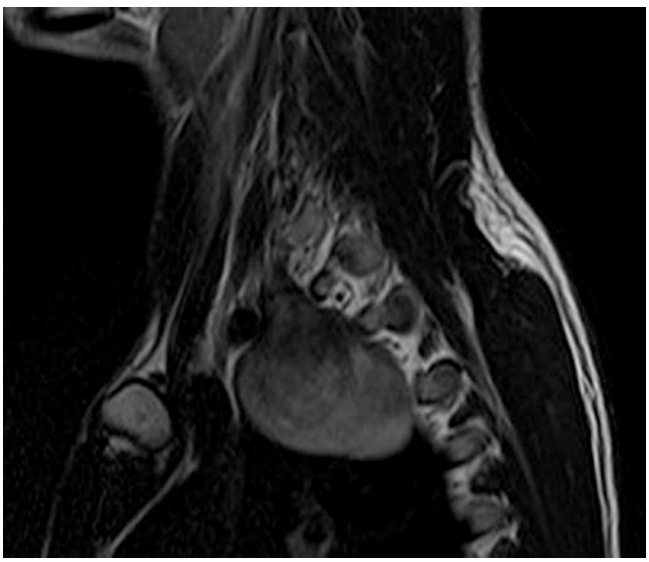

Fig. 9.75 T2WI showed a slightly higher signal

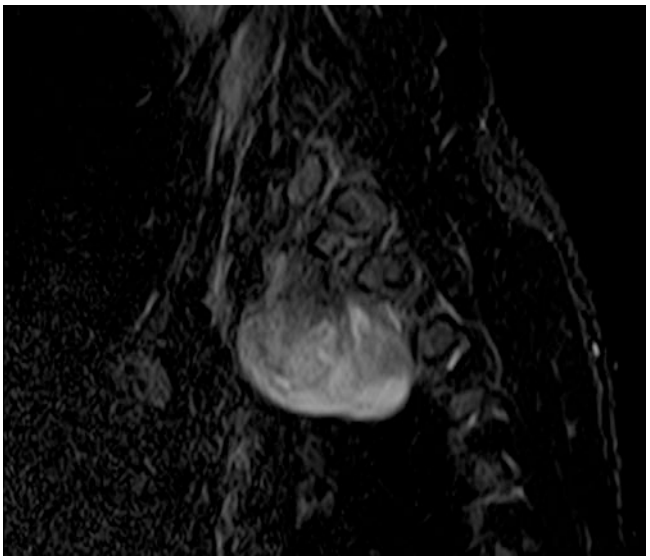

Fig. 9.76 T2WI fat-suppressed scan showed intermediate signal intensity mass with somewhat whorled appearance

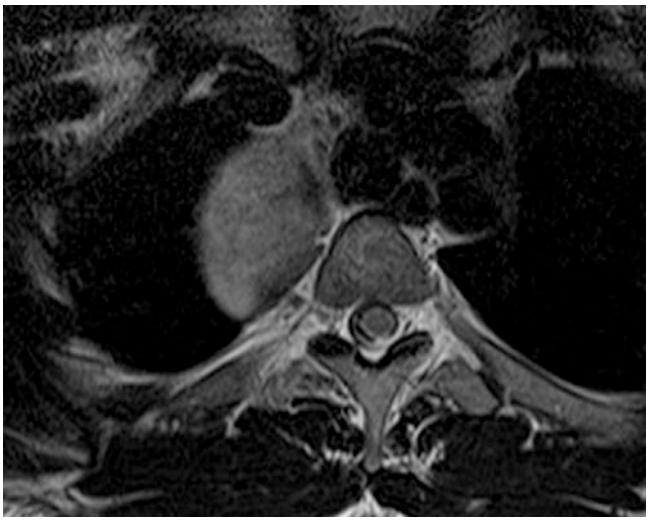

Fig. 9.77 Axial contrast-enhanced T1WI showed slightly enhancement

[**Analysis**] Ganglioneuromas are responsible for up to 35% of the intrathoracic neurogenic tumors. Ganglioneuroma generally manifests as broad-based, well-marginated, oblong masses along the anterolateral aspect of the spine, typically spanning three to five vertebrae. Compared with nerve sheath tumors, calcifications are more common in ganglioneuroma. On unenhanced CT, low internal attenuation relative to muscle corresponding to abundant myxoid matrix is characteristic. Some tumors may be slightly hyperattenuating when ganglion cells predominate. MRI features of ganglioneuromas include homogeneous, intermediate signal intensity on all sequences with an occasional whorled appearance of low-signal-intensity curvilinear or nodular bands on T1- and T2-weighted images.

Ganglioneuroma is composed of Schwann cells, nerve fibers, mature ganglion cells, and mucous matrix. The diagnosis depends on the observation of ganglion cells. When mucous matrix accounts for a large proportion, CT reveals hypodensity, while T2WI shows hyperintense signals. When ganglion cells and nerve fibers increase, CT reveals increased density, while T2WI shows slightly hyperintense signals. Heterogeneous hypointense signals in lesions on T2WI correspond to ganglion cells and nerve fibers. Curved or linear hypointense signals scattered was found in T2WI among the hyperintense signals, presenting with a whorled appearance. These hypointense signals represent scattered Schwann cells and collagenous fibers. Lonergan et al. [11] suggest that the whorled appearance is a typical feature of ganglioneuroma.

Some researchers believe that the adipose tissue in the posterior mediastinal lesion is a characteristic feature for diagnosis of ganglioneuroma. In this type of ganglioneuromas, two potential etiologies have been proposed to explain the presence of fatty components. One theory considers that the fatty component originates from involvement of paravertebral fat. Alternatively, ganglioneuroma may undergo fatty degeneration. The latter hypothesis can also explain why the older mean age of patients presenting with fat-containing ganglioneuromas. The average age of these patients is typically reported to be in the mid-forties, which is higher than the typical age for ganglioneuromas.

The imaging features of 14 pathologically confirming ganglioneuromas were defined by Kato et al. [12] on CT and MRI, and they reported that ganglioneuromas were typically well-delineated lesions that had oval or lobulated contours and appeared craniocaudal longitudinal growth with predominantly low attenuation on CT and seen as a hypointense lesion on T1-weighted and hyperintense lesions on T2-weighted sequences on MRI. Calcification on CT scan was seen in 38% of the cases. Whorled appearance (42%) and tailed-shaped edge (14%) were seen on both CT and MR images. Fat components (29%) observed histologically were also detected in tumors on CT and MR images. Contrast enhancement of the tumors was poor in 46% on dynamic CT study. All lesions were enhanced in all 5 contrast-enhanced MR examinations.

9.7.19 Case 19

A 17-year-old woman's physical examination revealed a mediastinal mass.

Chest radiograph and CT: Chest radiograph and coronal reconstruction showed bilateral posterior mediastinal lesion, which traveled longitudinally along the spine. The contrast-

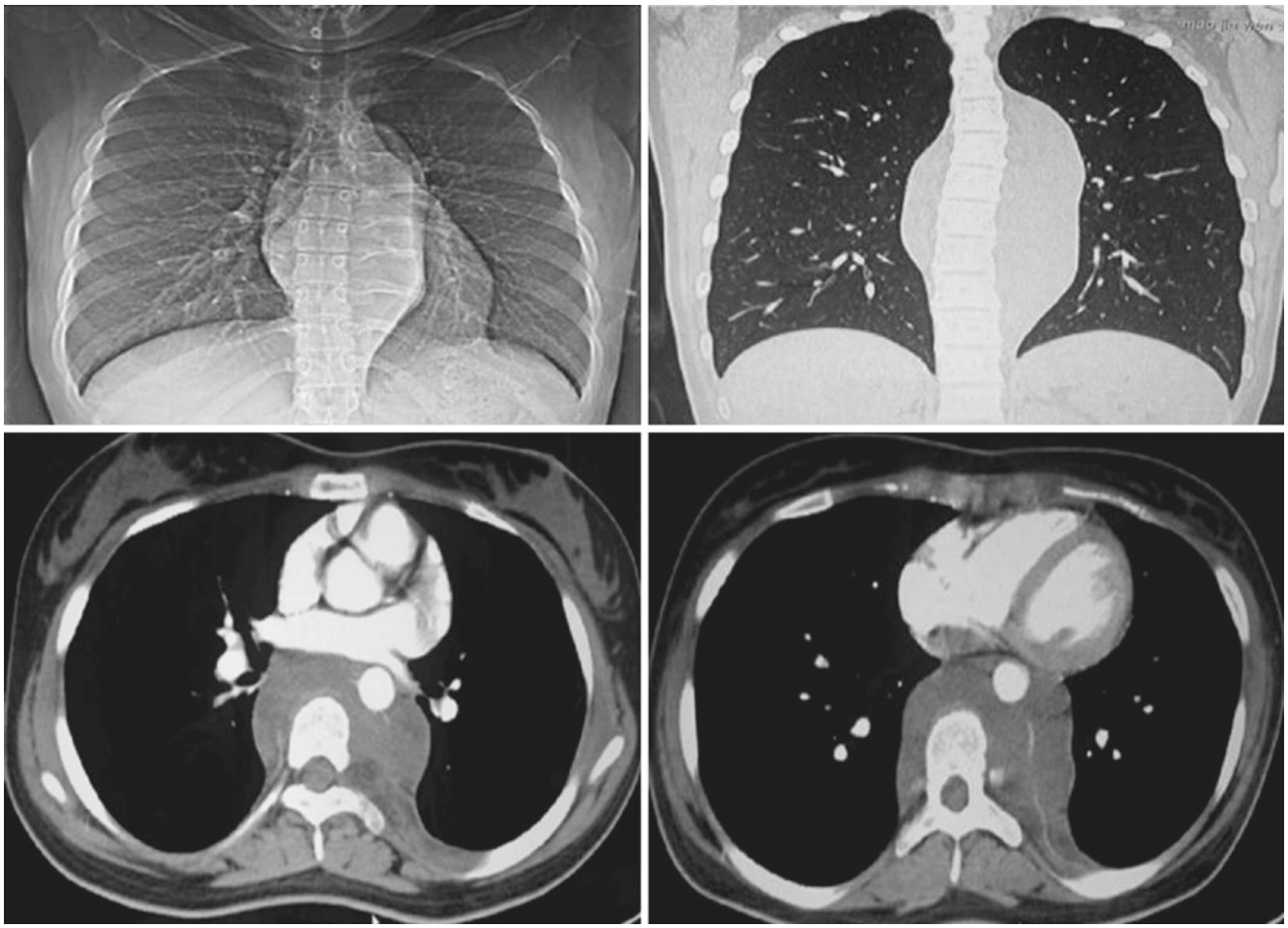

Fig. 9.78 Chest CT images of a 17-year-old woman's physical examination revealed a mediastinal mass

enhanced scan was slightly enhanced, and enhanced linear vascular shadows were visible (Fig. 9.78).

[**Diagnosis**] Ganglioneuroma

[**Diagnosis basis**] The differential diagnosis for posterior mediastinal lesions includes a benign or malignant tumor of neural origin, sarcoma, and lymphoma. Posterior mediastinal lymphoma is rare and the absence of mediastinal lymphadenopathy or other significant findings in the thorax made the diagnosis of lymphoma less likely. The tumor compressed surrounding structures rather than invading them, suggesting that the lesion is benign tumor. The lesions arising in the bilateral paraspinal space limit the differential diagnosis to ganglioneuroma and nerve sheath tumors. Posterior mediastinal tumors with a broad base along the anterolateral aspect of the spine are more likely to be ganglioneuroma rather than schwannoma or neurofibroma. Moreover, the patient's age is more consistent with ganglioneuroma, as schwannoma and neurofibroma are more common among adults. The other features such as hypodense, mildly heterogeneous, and fatty components further narrow the differential diagnosis to ganglioneuroma. Histologically, the lesion was composed of numerous clusters of ganglion cells and a small amount of mature fat cells, typical for ganglioneuroma.

[**Analysis**] Located on the side of the vertebral bodies, the thoracic sympathetic trunks and their associated ganglia form the autonomic nervous system. Ganglioneuromas are benign neuronal tumors that grow slowly and can potentially occur anywhere along the peripheral sympathetic chains. Therefore, although the growth of the lesion along bilateral sides of the spine is rare, it still meets its distribution characteristics. The ganglioneuromas are often found in females, while the male/female ratio is approximately two-third.

Scoliosis may occur in the posterior mediastinum. Although most cases of scoliosis are idiopathic, scoliosis may also be congenital or may be associated with neuromuscular diseases, developmental dysplasia, infections, or tumors. In rare cases, ganglioneuromas may cause painless progressive spinal deformity. There are three types of paravertebral ganglioneuroma and scoliosis: (1) the tumor grows expansively, leading to damages in the side and front vertebrae and eventually to scoliosis; (2) scoliosis is mechanically

stimulated, induced the tumor; and (3) paravertebral ganglioneuroma and scoliosis occur simultaneously. Scoliosis may be caused by irregular tumor location, but the exact mechanism remains unknown. Some scholars propose that tumors stimulate the epiphyseal plate and hence cause osteoepiphysis hyperplasia. Some scholars believe that the tumor involved paravertebral muscle of convex side, causing the convex side muscle atrophy.

9.7.20 Case 20

A 16-year-old girl's physical examination revealed a mediastinal mass for 5 days.

Chest CT: A large mass measured 9.4 cm × 11.5 cm located in the left lung, with speckled calcifications and slight enhancement (Fig. 9.79).

[**Diagnosis**] Ganglioneuroma

[**Diagnosis basis**] An adolescent female had large soft tissue mass in the left lung, with complete capsule (red arrow), spotty calcifications, and no obvious enhancement. CT reconstruction shows that the mass grows in the adjacent structural space, embeds the left subclavian artery (black arrow), pushes the left common carotid artery and left innominate vein, and the left subclavian artery emits small blood vessels passing through the mass (white arrow), showing "vascular floating sign." Surrounding adjacent blood vessels but showing little or no lumen narrowing is a more specific imaging manifestation of ganglioneuroma, and is related to the characteristics of tumors often extending along the vascular structure and sympathetic nerve. Based on the patient age, gender, and imaging characteristics of this case, the possibility of ganglioneuroma is first considered. The patient underwent biopsy, and the pathology was consistent with ganglioneuroma.

[**Analysis**] Ganglioneuroma needs to be distinguished from other tumors that originate in the peripheral nervous system. Ganglion-origin tumors include completely mature ganglioneuroma, partially mature ganglioneuroblastoma and lowly differentiated neuroblastoma. Neuroblastoma and ganglioneuroblastoma are evidently enhanced at an early stage and may invade adjacent tissues and blood vessels. They may have osseous metastasis with coarse calcification in the lesions and appear early enhancement in imaging. Schwannoma is mostly prone to cystic changes and necrosis. In CT and MRI, there is heterogeneous density/signals in schwannoma, mostly enhanced moderately and even enhanced apparently in the arterial phase, while homogeneous density/signals are shown in ganglioneuroma, enhanced or non-enhanced in the arterial phase and progressively mildly enhanced in the delayed phase. Ganglioneuroma can grow around the blood vessel but does not invade the blood vessel wall, schwannoma and neurofibroma have no such characteristics.

Thoracic ganglioneuroma needs to be differentiated from other cystic tumors. Cystic teratoma has multiple cavities, as well as calcification in the cystic wall. CT may show fat density and calcification shadow in the lesion. Fat, calcification, and fat tissue/fluid level are specific features of cystic teratoma. With homogeneous density higher than water, bronchocoele and oesophageal cyst are congenital mediastinal cystic lesions. They are not enhanced in the early phase and delayed phase. Ganglioneuroma is progressively enhanced in the delayed phase, which can be differentiated from other cystic tumors.

Ganglioneuroma is benign posterior mediastinal tumor requiring complete surgical excision as they can cause severe pain and compression symptoms. Knowing the patient's age and clinical course and typical imaging findings will increase the percentage of correct diagnoses.

9.7.21 Case 21

A 5-year-old girl complained of cough and chest tightness for 1 month.

Chest CT: An elliptical mass in the left posterior mediastinum, with localized calcification, invading adjacent ribs and chest wall, and linear enhancement seen on the contrast-enhanced scan (Fig. 9.80).

[**Diagnosis**] Ganglioneuroblastoma

[**Diagnosis basis**] Chest CT revealed a giant posterior mediastinal tumor with spotty calcification (red arrows) and slightly, line-like enhancement (white arrow). The boundary between the lower margin of the lesion and the pleura is unclear, combined with the patient age, the possibility of ganglioneuroblastoma or neuroblastoma is considered. The lesions were mildly invaded and the necrosis was not obvious, which is more in line with the characteristics of ganglioneuroblastoma and confirmed by surgical pathology.

[**Analysis**] Ganglioneuroblastoma (GNB) is a rare peripheral neuroblastic tumor. GNB represents 20% of all neuroblastomas and has pronounced cell polymorphism with ganglionic cells with different degrees of maturation and calcification areas. GNB accounts for 33% of sympathetic nerve tumors of the chest. It consists of gangliocytes and immature neuroblasts, indicating an intermediate malignancy. Gross features are composed of a well-defined or infiltrating tumor, usually encapsulated. Microscopic features are characterized by the coexistence of neuroblasts and typical ganglion cells with varying aspects based on the differential degree of the tumor cells. Neuroendocrine markers may be expressed in neural and ganglion cells. Schwann cells express S100 protein.

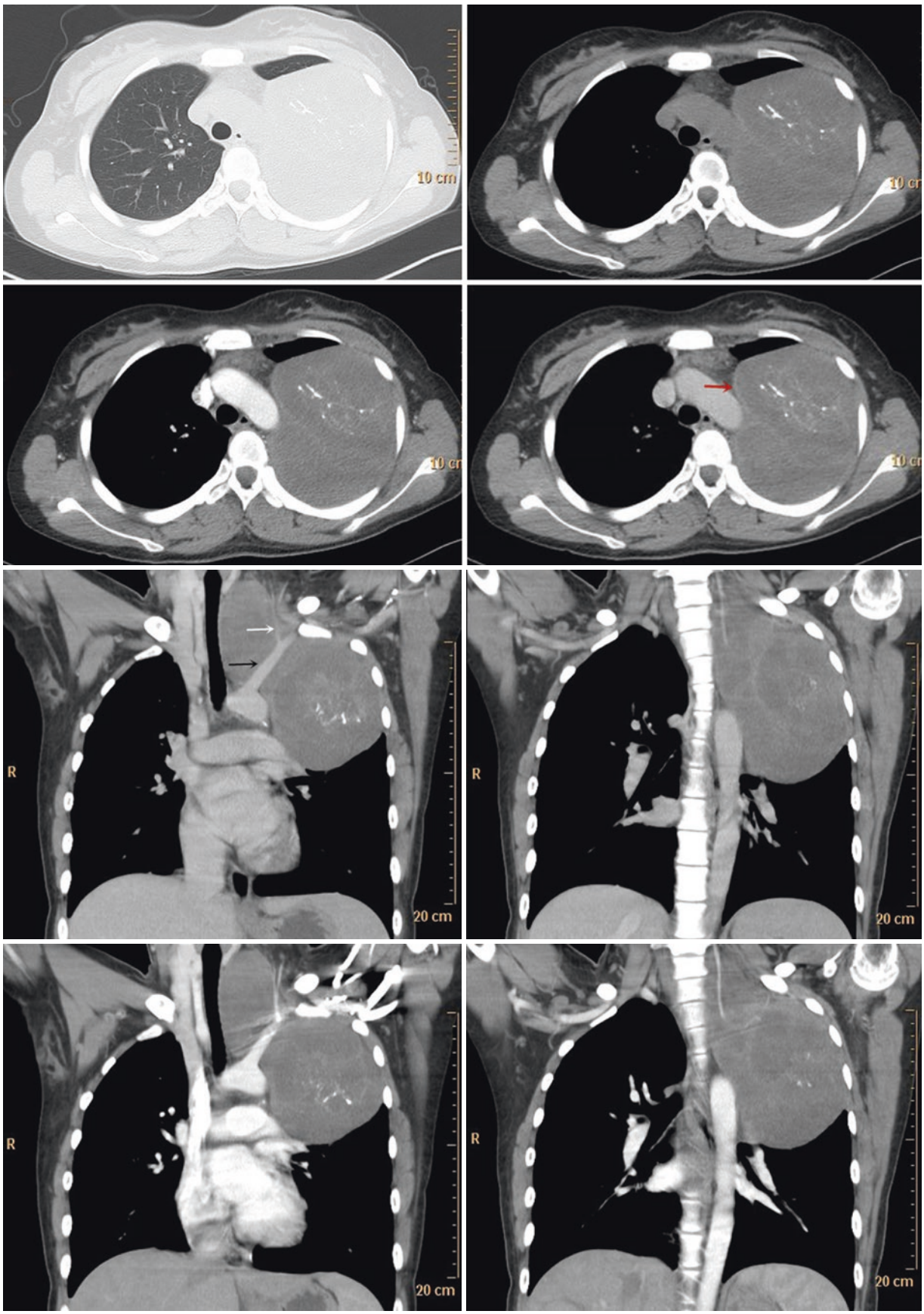

Fig. 9.79 Chest CT images of a 16-year-old girl's physical examination revealed a mediastinal mass for 5 days

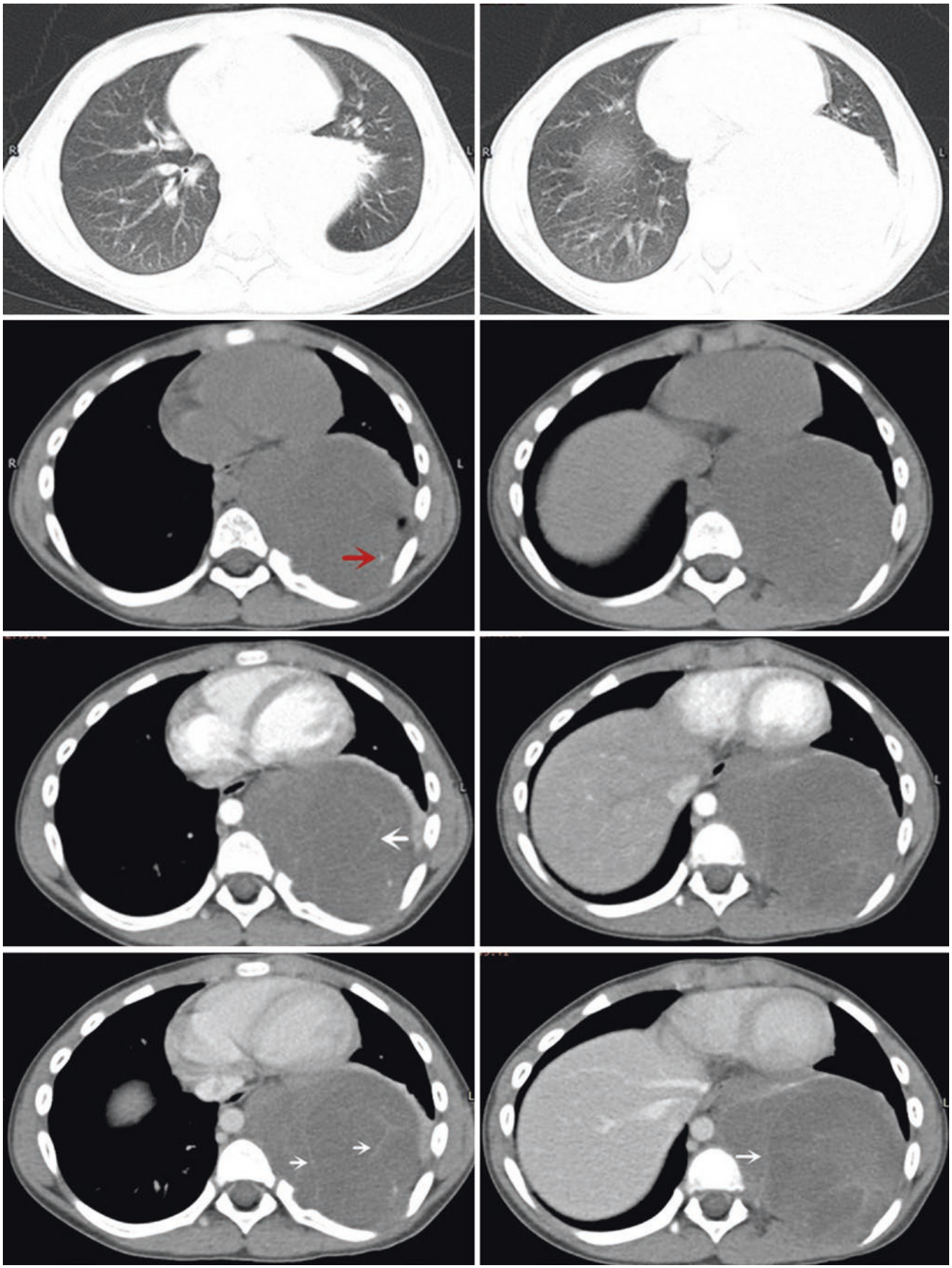

Fig. 9.80 Chest CT images of a 5-year-old girl complained of cough and chest tightness for 1 month

GNB is most common in children, especially age 1–2 years, with a median age at diagnosis of 22 months; most cases are diagnosed by 10 years. GNB can be located anywhere in the sympathetic nervous system: abdominal (65%), adrenal (25%), posterior mediastinal (20%), pelvic (4%), and cervical (1%) location. In 60%–70% of cases, metastases are present at diagnosis. Patients with mediastinal tumors may present stridor and respiratory difficulties secondary to tracheal compression. Large chest tumors may cause mechanical obstruction leading to superior vena cava syndrome. Most of them are unilateral, encapsulated, vascular, and do not cross the mid-abdominal line.

CT and MRI are the most commonly used imaging modalities for the assessment of GNB. The features of GNB are variable on enhanced CT, ranging from well-marginated, oblong paravertebral masses with homogeneous enhancement to irregular, cystic, hemorrhagic, or locally invasive masses. Approximately 50% of thoracic neuroblastomas/GNB have coarse, finely stippled, or curvilinear calcifications. On MRI, neuroblastomas and GNB are typically heterogeneous with variable enhancement and high signal intensity on T1W1 in hemorrhagic areas and hyperintense signals on T2W1 in cystic lesions.

Early and radical surgery is the best treatment available for mediastinal GNB. Prognosis depends on the disease stage, the degree of differentiation of neuroblastoma, the location of the primary tumor, and nutritional status. It is usually in good condition, with 2- and 5-year survival rates of 92% and 88%, respectively. Generally, older children with neuroblastoma/GNB had a worse prognosis than younger children. In addition, tumor size at diagnosis may be related to the prognosis in adult GNB. Adult GNB tumors >8 cm in diameter originating from the retrospective cavity tend to metastasize to other distant organs.

9.7.22 Case 22

A 6-year-old boy's physical examination revealed a left chest mass.

Chest CT: A huge spherical mass in the left mediastinum with calcifications (Fig. 9.81).

[**Diagnosis**] Neuroblastoma

[**Diagnosis basis**] In children, the lesions are huge, and calcification is obvious. Neuroblastoma is considered and confirmed by pathology.

[**Analysis**] Arising from neural crest cells, neuroblastoma is a solid tumor, which mature and develop into other cell types such as melanocytes, cranial neurons and glia, bone, cartilage, connective tissue as well as peripheral sympathetic neurons and Schwann cells. Neuroblastoma was originally described by Virchow in 1863; early reports considered the tumor as a glioma of the adrenal gland. By the beginning of the twentieth century, Zückerkandl and Kohn determined its origin in sym-

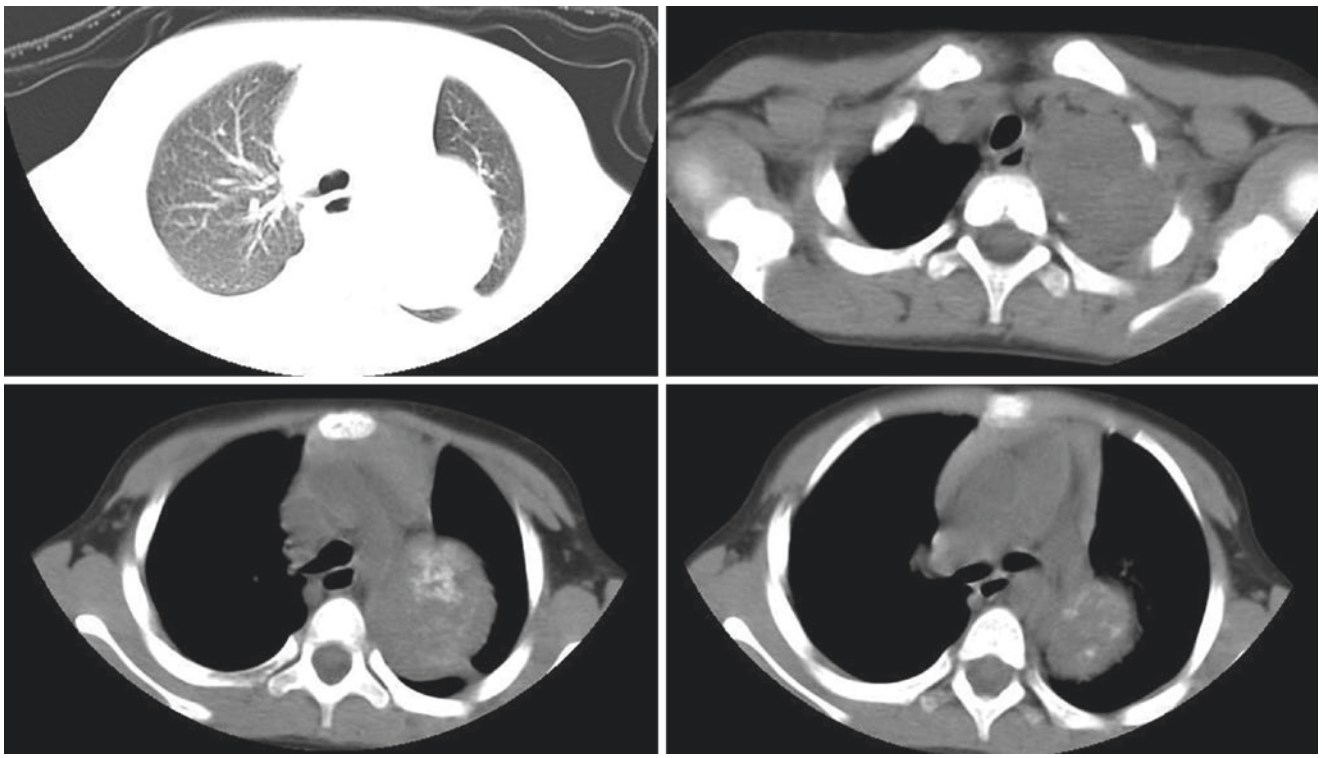

Fig. 9.81 Chest CT images of a 6-year-old boy's physical examination revealed a left chest mass

pathetic tissue. The surprising discovery that neuroblastoma could mature to ganglioneuroma was made in 1927.

Many genomic studies have proved that single nucleotide polymorphisms (SNPs) in DUSP12 and HSD17B12 locus at chromosome 5q11.2 are connected with low-risk neuroblastoma, whereas SNPs within or upstream of CASC15 and CASC14 on chromosome 6p22, BARD1, LMO1, HACE1, and LIN28B as well as a common copy number variation at 1q21 within NBPF23 have been associated with high-risk disease. Furthermore, a significant association of African genomic ancestry with high-risk neuroblastoma supported genetic etiology for the racial disparities in survival observed in neuroblastoma. Additional sequencing studies are needed to find new risk variants and develop deeper understanding of the genetic etiology of neuroblastoma.

Patients with neuroblastoma may present with symptoms affecting a variety of organ systems: respiratory (distress, infection, pneumonia), neurologic (Horner's syndrome, ataxia, myoclonic jerk), or urogenital (urinary tract infections). The most often symptom is pain, caused by either local effects from the primary tumor or metastatic disease. Up to 2/3 of patients have metastatic bone disease at presentation. The next most frequent complaint is abdominal distention. Other presenting symptoms include irritability, malaise, weight loss, shortness of breath (from a large abdominal tumor), and peripheral neurologic deficit (from neural foraminal invasion and nerve compression by tumor). Less common presentations include Horner syndrome (pupillary constriction, ptosis, and ipsilateral facial anhidrosis and flushing from a mediastinal tumor) and opsoclonus-myoclonus. Opsoclonus-myoclonus is jerking movements of the extremities and eyes, sometimes with cerebellar ataxia. The cause is unclear but it is seen in 2% of patients and is related to a thoracic primary tumor and a better prognosis.

Neuroblastic tumors are remarkable for their varied tumoral biologic behavior. One of the hallmarks of neuroblastoma and ganglioneuroblastoma is their tendency to secrete catecholamines. Most of catecholamines secreted are vanillylmandelic acid (VMA) and homovanillic acid (HVA). The vast majority (90–95%) of neuroblastoma and ganglioneuroblastoma secrete catecholamines, although the symptoms of catecholamine excess are rarely caused. Generally, the better differentiated the tumor, the more mature the catecholamine. Secreted as a metabolite of dopamine, the level of HVA may be elevated in more mature neuroblastoma and ganglioneuroblastoma. In contrast, VMA is a less mature metabolite of epinephrine and norepinephrine. Some centers evaluate a VMA-to-HVA ratio as an indicator of maturity. Ratios of less than 1 are considered favorable; ratios greater than 1 indicate an immature tumor and therefore a worse prognosis. Vasoactive intestinal peptide (VIP) may also be secreted by the tumor and may cause hypokalemia, watery diarrhea, and acidosis. VIP is believed to be elaborated by ganglion cells within the tumor. VIP-producing tumors tend to be more mature, and have a better prognosis.

The Children's Oncology Group (COG) has traditionally used the following factors to stratify patient risk. (1) Age at diagnosis, (2) stage to define extent of disease by the International Neuroblastoma Staging System (INSS), (3) tumor histology using the International Neuroblastoma Pathology Classification (INPC) criteria, (4) *MYCN* status (amplified versus nonamplified), and (5) DNA index or tumor cell ploidy. Older age has been prognostic of poor outcome in neuroblastoma since the 1970s. Compared with older children, younger children, especially infants <1-year old, have significantly better disease-free survival outcomes, for that all stages of neuroblastoma beyond stage 1, where the tumor is still in the localized state.

9.7.23 Case 23

A 8-year-old girl's physical examination revealed mediastinal mass.

Chest CT: A large mass in the left posterior mediastinum with necrosis and calcification (Fig. 9.82).

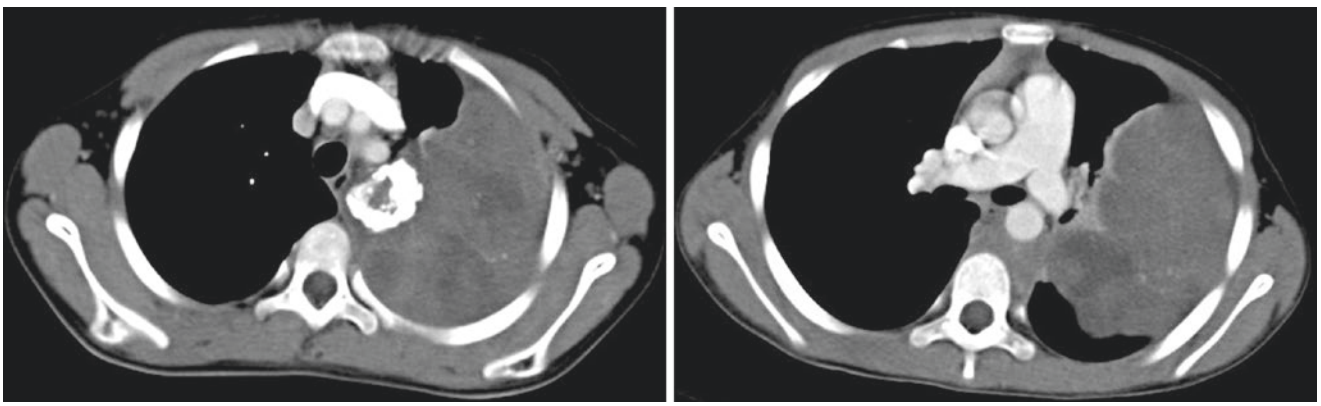

Fig. 9.82 Chest CT images of an 8-year-old girl's physical examination revealed mediastinal mass

[**Diagnosis**] Neuroblastoma

[**Diagnosis basis**] A child with mediastinal space-occupying lesions, gross calcification, and obvious necrosis is seen. The diagnosis first considers neuroblastoma and is confirmed by pathology.

[**Analysis**] The age and lesion location of patient are important for the diagnosis of mediastinal neurogenic tumors. Most mediastinal neurogenic tumors are benign in adults, but they are frequently malignant in children. The most common neurogenic tumors in adults are neurofibroma and schwannoma, which are most common between 20 and 55 years. The most common types in children are neuroblastoma and ganglioneuroma, most of which occur within the age of 10 years.

Neurogenic tumors on CT are mostly round or circular-shaped mass with smooth, clear borders, and uniform density in mediastinum. Some tumors can have calcifications (schwannoma, ganglioneuroma, and neuroblastoma) and cystic changes (mainly schwannoma). Completely cystic schwannoma is easily misdiagnosed as a mediastinal cyst in the clinic. CT findings of neurogenic tumors of different origins in the posterior mediastinum have their own characteristics. Neuroblastoma has the largest and most calcification. Paraganglioma has the most obvious enhancement in parenchyma. Ganglioneuroma has the most significant difference in the ratio of tumor length to width. Schwannoma has the most cystic changes. Neurofibroma is histologically more similar to schwannoma, therefore the differential diagnosis in CT is difficult when they are single. But it is easy to diagnose neurofibromatosis when there are multiple lesions slightly or no enhancement.

Comprehensive consideration of the patient's age and clinical manifestations, lesion location, and imaging findings is important in the diagnosis of mediastinal neurogenic tumors.

9.7.24 Case 24

A 36-year-old male complained of chest tightness for 1 month.

Chest CT: An elliptical mass in the right posterior mediastinum, with high degree of enhancement and a necrotic or cystic component (Fig. 9.83).

[**Diagnosis**] Paraganglioma

[**Diagnosis basis**] The posterior mediastinal tumor showed high degree of enhancement and extensive unenhanced area with necrotic or cystic component. The imaging performance was consistent with paraganglioma and confirmed by surgical pathology.

[**Analysis**] Paragangliomas are rare neuroendocrine tumors originating from extra-adrenal chromaffin cells. Glenner et al. divide mediastinal paraganglioma into two types: aorticopulmonary paraganglioma (APPG), arising in the anterior or middle mediastinum (along the great vessels) and aorticosympathetic paraganglioma (ASPG), occurring in the posterior mediastinum. APPGs usually occur in persons older than 40 years. Among APPGs, nonfunctioning tumors are more common than functioning tumors. In contrast, ASPGs occur in younger adults (mean 29 years), and approximately 50% of patients present with symptoms related to the functional activity of the tumor.

Pheochromocytomas and paragangliomas (PPGLs) have a high degree of heritability with 40% of cases carrying a germline mutation. More than 20 susceptibility genes have been identified. The underlying mutation influences PPGL clinical presentation such as cell differentiation, tumor location, specific catecholamine production, malignant potential, and genetic anticipation.

CT and MRI are useful imaging methods in the diagnosis of mediastinal paraganglioma, which provide information about the location and size of lesions. Because mediastinal paragangliomas are hypervascular tumors, they can exhibit remarkable contrast agent enhancement on CT or MRI. Based on the hypervascular characteristic, transthoracic needle biopsy is not recommended for preoperative diagnosis because this process may lead to catastrophic bleeding. Hyaline-vascular type Castleman's disease appears pronounced contrast enhancement in the arterial phase on dynamic imaging, which resembles paraganglioma. However, necrosis and cystic changes are rare in Castleman's disease, which is thought to be helpful in the differential diagnosis.

Paragangliomas are usually low-grade indolent tumors. It is estimated that 0% to 36% of paragangliomas can metastasize depending on the type of tumor. Metastasis is the most common negative predictor for long-term survival. The most common regions of metastasis include lung, lymph nodes, and bone, which indicates both lymphatic and hematogenous route of transmission. Mediastinal paragangliomas are particularly aggressive tumors and are related to a higher morbidity and mortality. Complete resection is the preferred treatment for mediastinal paraganglioma. Nevertheless, the highly vascular nature of these tumors also causes huge surgical risks. Massive bleeding during tumor excision has been reported. Therefore, it is recommended to perform preoperative angiography to assess the vascular supply of the tumor. Preventive embolization can reduce perioperative bleeding if necessary.

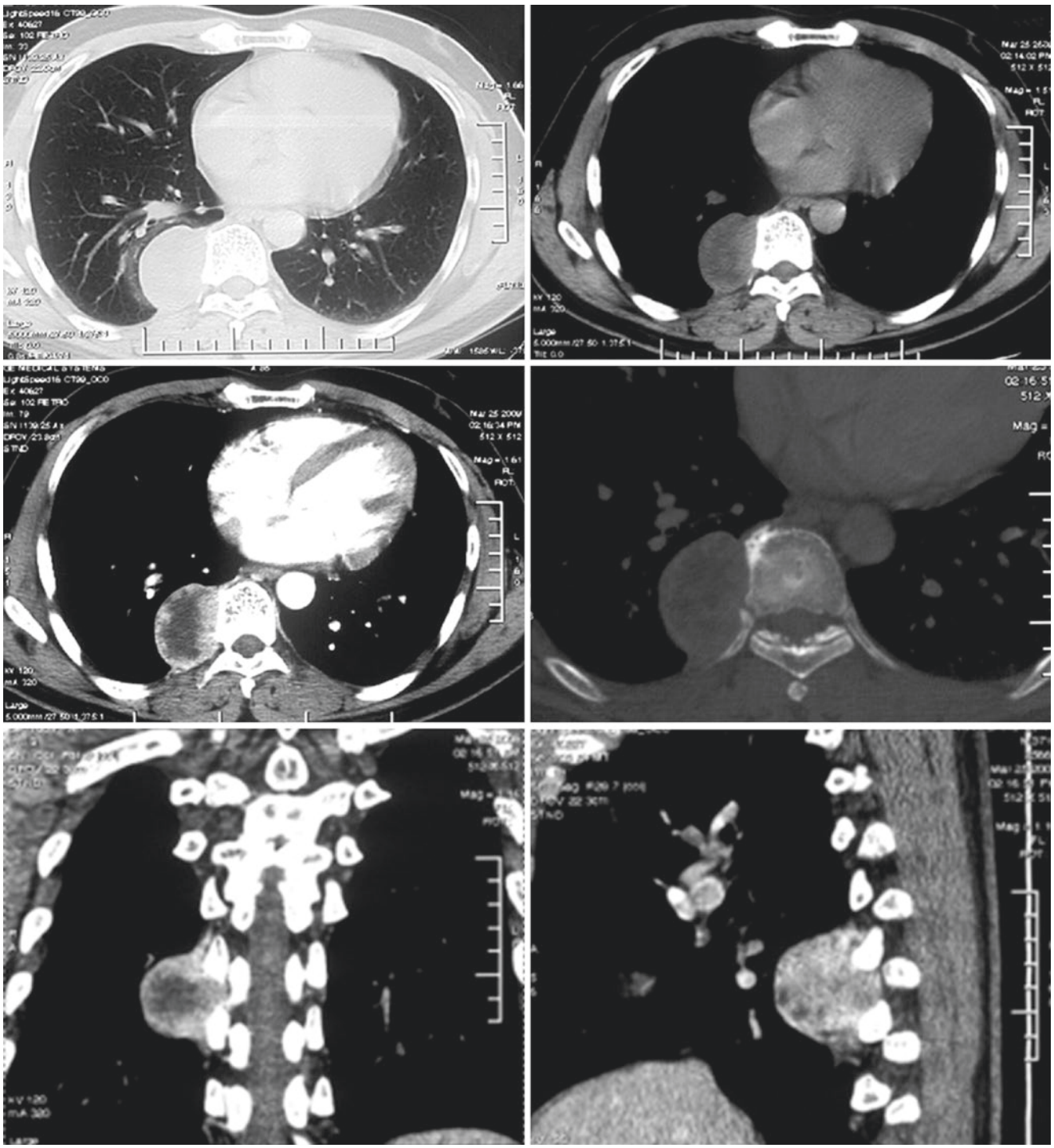

Fig. 9.83 Chest CT images of a 36-year-old male complained of chest tightness for 1 month

References

1. Isoda H, Takahashi M, Mochizuki T, et al. MRI of dumbbell-shaped spinal tumors. J Comput Assist Tomogr. 1996;20:573–82.
2. Wiener MF, Chou WH. Primary tumors of the diaphragm. Arch Surg. 1965;90:143–52.
3. Straus GD, Guckien JL. Schwannoma of the tracheobronchial tree: a case report. Ann Otol Rhinol Laryngol. 1951;60:242–6.
4. Kasahara K, Fukuoka K, Konishi M, et al. Two cases of endobronchial neurilemmoma and review of the literature in Japan. Intern Med. 2003;42:1215–8.
5. Jo VY, Fletcher CDM. Epithelioid malignant peripheral nerve sheath tumor: clinicopathologic analysis of 63 cases. Am J Surg Pathol. 2015;39:673–82.
6. Varma DG, Moulopoulos A, Sara AS, et al. MR imaging of extracranial nerve sheath tumors. J Comput Assist Tomogr. 1992;16:448–53.
7. Davies PBD. Diffuse pulmonary involvement in von Recklinhausen's disease: a new syndrome. Thorax. 1963;18:198.
8. Zamora A, Collard H, Wolters P, et al. Neurofibromatosis-associated lung disease: a case series and literature review. Eur Respir J. 2006;29:210–4.
9. Ueda K, Honda O, Satoh Y, et al. Computed tomography (CT) findings in 88 neurofibromatosis 1 (NF1) patients: prevalence rates and correlations of thoracic findings. Eur J Radiol. 2015;84:1191–5.
10. Massaro D, Katz S. Fibrosing alveolitis: its occurrence, roentgenographic, and pathologic features in von Recklinghausen's neurofibromatosis. Am Rev Respir Dis. 1966;93:934–42.
11. Lonergan GJ, Schwab CM, Suarez ES, et al. Neuroblastoma, ganglioneuroblastoma, and ganglioneuroma: radiologic–pathologic correlation. Radiographics. 2002;22:911–34.
12. Kato M, Hara M, Ozawa Y, et al. Computed tomography and magnetic resonance imaging features of posterior mediastinal ganglioneuroma. J Thorac Imaging. 2012;27:100–6.